Pyrolysis of contaminated PS single-layer and LDPE/PET multi-layer waste plastic packaging to optimise the production of oil for fuel applications

by

Salomie van der Westhuizen

Thesis presented in partial fulfilment
of the requirements for the Degree

of

MASTER OF ENGINEERING
(CHEMICAL ENGINEERING)

in the Faculty of Engineering
at Stellenbosch University

Supervisor

Prof. Johann F. Görgens

Co-Supervisor

Dr. François-Xavier Collard

March 2020

Declaration

By submitting this thesis electronically, I declare that the entirety of the work contained therein is my own, original work, that I am the sole author thereof (save to the extent explicitly otherwise stated), that reproduction and publication thereof by Stellenbosch University will not infringe any third party rights and that I have not previously in its entirety or in part submitted it for obtaining any qualification.

Date: March 2020

Plagiarism declaration

1. Plagiarism is the use of ideas, material and other intellectual property of another's work and to present is as my own.

2. I agree that plagiarism is a punishable offence because it constitutes theft.

3. I also understand that direct translations are plagiarism.

4. Accordingly, all quotations and contributions from any source whatsoever (including the internet) have been cited fully. I understand that the reproduction of text without quotation marks (even when the source is cited) is plagiarism.

5. I declare that the work contained in this assignment, except where otherwise stated, is my original work and that I have not previously (in its entirety or in part) submitted it for grading in this module/assignment or another module/assignment.

Initials and surname: S van der Westhuizen

Date: 15 November 2019

Abstract

It has been predicted that by 2050 there will be more plastic in the ocean than fish by weight. Besides the obvious environmental threat, plastic waste also poses a loss of valuable hydrocarbon-based materials.

Pyrolysis has been identified as a promising technology for the recycling of waste plastics that cannot be recycled by conventional means due to their mixed and/or contaminated nature. Two such waste plastics are black PS punnets and LDPE/PET multi-layer films used to package raw meat and dry dog food respectively. However, little has been reported on the conversion of multi-layers, the influence of contamination, or the scale-up of the process to larger scale. The pyrolysis process performance has been found to be highly dependent on the composition of the feedstock and process parameters. Additionally, large-scale processing can present added difficulties. Therefore, to make pyrolysis a viable option for processing of these particular waste plastics at a large scale, it is necessary to study its optimisation and scale-up to pilot scale.

The aim of this study was to convert these two waste plastics into fuel (oil/wax) products by pyrolysis. To meet this aim, the waste plastics were characterised to determine their suitability as fuel precursors and estimate the amount of contamination. The pyrolysis process was optimised in a bench scale semi-batch reactor for the yield and quality of the oil/wax. Based on optimised conversion, the process was scaled-up in a pilot semi-continuous rotary kiln reactor.

Feedstock characterisation proved that the waste plastics were suitable as oil/wax fuel precursors. Contamination in PS negatively affected the characterisation. However, both volatile matter and the sum of carbon and hydrogen contents still represented more than 95 wt.%. Contamination in the LDPE/PET multi-layer resulted in insignificant characterisation differences.

Oil yield of 89.8-93.2 wt.% was achieved during bench scale testing of the clean PS. Heavy meat juice contamination (about 16 wt.%, dry basis) decreased the oil yield by 7.3 wt.% but did not affect the HHV. Conversion of post-consumer densified PS resulted in similar oil yield and HHV to the clean PS. Scale up to the pilot reactor resulted in lower oil yield of 82.5±1.4 wt.% with HHV similar to oils obtained at bench scale in the range of 41.9-42.5 MJ/kg (comparable to gasoline). The gross energy recovered from the oil was 88±3%. Fuel characterisation indicated the oils similarity to gasoline. However, with aromatic content greater than 68 wt.%, blending with conventional fuel will be necessary to make it commercially suitable.

Maximum oil/wax yield of 75.37±0.04 wt.% was achieved during bench scale testing of the clean multi-layer. Contamination decreased the oil/wax yield to 71.45±0.03 wt.%, potentially due to a

catalytic effect, but did not affect the HHV. Scaling up to pilot scale resulted in lower oil/wax yield of 62 ± 12 wt.% and unaffected HHV in the range of 43.5-44.13 MJ/kg (similar to diesel). This represented a gross energy recovery of $66\pm12\%$. Fuel characterisation indicated the flowable oils similarity to diesel. However, further upgrading will be necessary to make it suitable as commercial diesel.

Opsomming

Dit is voorspel dat teen 2050 daar meer plastiek as visse per gewig in die oseaan gaan wees. Buiten die vanselfsprekende omgewingsbedreiging, hou plastiekafval ook 'n verlies van waardevolle koolwaterstof-gebaseerde materiale in.

Pirolise is geïdentifiseer as 'n belowende tegnologie vir die herwinning van afvalplastiek wat nie herwin kan word deur konvensionele maniere nie as gevolg van hul gemengde en/of gekontamineerde aard. Twee sulke afvalplastiekstowwe is swart PS-bakkies en LDPE/PET-multilaag films wat gebruik word om rou vleis en droë hondekos, onderskeidelik, te verpak. Daar is egter min gerapporteer oor die omsetting van multilae, die invloed van kontaminasie, of die opskalering van die proses na groter skaal. Die doeltreffendheid van die pirolieseproses is gevind om hoogs afhanklik te wees van die komposisie van die voermateriaal en prosesparameters. Daarby kan grootskaalse prosessering toegevoegde moeilikheid inhou. Daarom, om pirolise 'n uitvoerbare opsie vir die prosessering van hierdie spesifieke afvalplastiekstowwe op grootskaal te maak, is dit nodig om sy optimering en opskalering na loodsskaal te bestudeer.

Die doel van hierdie studie was om hierdie twee plastiekstowwe in brandstofprodukte (olie/was) deur middel van pirolise om te skakel. Om hierdie doel te bereik is afvalplastiekstowwe gekarakteriseer om hul gepastheid as brandstofvoorlopers te bepaal en die hoeveelheid kontaminasie te beraam. Die piroliseproses is geoptimeer in 'n banktoetsskaal semilotreaktor vir die opbrengs en kwaliteit van die olie/was. Gebaseer op geoptimeerde omsetting, is die proses opgeskaal in 'n loodssemi-aaneenlopende draaioondreaktor.

Karakterisering van voermateriaal het bewys dat die afvalplastiekstowwe gepas was as olie/was-brandstofvoorlopers. Kontaminasie in PS het die karakterisering negatief geaffekteer. Beide vlugtige stowwe en die som van koolstof- en waterstofinhoud het egter steeds meer as 95 wt.% verteenwoordig. Kontaminasie in die LDPE/PET-multilaag het onbeduidende karakteriseringsverskille tot gevolg gehad.

Olie-opbrengs van 89.8–93.2 wt.% is bereik gedurende banktoetsskaaltoetsing van die skoon PS. Swaar vleissapkontaminasie (omtrent 16 wt.%, droë basis) het die olie-opbrengs met 7.3 wt.% verminder maar het nie die HHV geaffekteer nie. Omsetting van post-verbruiker gedigte PS het soortgelyke olie-opbrengste en HHV as die skoon PS tot gevolg gehad. Vergroting van skaal na die loodsreaktor het laer olie-opbrengs van 82.5±1.4 wt.% tot gevolg gehad met HHV soortgelyk aan olies verkry by banktoetsskaal in die bestek van 41.9–42.5 MJ/kg (vergelykbaar met petrol). Die bruto-energie herwin uit die olie was 88±3%. Brandstof karakterisering het aangedui dat die olies soortgelyk aan petrol is. Met aromatiese inhoud groter as 68 wt.%, sal vermenging met konvensionele brandstof noodsaaklik wees om dit kommersieel geskik te maak.

Maksimum olie/was-opbrengs van 75.37±0.04 wt% is bereik gedurende banktoetsskaaltoetsing van die skoon mulitlaag. Kontaminasie het die olie/wasopbrengs na 71.45±0.03 wt.% verminder, moontlik as gevolg van 'n katalitiese effek, maat het nie die HHV geaffekteer nie. Vergroting van skaal na loodsskaal het in laer olie/wasopbrengs van 62±12 wt.% gelei en ongeaffekteerde HHV in die bestek van 43.5-44.13 MJ/kg (soortgelyk aan diesel). Hierdie het 'n bruto-energieherwinning van 66±12% verteenwoordig. Brandstof karakterisering het aangedui dat die vloeibare olies soortgelyk aan diesel is. Verdere opgradering is nodig om dit gepas vir kommersiële diesel te maak.

Acknowledgements

Foremost, I wish to express my gratitude to my supervisor, Prof Johann F Görgens for his support, guidance and commitment to a higher standard that has made me a better researcher. My enduring appreciation to my co-supervisor, Dr François-Xavier Collard, for his generosity with his time, exceptional knowledge, guidance, moral support and ever calm demeanour. In addition, I hereby express my appreciation for the financial support and research question provided by PlasticsSA.

Special thanks to the following people:

- Mr Jaco van Rooyen, Ms Hanlie Botha and Ms Levine Simmers for their assistance with many analyses and offering support beyond what was required.

- Mr Jos Weerdenburg, Mr Anton Cordier and Mr Bevan Koopman for invaluable technical support and wealth of know-how.

- Mr Alvin Petersen and Mr Oliver Jooste for helping me stay on schedule with technical support.

- Dr Danie Diedericks for consistent moral support.

- Mr Henry Solomon for assistance with feedstock processing and always offering a smile.

- Ms Anita Kleinschmidt for assistance with funding administration.

- Ms Mieke De Jager for her expert administrative skills.

- To my colleagues who provided a discussion platform and assisted with experiments: Ms Wendy Mfana, Mr Farai Chireshe and Mr George Parku.

- Lastly, yet the most important, to my family without whom getting to this point would have been impossible and a lot less rewarding.

Table of contents

List of figures

List of tables

Nomenclature

DTG	Derivative of TGA mass loss curve
ESP	Electrostatic precipitator
GC	Gas chromatography
GC/MS	Gas chromatography/mass spectrometry
HDPE	High density polyethylene
HHV	Higher heating value
Induction	Heating via electromagnetic waves creating eddy currents in iron-based metal
IS	Internal standard
LDPE	Low density polyethylene
LOD	Limit of detection
MW	Molecular weight
PAH	Polycyclic aromatic hydrocarbon
PET	Polyethylene terephthalate
PS	Polystyrene
PVC	Polyvinyl chloride
SABS	South African Bureau of Standards
SANS	South Africa National Standard
T	Temperature
TGA	Thermogravimetric analysis

1 Introduction

Plastic products have become an integral part of modern society and have replaced many other materials such as metals, ceramics, glass, and wood, due their affordability, low weight, durability, versatile applications, resistance to degradation by many chemicals, and ease of processing (Diaz-Silvarrey *et al*., 2018; Wong *et al*., 2015). These characteristics ensure an economic benefit in the industrial sector, but also promote environmental benefits by for example being able to transport more plastic products (as opposed to alternatives such as paper, metal and glass) and therefore reducing the carbon footprint of products manufactured from plastic.

However, typically plastic products have a very short commercially usable life (single-use plastics) before it is classified as post-consumer and discarded as waste (some prime examples include food packaging, straws, and grocery bags). Plastic packaging, which comprises about 51.4% of the plastics produced locally, is likely to reach its end of life in a matter of days to a couple of months (National Plastics Recycling Survey-2016, 2017). Internationally about 14% of post-consumer plastic waste is recycled annually (The New Plastics Economy, 2016), while in South Africa in 2016, 41.8% of post-consumer waste plastic was recycled (National Plastics Recycling Survey-2016, 2017). The rest (0.667 million tonnes in South Africa in 2016 (National Plastics Recycling Survey-2016, 2017)) was land-filled or ended up as plastic pollution in the earth's natural environment. Furthermore, plastic waste remains intact for hundreds of years due to the fact that they are so durable and not easily degraded (Wong *et al*., 2015). Therefore, the presence of plastic waste in natural environments and in landfills wreaks havoc on plant and animal life, and further strains already full landfill areas (especially due to the very low bulk density of plastics). The global environmental plastic waste issue can be very clearly illustrated by the often-cited prediction that by 2050 there will be more plastic in the ocean than fish by weight (The New Plastics Economy, 2016). Aside from the obvious environmental threat, plastic waste also represents an economic loss in terms of the energy and valuable chemical content that can be recovered from the waste plastic, as virgin plastics are manufactured from depleting fossil fuels and in fact the energy value of most plastics is similar to that of hydrocarbon fuels such as diesel and gasoline (Wong *et al*., 2015).

In South Africa, where recycling is largely economically driven, there currently exist well-established markets for the primary and secondary recycling of suitable plastics (which accounts for the 41.8% recycled), i.e. the recycling of pure and very clean plastic waste to produce new plastic products (National Plastics Recycling Survey-2016, 2017). However, some waste plastics cannot be recycled via primary or secondary methods, because they are composed of multiple different kinds of plastic polymers (such as multi-layers) and/or are highly contaminated, such as food packaging. This

is problematic since recycling requires a high degree of purity and cleanliness. The pre-processing required for the mixed and contaminated plastics, such as separation and cleaning, to be able to recycle them via primary and secondary means, would incur extra costs and reduce the economic and practical viability of the recycling process. Therefore, in order to increase the recycling rate of plastic waste, different technologies, that are better able to deal with mixed and contaminated plastics, have to be developed and optimised. This will aid in establishing suitable markets for the recycling of these plastics and this is where tertiary recycling can play an important role.

The different technologies available that are classified as tertiary recycling include pyrolysis, glycolysis, hydrolysis, and gasification among others (Wong *et al*., 2015). Their goal is to recover value-added products in terms of their chemical or energy content. Pyrolysis has the advantage over primary, secondary, and other tertiary recycling methods of being a very robust process (especially when coupled with a robust reactor design such as a rotary kiln) that is able to deal with different kinds of plastics (even mixed plastics) and a greater degree of contamination. During pyrolysis the plastic waste is processed to obtain value-added products such as chemicals and a more homogeneous oil/wax (compared to the raw plastic waste) that can be used as fuel. This fuel can possibly be used in a transportation context as diesel or gasoline. For these applications it would need to meet diesel or gasoline property specifications, which in South Africa are set out by SABS standards SANS 342 for diesel and SANS 1598 for gasoline.

Pyrolysis is a thermal treatment (with or without catalyst) whereby an organic material is heated to within a range of 400-700 °C, in an inert environment (such as N_2 atmosphere) to produce three products: oil/wax, char, and gas. These products have value for either their chemical or energy content, as the components of the products are hydrocarbon based (Sharuddin *et al*., 2016).

The pyrolysis process has been found to be highly dependent (in terms of the yield and quality of the products) on the type of feedstock processed and other operating parameters such as temperature, heating rate, feedstock residence time, volatile residence time, and the reactor configuration, among others (Sharuddin *et al*., 2016), as outlined in Section 2.2.2. Some research studies have been performed on the most common plastic waste types, which are polyethylene terephthalate (PET), high density polyethylene (HDPE), polyvinyl chloride (PVC), low density polyethylene (LDPE), polypropylene (PP), and polystyrene (PS) (Letcher *et al*., 2011), using different reactor configurations and testing the influence of the operating parameters. However, these studies mainly focus on individual plastics that are clean and scale up to pilot scale is not typically investigated.

The governing body of the plastic industry in South Africa, PlasticsSA, has identified particularly problematic plastic waste fractions that cannot be recycled via primary or secondary methods due to being composed of mixed plastics (such as multi-layers) and/or being too contaminated. Therefore, these plastics do not currently have viable recycling markets, which necessitates their disposal to landfill. This study explores the tertiary recycling of two of these problematic plastic waste fractions via pyrolysis. The two types of waste plastics are first a single-layer, high-absorbent polystyrene (PS) plastic used as packaging for raw meat, which makes it highly contaminated with meat juice. The second waste plastic is a multi-layer plastic composed of low density polyethylene (LDPE) and polyethylene terephthalate (PET) used to package dry dog food.

The main aim of this study is to optimise the pyrolysis conversion of the two waste plastic fractions, in terms of yield and quality of the oil/wax product for transportation fuel applications such as diesel or gasoline. The approach consists of an optimisation at bench scale in a semi-batch reactor followed by an investigation of the scale-up in a continuous, pilot scale, rotary kiln reactor. The key objectives include to characterise the plastic feedstock (both pure and contaminated) and to study the influence of operating parameters at bench scale and the effect of contamination. Based on these results, an optimisation study is undertaken at pilot scale. As it has been reported that pyrolysis of mixtures of plastics and/or contaminated plastics can cause interaction between the different plastic components and/or the contamination (Brems *et al*., 2011; Wong *et al*., 2015), it is essential that optimisation of the two problematic plastic wastes be performed and scaled up to pilot scale, to aid in establishing viable markets for its recycling.

In the following chapters, a review of the relevant literature is considered in Section 2, which includes literature pertaining to pyrolysis of PS, LDPE and PET; the effect of contamination; and interaction effects in mixed and/or contaminated plastics. Thereafter, the key questions and objectives are clarified in Section 3 and the methods used to answer the key questions and meet the objectives are detailed in Section 4. Following this, the results are presented and discussed in Section 5, which starts with characterisation and bench scale pyrolysis of the waste plastics, followed by pilot scale pyrolysis results and relating major operational difficulties. Finally, the conclusions drawn from the study, along with recommendations for further work are presented in Section 6.

2 Literature review

The literature review is organised by first defining plastic and the management strategies employed for waste plastic in Section 2.1. Secondly, in Section 2.2, pyrolysis is defined in detail including the factors that effect it such as the type of plastic being processed, the reactor configuration and type of pyrolysis, temperature, heating rate, feedstock residence time, volatile residence time, particle size, pressure, and catalyst. Thirdly, Section 2.3 considers commercial grade fuel (diesel and gasoline) in terms of the fuel constituents, boiling points, energy content, and other fuel quality characteristics for better comparison of the pyrolysis oil. Thereafter, Sections 2.4, 2.5.1 and 2.5.2 detail the research available for the individual plastics (PS, LDPE, PET) and their pyrolysis conversion in terms of the composition of the plastics, their thermal degradation behaviour, the degradation mechanisms, the yield of the three product fractions and the quality of the oil/wax as fuel. Finally, the multi-layer of LDPE and PET is considered (Section 2.5.3), particularly potential interaction effects, and the possible effect of contamination is explored in Section 2.6. Conclusion drawn from the literature including the proposed limitations are presented in Section 2.7.

2.1 Plastic waste

2.1.1 Plastic definition

Plastics are synthetic organic polymers made up of a large number of repeating monomers (from hundreds to tens of thousands) that are chemically joined (Kotz *et al*., 2009; Silderberg, 2009). Polymer chains consist primarily of carbon (C) and hydrogen (H). Some polymers consist only of these two elements such as polyethylene and polystyrene. Others also contain chlorine (Cl) such as PVC, while some contain oxygen (O) such as PET, and nitrogen (N) such as polyamides (nylon) (Kotz *et al*, 2009). The plastic polymers that make up the majority of plastic wastes are polyethylene terephthalate (PET), high-density polyethylene (HDPE), polyvinyl chloride (PVC), low-density polyethylene (LDPE), polypropylene (PP), and polystyrene (PS) (Letcher *et al*., 2011; Williams & Williams, 1999a; Park *et al*., 2003).

2.1.2 Management strategies

South Africa's National Waste Management Strategy defines the following hierarchy for waste management: 1) waste avoidance; 2) re-use; 3) recycle; 4) recover, and finally 5) treatment and disposal to landfill (National Waste Information Baseline Report, 2012). Therefore, to prevent plastic waste from being disposed to landfill, it has to undergo processes in order to either be recycled into new products or to recover some chemicals or the energy inherent in the polymer chains. The recycling and recovery of plastic waste can further be classified as primary, secondary, tertiary and quaternary

recycling (Al-Salem *et al*., 2009).

Primary recycling, or re-extrusion, is the recycling of scrap plastic in the plastic manufacturing process to produce a final plastic product of similar quality (Al-Salem *et al*., 2009). An example is the injection moulding of LDPE crates. Final crates that do not adhere to the required product specifications are pelletised and reintroduced to the manufacturing process (Al-Salem *et al*., 2009). For plastic to be recycled in this way, the plastic must be of the same type as being manufactured with a high purity. Additionally, it requires that the plastic be very clean. This can introduce complications and added costs when the plastic waste is mixed with other plastics or is contaminated (Al-Salem *et al*., 2009).

Secondary, or mechanical recycling is when solid plastic waste is used to produce plastic products via mechanical means (Al-Salem *et al*., 2009). Products from the secondary recycling of plastic solid waste usually have lower quality compared to the original plastic product due to degradation caused by the reprocessing techniques and impure or contaminated plastic feedstock (Al-Salem *et al*., 2009). Examples of products from secondary recycling are grocery bags, pipes and gutters (Al-Salem *et al*., 2009).

Quaternary recycling is the incineration of plastics to recover energy as heat. Mixtures of contaminated plastics are typically used. This makes efficient incinerator reactor design and process control difficult due to plastic waste being heterogeneous. Additionally, extensive treatment technologies are necessary to clean the high volumes of toxic off-gasses (Brems *et al.*, 2011).

Tertiary, or chemical recycling is when advanced technologies are used to break down the large plastic polymer chains to produce smaller molecules, which may be in the form of liquid/wax or gas (Al-Salem *et al*., 2009). These technologies include thermochemical conversions such as gasification and pyrolysis. The products from these processes can be used to either make new plastic products (from the chemicals produced) or as fuel (due to the inherent energy value) (Al-Salem *et al*., 2009). Of particular interest in this study is the use of pyrolysis for transportation fuel production.

Pyrolysis can better deal with mixed plastics as feedstock as well as a certain degree of contamination, compared to primary or secondary recycling methods. It also produces a more homogenous oil/wax and gas, which are value-added products, that can be exploited for their energy value more efficiently than with incineration. Therefore, pyrolysis has the benefits of easier and more flexible handling and processing (Sharuddin *et al*., 2016) and production of value-added products.

2.2 Pyrolysis of plastic waste for fuel production

2.2.1 Pyrolysis definition and products

Plastic pyrolysis is the degradation of plastic polymer (long chains) feedstock at high temperature (400-700 °C) in an inert environment to produce smaller chains and compounds (Sharuddin *et al*., 2016). Pyrolysis is an endothermic reaction, and the high temperature provides the energy required to break the intermolecular bonds of the polymer, while the absence of oxygen (inert environment) ensures that combustion of the feedstock does not occur (Sharuddin *et al*., 2016). Three products are formed from the pyrolysis process: a gas product, an oil/wax product, and char product.

Figure 2.1 provides a basic schematic explanation of the pyrolysis process. In this example, nitrogen flow provides the inert environment and the heating supplies the energy to break up the long polymer chains of the plastic into smaller units. When small enough, these units become volatile. The hot volatiles from the pyrolysis reactor contain a condensable and a non-condensable fraction. The non-condensable fraction is the gas product and is composed of the smallest molecules. At ambient temperature, the condensable fraction becomes an oil/wax product. The char is the solid residue. The oil/wax is the marketable product of interest for fuel applications in this study due to its hydrocarbon nature and therefore high energy content, comparable to other hydrocarbon fuels such as diesel or gasoline (Miandad *et al*., 2016b; Li *et al*., 1999; Wiriyaumpaiwong & Jamradloedluk, 2017; Sharuddin *et al*., 2016). A condensable product with a high proportion of long (respectively short) chain compounds will be characterised by a waxier (respectively oily) aspect. The gas product has been found to also have a high energy content, similar to natural gas at 48-53 MJ/kg (López *et al.*, 2011). In pyrolysis processes, the gaseous product is typically combusted onsite to provide process heat for the pyrolysis reactor (Chen *et al*., 2014).
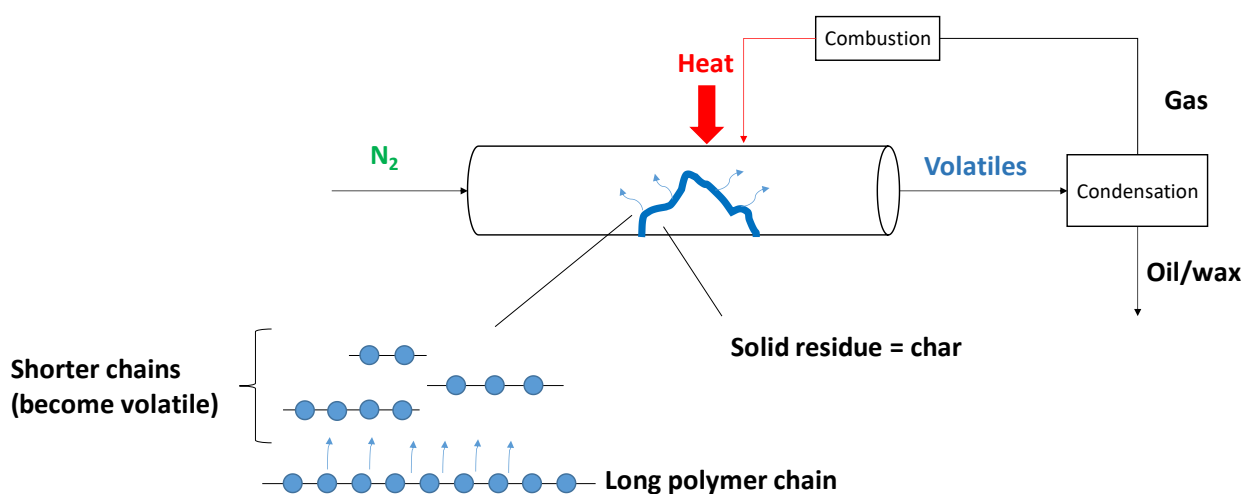
Figure 2.1: Simplified schematic of pyrolysis

2.2.2 Important factors that affect the pyrolysis process performances

The following factors are important to consider during the pyrolysis process and will be discussed in more detail in this section:

- Types of polymers

- Types of pyrolysis and reactors

- Temperature

- Heating rate

- Residence time of the feedstock

- Residence time of the volatiles

- Particle size of the plastic feedstock

- Pressure

- Catalyst

A study of the available literature is useful to describe the effects of some of the parameters. However, it lacks the capability to determine the optimum conditions for a specific plastic, due to the fact that the studies typically investigate one parameter at a time and therefore do not account for the interaction between the parameter. Additionally, the combination of different plastics and the proportion of their combination have been found to affect the results. Lastly, the effects of the parameters are a function of the reactor configuration.

2.2.2.1 Types of polymers

Different types of plastic polymers have different compositions, structures and reactivities. This is an essential consideration in evaluating both the yield and the properties of the pyrolysis products. A more complete discussion on how the composition and structure of PS, LDPE and PET can affect the pyrolysis process is given in Sections 2.4 and 2.5.

The composition of a feedstock considered for fuel properties is commonly characterised in terms of the ultimate and proximate analysis thereof (Sharuddin *et al*., 2016). This characterisation can provide an indication of the suitability of the feedstock for fuel applications. The ultimate analysis provides the composition of the feedstock in terms of the following elements (normally reported on a

dry, ash free basis): carbon (C), hydrogen (H), nitrogen (N), and sulphur (S). The oxygen content is determined by the difference. A feedstock having a higher content of carbon and hydrogen is an indication of a better potential in terms of energy content. Additionally, a plastic with a higher H/C ratio could produce a fuel oil with a higher H/C ratio when processed. This is important as the H/C ratio is considered as an important parameter in fuel characterisation, with Yue *et al.* (2016) and Li *et al*. (1999) stating that it has been found to be correlated with the cracking performance of fuel in a refinery, i.e. a fuel feedstock with a higher H/C ratio has been found to generally perform better. The presence of oxygen in significant amounts is not recommended as oxygenated compounds can make the fuel unstable and acidic, resulting in complicated processing due to problems such as corrosion (Fahim *et al*., 2010). The presence of high amounts of nitrogen and sulphur compounds is undesirable in fuel and fuel feedstocks as they cause harmful emissions such as NO_x and SO_x on combustion (Fahim *et al.,* 2010).

The proximate analysis decomposes the feedstock into four components: the moisture content, the volatile matter, the fixed carbon and the ash content (Sharuddin *et al*., 2016). The moisture corresponds to the water physically adsorbed at the surface of the plastic. After pyrolysis and condensation, it is found in the oil product. Therefore, the moisture content of the plastic feedstock is desired to be low for efficient heating (during pyrolysis) of the sample and to ensure that the oil does not contain a significant amount of water, which would cause the oil to have a lower HHV and can also result in complications when combusted in conventional engines. When targeting the conversion of the feedstock into an oil/wax product, the percentage of volatile matter is desired to be high as this relates to the degree of conversion possible for the feedstock. The fixed carbon and ash content directly relate to the minimum amount of char that can be expected for the pyrolysis of the feedstock (Nunes *et al*., 2018). The source of the ash is the inorganic fraction of the feedstock. The presence of inorganics is usually due to additives (such as fillers, plasticisers, stabilisers and colourants (Callister & Rethwisch, 2011)) used in the plastic product processing.

2.2.2.2 Types of pyrolysis and reactors

Pyrolysis type is usually defined as either slow, fast or intermediate. Slow pyrolysis is characterised by low heating rates of 10-100 °C/min (Gao, 2010). Fast pyrolysis is characterised by very fast heating rates of up to 1000 °C/min (Gao, 2010). Additionally, fast pyrolysis is often associated with very short volatile residence times of about 0.5-5 s (Gao, 2010; Bridgwater, 2012) in order to limit secondary cracking of the volatiles, and therefore limit the formation of gas while promoting the production of the oil/wax fraction. Intermediate pyrolysis is characterised by heating rates between that of slow and fast pyrolysis and/or with an intermediate volatile residence time of about 10 to 30 s (Bridgwater, 2012).

The type of reactor is selected based on the type of pyrolysis process, i.e. the type of reactor determines the type of pyrolysis by typically effecting the heating rate and volatile residence time by facilitating differing degrees of heat and mass transfer. For example, a reactor that employs mixing will result in better heat and mass transfer and therefore a faster heating rate of the particles and shorter volatile residence time. The two most widely used reactors for plastic pyrolysis, as observed from literature studies, are semi-batch reactors (Williams & Williams, 1997; Demirbas, 2004; Miandad *et al*., 2016a) and continuous reactors (e.g. rotary kiln, auger or fluidised bed) (Williams & Williams, 1999a; Liu, *et al*., 2000; Kaminsky *et al*., 2004).

In semi-batch reactors the plastic feedstock is placed inside the reactor before heating begins. The reactor is then heated at a fixed heating rate to the desired temperature. The volatiles produced are continuously removed with an inert fluidising medium (or via vacuum suction). This type of process can be operated at conditions corresponding to either slow or intermediate pyrolysis, typically characterised by low heating rates of 10-100 ℃/min and feedstock residence times of more than 20 min (Williams & Williams, 1999a). Semi-batch reactors are more suited for bench scale experiments than for pilot-scale or industrial scale and their advantages include more control over process parameters and quantification of products, while their disadvantages include that they are labour intensive and require frequent recharging (Wong *et al*., 2015).

In a continuous reactor, the plastic feedstock is continuously fed into the reactor, which is already at the desired temperature, making this type of reactor more suited to industrial scale applications than semi-batch reactors. In the case of a fluidised bed (Figure 2.2), the inert fluidising gas is pre-heated and flows in at the bottom of the reactor, which then fluidises the small plastic particles (particle size < 5 mm) together with a fluidising medium, such as sand. The volatiles exit the reactor at the top with the fluidising gas. The fact that the small plastic particles are introduced into an already hot reactor and rapidly mixed with the hot sand, means that the heating rates (of the feedstock) in fluidised beds are fast (up to 1000 ℃/min) (Wong *et al*., 2015). Typically, the residence times of the volatiles in the reactor are also short (< 1 s to a few minutes) (Williams & Williams, 1999a). Disadvantages of the fluidised bed include the design complexity of the reactor and scaling difficulties particularly with the processing of plastics, which can agglomerate with the sand and cause de-fluidisation of the bed (Aguado, 2003).
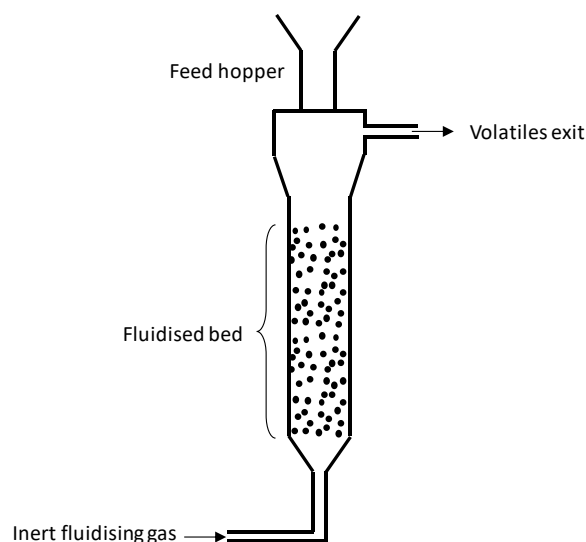
Figure 2.2: Simplified schematic of a fluidised bed reactor (adapted from Williams and Williams (1999a))

Another type of continuous reactor used in plastic pyrolysis is the rotary kiln reactor. The plastic feedstock is charged continuously into the hot reactor, which moves the plastic to the exit by rotation and with the help of baffles on the inside of the reactor and/or inclination of the reactor (Chen *et al*., 2014). This type of reactor is expected to have higher heating rates (of the plastic feedstock) than semi-batch reactors because it is already at the desired temperature when the feedstock is charged, and it facilitates mixing inside the reactor by the rotation action. However, it is also expected to have lower heating rates than a fluidised bed reactor because the mixing in the rotary kiln will not be as efficient as in the fluidised bed resulting in heat transfer limitation. Therefore, pyrolysis in a rotary kiln can be considered as an intermediate type, with expected heating rates between that of semi-batch and fluidised bed of ±100 °C/min (Chen *et al*., 2014). The rotary kiln is frequently used in industry because its robust design ensures that many different feedstock can be processed, whether it be heterogeneous or have a larger particle size (Chen *et al*., 2014).

2.2.2.3 Temperature and heating rate

Temperature is considered as the parameter that has the greatest effect on pyrolysis results and has also been the most studied parameter (López *et al*., 2011; Sharuddin *et al*., 2016). The heating rate is the rate at which the feedstock is heated from ambient temperature to the final pyrolysis temperature. The two parameters are explained together in this section as they have an integrated relationship in the pyrolysis process.

The temperature affects the reaction kinetics with faster rate of reaction at higher temperatures due to increased instability of chemical bonds (Fogler, 2014; Gao, 2010). The relationship between reaction conversion rate and temperature is typically analysed using thermogravimetric analysis (TGA) (Sharuddin *et al*., 2016). TGA measures the mass loss of a feedstock sample (under simulated pyrolysis

conditions) as a function of temperature. With TGA the pyrolysis of very small samples (μg to mg-scale) can be investigated and therefore the effect of heat and mass transfer is eliminated, giving a more accurate representation of the reaction kinetics. The derivative of the resulting TGA curve is known as the DTG curve and corresponds to the conversion rate (mass loss per time). TGA can be used to identify the temperature range within which the plastic feedstock will degrade. This range has been found to be different for different plastics. For example, at a heating rate of 40 °C/min, PS degrades within 400 to 460 °C, and LDPE degrades within 415 to 510 °C (Diaz-Silvarrey & Phan, 2016).

Figure 2.3 presents a simplified DTG curve at different heating rates. As the heating rate increases, the maximum rate of degradation increases (peaks of curves) due to more mass degrading at higher temperatures. The temperature at which maximum degradation occurs increases as the heating rate increases due to heat transfer limitation at higher heating rates (Brems *et al*., 2011) and this is not an indication of a change in the reaction kinetics.
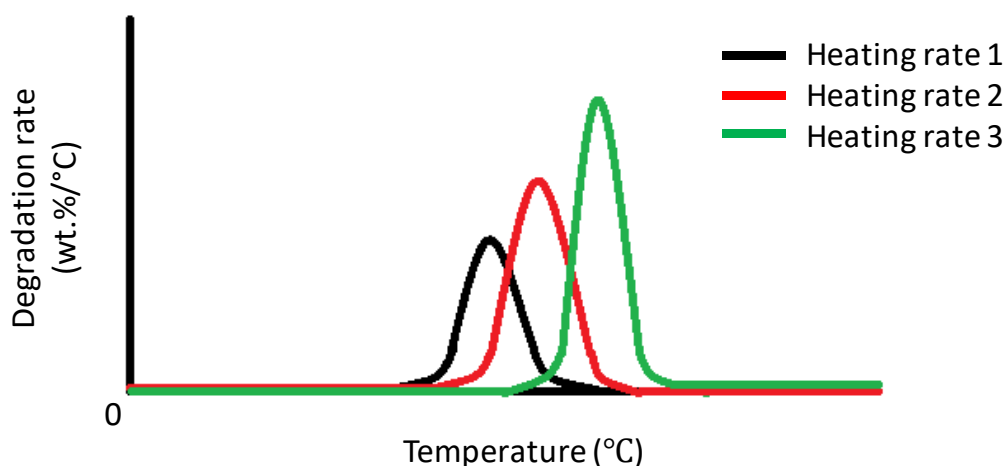
Figure 2.3: Simplified DTG curves (heating rate 1 < heating rate 2 < heating rate 3) (Adapted from Diaz-Silvarrey and Phan (2016) and Kim and Kim (2004))

From the above discussion, the conclusion can be drawn that with higher temperatures and faster heating rates, faster degradation of the plastic feedstock will be promoted. Additionally, it should be noted that if the rate of degradation is slower, then the feedstock will need longer residence times in order to be completely converted to volatiles.

Temperature has also been found to affect the mechanism of thermal degradation, which would result in different product distributions at different temperatures. When temperature increases, cracking of the different types of bonds in the plastic feedstock is promoted, which leads to a reduction of the mass of the char residue. At relatively high temperature, extensive cracking produces smaller primary and secondary volatile products, resulting in increased gas and decreased wax yield (Gao, 2010). Here, the primary volatiles are defined as the first volatile compounds that are formed. Reactions of these

primary volatiles (before exiting the hot part of the reactor) produce secondary products. Therefore, an optimum temperature, which will maximise the oil yield by extensive conversion of the char, while limiting gas and wax formation, will exist.

2.2.2.4 Residence time (feedstock)

This parameter describes how long the solid plastic feedstock remains in the reactor. Short residence times can lead to incomplete conversion (especially at low degradation rates at low temperatures and heating rates) and therefore decreased oil yield. In this document, the feedstock residence time is defined as the time that the feedstock spends in the reactor at the final pyrolysis temperature.

2.2.2.5 Residence time (volatiles)

The volatiles residence time describes how long the volatiles, formed from the pyrolysis of the plastic feedstock, remains in the hot part of the reactor. Volatiles remaining for longer periods in the reactor means that there is more time for secondary reactions of the primary volatiles to occur, which will lead to the formation of smaller compounds, resulting in increased gas and decreased wax yield and ultimately decreased oil yield (Williams & Williams, 1999a; Sharuddin *et al*., 2016). While pyrolysis studies with biomass have reported that longer volatile residence times promote the formation of char (Collard and Blin, 2014), that is usually not observed in pyrolysis studies focussing on most kinds of plastics.

2.2.2.6 Particle size

Particle size influences heat and mass transfer. In smaller particles heat and mass transfer is facilitated, which is recommended for uniform heating of the feedstock and fast removal of the volatiles. If the particle sizes are bigger, then the feedstock will take longer to thermally degrade, especially the core of the particle. In the case of plastic, the particle size is less of a factor than with biomass pyrolysis, due the plastic melting into a single cohesive unit, which then promote further heat and mass transfer within the melt. Therefore, the size of the plastic sample is of greater importance than the particle size. In fact, Aguado and Serrano (1999) stated that it has been found by many studies that the surface area and thickness of the plastic sample, affects the thermal degradation rate of the sample, meaning that a larger amount of sample will degrade slower than a small amount.

2.2.2.7 Pressure

Pressure affects the evaporation (boiling point) of compounds. Therefore, in pyrolysis, high pressure will have the effect of inhibiting larger molecules from becoming volatile and facilitating further reactions, resulting in the production of smaller molecules, which is likely to promote gas yield or

decrease the formation of wax. Vacuum pressure would have the opposite effect by facilitating shorter volatile residence times and fewer secondary reactions.

2.2.2.8 Catalyst

Catalysts can be used in pyrolysis processes to improve the reaction kinetics (faster conversion) and to obtain a greater selectivity toward a targeted product (Sharuddin *et al.*, 2016) by changing the pyrolysis reaction mechanism (Wong *et al*., 2015). This can allow the pyrolysis process to be performed at lower temperatures than would be possible with only thermal degradation (Wong *et al*., 2015). However, using a catalyst comes with an additional cost and issues pertaining to the recycling of the catalyst.

2.3 Fuel quality considerations

Conventional petroleum products typically consist of the following compounds (Aguado & Serrano, 1999):

- Paraffins (alkanes): linear hydrocarbons with only single bonds between the carbon atoms, also known as saturated hydrocarbons.

- Olefins (alkenes): Linear hydrocarbons that contain double bonds between some carbon atoms, also known as unsaturated hydrocarbons.

- Naphthenes (cycloalkanes): hydrocarbons containing rings that have only single bonds between the carbons in the rings.

- Aromatics: hydrocarbons containing rings with conjugated double bonds (benzene for instance). Aromatic compounds have a high stability (Aguado & Serrano, 1999; Miandad *et al*., 2016b), which means that the bonds are more difficult to break during thermal degradation. Generally, if the aromatic composition is high, this will have the effect of decreased combustion efficiency and increased toxic emissions and soot formation (Zetterdahl *et al.*, 2017). However, the presence of aromatics in jet fuels are considered beneficial as they prevent leaks (Hemighaus *et al.*, 2006). Commercial gasoline is limited to 35 vol% aromatic compounds (SANS 1598, 2006). Commercial diesel and marine grade diesel have been reported to have an aromatic concentration of 4 to 5 vol% and 20 to 30 vol% respectively (Zetterdahl *et al*., 2017). Aromatic compounds in fuels are either mono-aromatic or poly-aromatic. Compounds containing benzene rings that are fused together are known as polycyclic aromatic hydrocarbons (PAH). PAH compounds are undesirable in fuels because they cause

emissions that are harmful to the environment, with some PAH's being carcinogenic.

- Compounds containing sulphur (S), oxygen (O), or nitrogen (N): It is desired to minimise the concentrations of these compounds in fuel products as the presence of S and N causes SO_x and NO_x emissions respectively during combustion, while the presence of O affects its calorific value and possibly other properties such as its stability and acidity.

Hydrocarbon fuels are classified according to their boiling point ranges. The SABS standard for gasoline (SANS 1598, 2006) specifies gasoline as having a maximum final boiling point of 210 °C. The SABS standard for diesel (SANS 342, 2006) specifies the maximum boiling point where 95 vol% of the fuel is recovered at 360 °C. Plastic pyrolysis typically produces oil products that can be classified as a mixture of gasoline and diesel (Kunwar *et al*., 2016).

In order to better understand the influence of different conditions on the pyrolysis mechanism and estimate the gasoline/diesel proportions of the pyrolysis products, based on the number of carbons of the compounds, some researchers characterise the oil/wax product using GC/MS. Though carbon number is correlated with boiling point (e.g. when comparing alkanes, an increased carbon-number results in a higher boiling point), the structure of the compounds also influences the boiling point. The carbon number of gasoline can be considered to be C_3-C_{12}, while that of diesel can be considered as C_8-C_{20} (Fahim *et al*., 2010; Speight, 2015).

However, boiling point is not enough to classify a hydrocarbon fuel as suitable for commercial use. To this end, quality specifications as set out by the SABS standards for gasoline (SANS 1598, 2006) and diesel (SANS 342, 2006) must be met so that the fuel can be commercialised. Following are some of the properties that are frequently considered:

- Higher heating value (HHV): The HHV determines the energy content of the fuel.

- Ash content: This is a measure of the inorganics present in the fuel.

- Density

- Viscosity: This property indicates the fuels resistance to flow and is usually reported in centiStokes (cSt) (Fahim *et al*., 2010).

- Pour point: This is the lowest temperature at which the fuel flows. This property is especially important in cold climates (Fahim *et al*., 2010).

- Flash point: This is the lowest temperature where enough volatiles are produced at the surface

of the fuel so that it would ignite if an ignition source is present (Fahim *et al*., 2010).

- Octane number (gasoline): This property indicates the knocking tendency of the gasoline fuel. A high octane number is an indication that the fuel can resist auto-ignition when compressed, which is an important ability in spark-ignition engines (Fahim *et al*., 2010).

- Cetane number (diesel): The cetane number indicates the auto-ignition ability of diesel. A high cetane number indicates that the fuel will readily combust when compressed, which is an important feature for diesel fuels (Fahim *et al*., 2010).

When plastic waste is predominantly composed of hydrocarbons, oil from pyrolysis conversion have been found to have Higher Heating Values (HHVs) comparable to that of gasoline (43.4-46.5 MJ/kg) and diesel (42.8-45.8 MJ/kg), which make them attractive for fuel applications (Sharuddin *et al*., 2016). However, the pyrolysis oils are not expected to have the quality required for application as commercial fuel in high speed automobile engines as set out by standards such as SANS 342 (diesel) and SANS 1598 (gasoline). The lower quality of pyrolysis oil can be due to various reasons for example: the contamination can introduce inorganics, which will increase ash content; a high proportion of aromatic compounds can be produced during pyrolysis, which has been correlated with soot formation during combustion (Zetterdahl *et al*., 2017). Additionally, the production of long hydrocarbon chains will translate to a higher viscosity than commercial grade gasoline and diesel. The oil can then possibly be used in slower speed engines such as marine engines and power plant engines that can handle a lower quality fuel (Speight, 2015; Kalargaris *et al*., 2017). For applications as transportation fuel, the pyrolysis conversion should be optimised to produce an oil following SABS standards and, if the quality is not good enough, blending the oil with commercial grade fuel or upgrading in a refinery can be considered (Miandad *et al*., 2016a; Kalargaris *et al*., 2017).

2.4 Pyrolysis of polystyrene single-layer plastic packaging

One of the two types of waste plastic packaging of interest in this study is a polystyrene single-layer. Particularly of interest in this study is the black polystyrene punnets used to package raw meat. This section deals with the following aspects pertaining to the pyrolysis of this feedstock: characterisation of the plastic feedstock; thermal degradation mechanism; effect of pyrolysis operating conditions on the product yields (oil/wax, gas and char); and the composition and fuel properties of the volatile products. The operating conditions that are studied most frequently and that will be focussed on are the pyrolysis temperature, the heating rate, the feedstock residence time and the volatile residence time. The purpose of this discussion will be to determine the suitability of the PS punnets as pyrolysis feedstock, and to identify ranges of operating conditions to be studied experimentally for

optimum oil or oil/wax yield and composition.

2.4.1 Feedstock characterisation

2.4.1.1 Structure

Polystyrene (PS) is formed by the polymerisation of the monomer unit, styrene, as shown in Figure 2.4. Each monomer unit consists of a benzene ring attached to a two carbon chain. PS is classified as a thermoplastic, i.e. it melts and flows when heated and upon cooling will harden again (Kotz *et al.*, 2009). It is also classified as an addition polymer, i.e. it is manufactured by the direct addition of the monomer units (Kotz *et al.*, 2009). PS melts at a temperature of 240°C (Callister & Rethwisch, 2011).
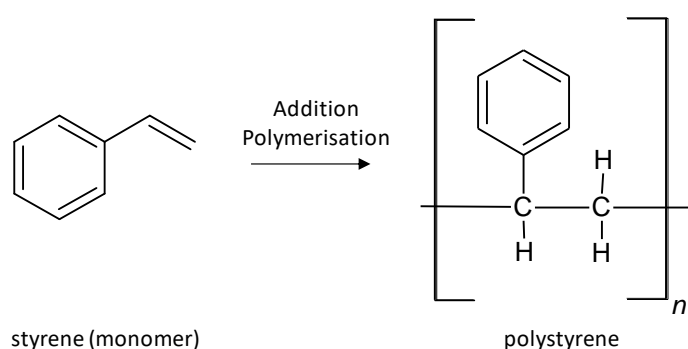
Figure 2.4: Polystyrene formed from the addition polymerisation of the styrene monomer (adapted from Callister and Rethwisch (2011))

2.4.1.2 Ultimate, proximate and energy content analysis of polystyrene

Properties of polystyrene samples as have been determined by various studies are summarised in Table 2.1, in terms of the ultimate, proximate and energy analysis. Based on the structure of PS (Figure 2.4), pure PS consists of only C (92.3 wt.%) and H (7.7 wt.%). However ultimate analysis showed that the actual elemental composition of waste samples differed slightly from the theoretical values. This difference can be due to the presence of additives (Diaz-Silvarrey & Phan, 2016), and/or contamination from waste. However, the samples were still largely of a hydrocarbon nature (> 95 wt.%), making it useful for energy application. This was confirmed by the HHVs of the samples (38.2-42.1 MJ/kg) as given in Table 2.1, which were only slightly lower than that of conventional diesel (42.8-45.8 MJ/kg) (Sharuddin *et al.*, 2016).

The proximate analysis (Table 2.1) indicated a low moisture content, which is beneficial from an energy efficiency and fuel quality standpoint. The volatile matter was high (98.5-99.6 wt.%), which is desirable for a pyrolysis process targeting the oil/wax product. The fixed carbon and ash content correlate with the minimum amount of char that can be achieved (Nunes *et al.*, 2018) and as these values were found to be quite low (< 1.5 wt.%), very little char is expected to be produced.

Table 2.1: Ultimate and proximate analysis, and energy value of PS

	Parameter	Value	References
Ultimate analysis (wt.%) dry, ash free basis	**C**	92.3 89.5-92.7	Based on pure PS structure (Park *et al.*, 2012; Diaz-Silvarrey & Phan, 2016)
	H	7.7 7.2-8.5	Based on pure PS structure (Aboulkas *et al.*, 2011; Diaz-Silvarrey & Phan, 2016)
	N	0 0.0-3.0	Based on pure PS structure (Park *et al*., 2012; Diaz-Silvarrey & Phan, 2016)
	S	0 0.0	Based on pure PS structure (Park *et al*., 2012)
	O*	0 0.0-0.5	Based on pure PS structure (Park *et al*., 2012; Diaz-Silvarrey & Phan, 2016)
Proximate analysis (wt.%)	**Moisture**	0.30-1.4	(Park *et al.,* 2012; Diaz-Silvarrey & Phan, 2016)
	Volatile compounds	98.5-99.6	(Park *et al*., 2012; Aboulkas *et al*., 2011; Diaz-Silvarrey & Phan, 2016)
	Ash content	0.0	(Park *et al*., 2012; Aboulkas *et al*., 2011; Diaz-Silvarrey & Phan, 2016)
	Fixed carbon	0.2-1.5	(Park *et al*., 2012; Aboulkas *et al*., 2011; Diaz-Silvarrey & Phan, 2016)
Energy value	**HHV (MJ/kg)**	38.2-42.1	(Park *et al*., 2012; Diaz-Silvarrey & Phan, 2016)

* by difference

2.4.1.3 Thermal degradation behaviour

As stated in Section 2.2.2.3 different plastics degrade within different temperature ranges and these ranges can be determined via mg-scale pyrolysis using TGA. The results obtained from pyrolysis using TGA are likely to be reaction limited instead of heat/mass transfer limited as the sample size is mg-scale. This is especially relevant at slower heating rates, which ensure small temperature gradients within the sample analysed (Brems *et al*., 2011). Therefore, TGA is often performed at heating rates between 5 and 20 °C/min. TGA results for PS, as has been determined by various researchers, illustrate that PS degrades in a single step (one single DTG peak) and the minimum temperature range in which it will degrade is 360-380 °C (Table 2.2). Below this temperature, there will likely not be enough energy for the endothermic pyrolysis reaction to happen. PS degrades at a lower temperature than other plastics such as LDPE, HDPE and PP due to the presence of the many tertiary bonded carbons (Pek & Ghosh, 2015). The maximum temperature in Table 2.2 is the temperature at which the degradation rate

is the highest. The temperature range where the maximum degradation rate occurs for PS is 400-430 °C. The maximum temperature can be seen to increase as heating rate increases, which as explained is due to heat transfer becoming the limiting factor at higher heating rates.

Table 2.2: Polystyrene conversion behaviour determined by TGA

Heating rate (°C/min)	Temperature range (°C)	Maximum temperature (°C)	References
10	360-380 (start) 420-480 (end)	400-430	(Diaz-Silvarrey & Phan, 2016; Park *et al*., 2003)
20	369-486	445	(Aboulkas *et al.*, 2011)
40	400-460	460	(Diaz-Silvarrey & Phan, 2016)
50	409-533	463	(Aboulkas *et al.*, 2011)
100	436-553	496	(Aboulkas *et al.*, 2011)

2.4.2 Degradation mechanism

Polystyrene, like other addition polymers, undergoes thermal degradation via a radical chain mechanism (Aguado & Serrano, 1999; Faravelli *et al*., 2001; Singh *et al*., 2019; Ojha & Vinu, 2015). The mechanism can be divided into 3 steps: initiation, propagation, and termination as described in Figure 2.5.

Initiation reactions can be either random scission or chain-end scission. Random scission cracks the hydrocarbon back-bone of the PS polymer chain at a random point forming a primary radical (R_p), and a secondary benzyl radical (R_{sb}). Primary, secondary and tertiary refer to the number of carbon atoms (respectively 1, 2 and 3) attached to the radical. During chain-end scission, the hydrocarbon back-bone is cracked at the end of the chain to form a secondary benzyl radical (R_{sb}) and an alkyl benzene radical (R_a).

The second step, propagation, can happen via H-abstraction (also known as H-transfer) or β-scission (also known as β-cleavage, β-decomposition, or unzipping in the case of monomer formation). H-abstraction describes the transfer of an H-atom to the radical point. It can happen either via intermolecular or intramolecular (also known as back-biting) transfer. During intermolecular abstraction, an H-atom from one molecule is transferred to a radical on another molecule. In Figure 2.5, a primary radical abstracts an H-atom from the tertiary position of a different molecule to form a tertiary radical. During intramolecular abstraction the H-atom that is transferred, and the radical it is transferred to are on the same molecule, which can be a primary or a secondary benzylic radical. During β-scission the C-C bond in the β-position to the radical is cleaved. In Figure 2.5 it is illustrated where

18

the tertiary benzylic radical (R_t) is cleaved to form secondary benzylic radical (R_{sb}) and a polymer with an unsaturated end. β-cleavage is also illustrated in Figure 2.5 where R_{sb} is cleaved to form the PS monomer, styrene, and another R_{sb} with one less monomer unit. This is the major reaction involved in the formation of the styrene monomer during thermal decomposition, i.e. repeated β-scission of R_{sb}.

The propagation reactions are ended with termination reactions. These can be either recombination reactions or disproportionation reactions (which forms an unsaturated end) as depicted in Figure 2.5.

The main products from PS pyrolysis are the PS monomer styrene, ethylbenzene, toluene, α-methylstyrene, and styrene dimers, with these compounds constituting 82-93% (by peak area) of the oil produced in the temperature range of 350-600 °C (Zhang *et al*., 1995; Park *et al*., 2003; Artetxe *et al*., 2015). These compounds are formed via different routes of the mechanism depicted in Figure 2.5. Investigation of the mechanism indicates that the formation of smaller non-condensable species would be limited as the benzene ring is generally stable in the investigated temperature range. All the compounds described above are characterised by boiling points higher than 80.09 °C (Engel & Reid, 2013) and would therefore be condensable at ambient conditions. This indicates that the gas yield will be relatively small. Indeed, based on the structure of PS (i.e. the proportion of benzene rings present), the non-condensable gas yield can be expected to be below a maximum of 24 wt.%.

Propagation: Intermolecular H-abstraction

R_p PS   PS R_t

Propagation: Intramolecular H-abstraction

R_{sb} (or R_p) R_t

Propagation: β-scission

R_t Polymer with unsaturated end R_{sb}

R_{sb} R_{sb} Monomer (styrene)

20
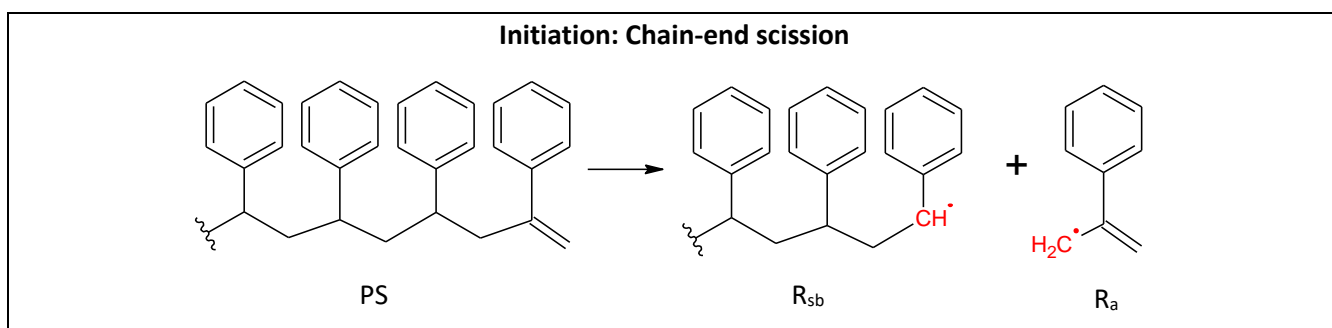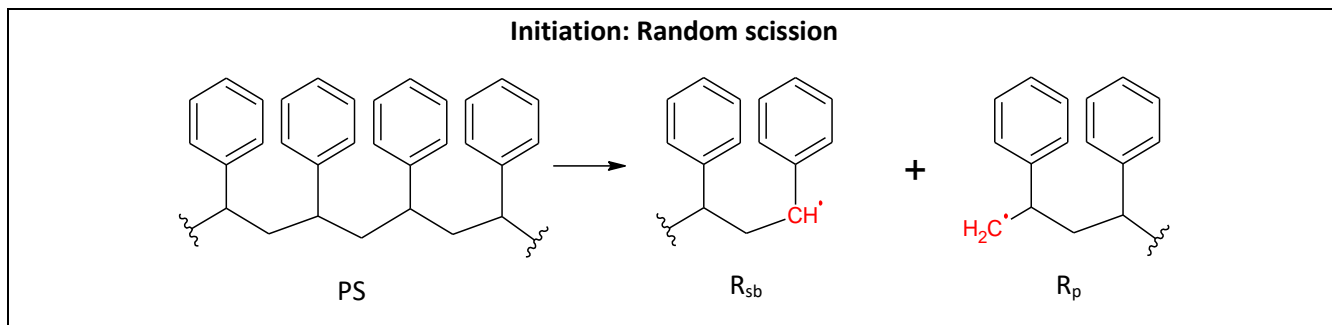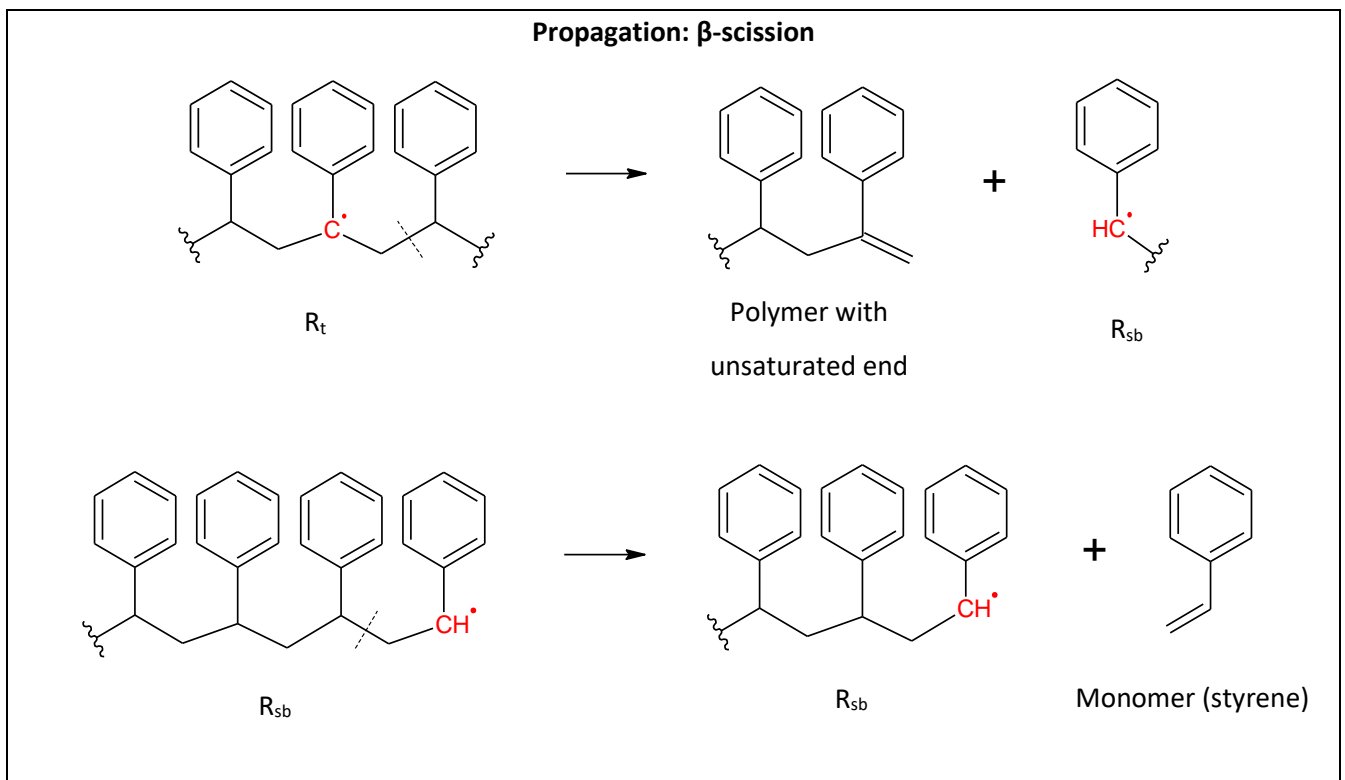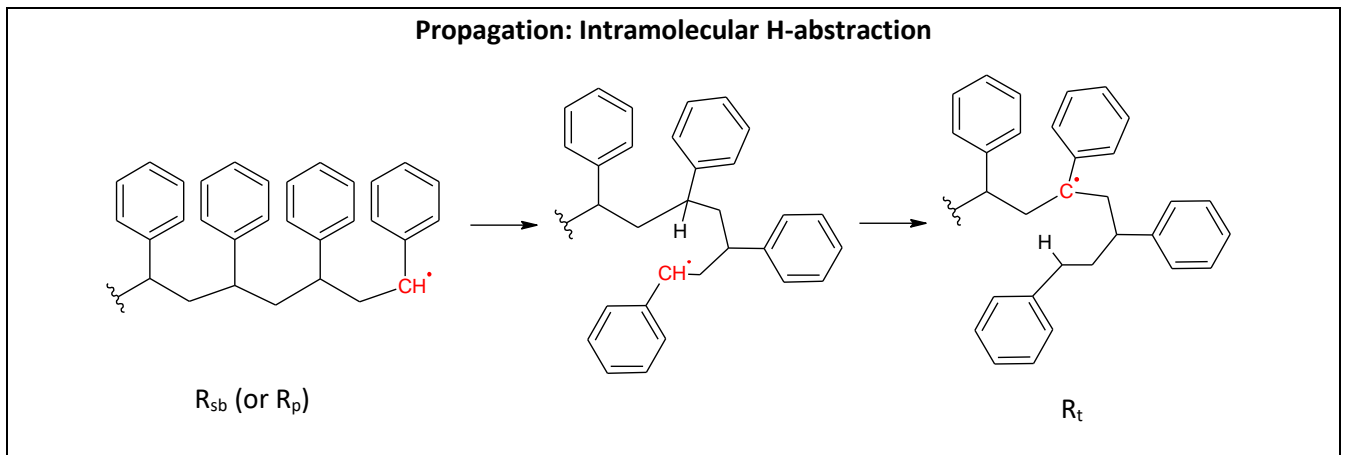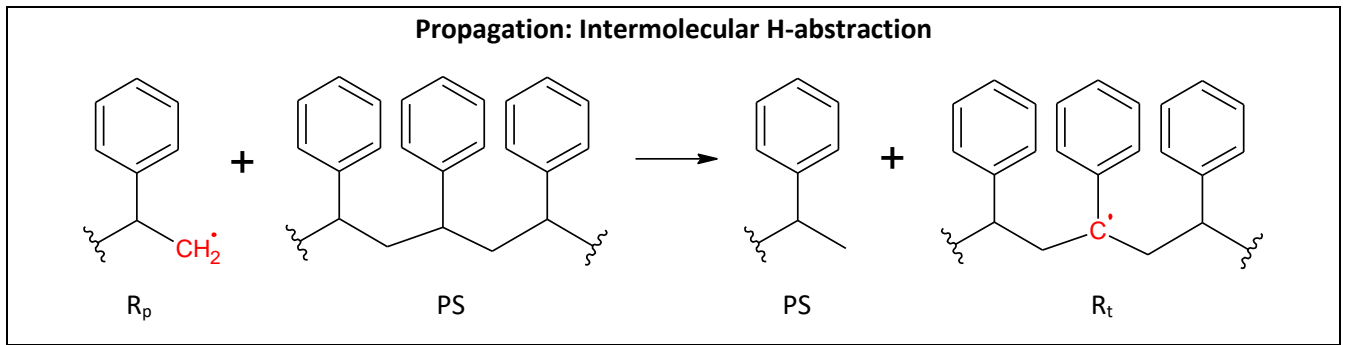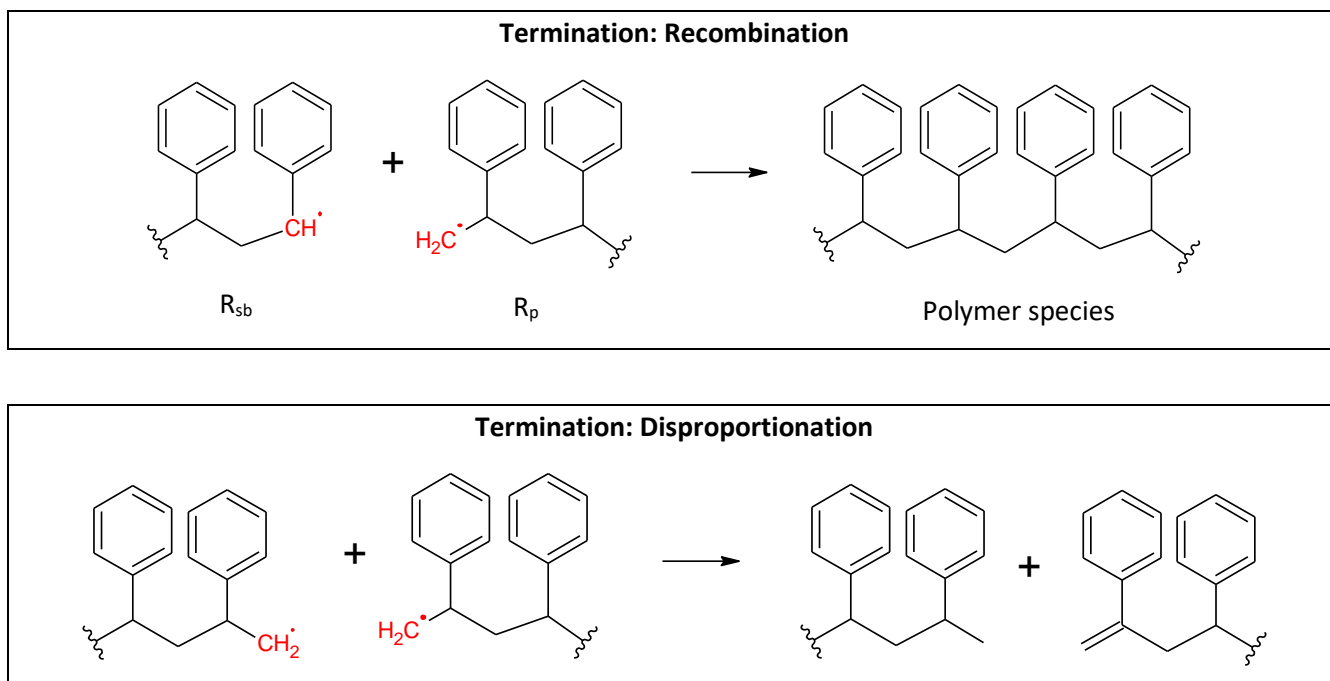
Figure 2.5: Reaction mechanism of polystyrene, adapted from Faravelli *et al.* (2001) *(radical positions indicated in red)*

2.4.3 Effect of operating parameters on product yields

This section focusses on the effect that the operating parameters have on the product yields from PS pyrolysis. The discussion is based on results from various studies as summarised in Table 2.4. The aim of this discussion will be to identify trends in the effects of the operating conditions, to suggest experimental ranges to be investigated for optimum oil or oil/wax yield.

As the three products from plastic pyrolysis are non-condensable gas, char, and an oil/wax fraction, the oil/wax fraction can be maximised by minimising the gas and char fractions. Therefore, in this section, the effect that the operating parameters have on the gas and char fractions will be discussed first.

2.4.3.1 Char yield

Temperature, heating rate and feedstock residence time have an interacting effect on char yield. Temperature and heating rate affect the rate of feedstock degradation as explained in Section 2.2.2.3, while feedstock residence time describes the time available for degradation to occur. For example, a higher temperature and heating rate will result in a faster degradation rate, which in turn will mean that a shorter feedstock residence time will be adequate for complete degradation of the feedstock. The feedstock residence time necessary for complete degradation is discussed further in Section 2.4.3.3.

The char yield has been reported to decrease and then become constant (when complete degradation is achieved) during a PS pyrolysis process and negligible char (< 5 wt.%) yields were reported (Williams & Williams, 1997, 1999b; Kaminsky *et al*., 2004; Shah & Jan, 2014; Miandad *et al*., 2016b).

21

This corresponds well with the low ash and fixed carbon contents of PS (Table 2.1), which indicated that the minimum char yield possible during complete conversion of the samples, would be negligible.

With feedstock such as biomass, it has been observed that long volatile residence time can lead to the recombination of some volatiles to form a heavier product, which is no longer volatile, thus resulting in the formation of additional char (Collard & Blin, 2014). Contrary to this trend, the effect of volatile residence time on char yield from PS pyrolysis has been found to be negligible. Mo *et al*. (2014) studied an inert gas (N_2) flow rate in the range of 50-200 mL/min (with the low and high ends giving longer and shorter volatile residence times respectively) and its effect on oil yield via a Box-Behnken experimental design in a semi-batch reactor. Statistical analysis of the results obtained in this study indicated a non-significant effect of the volatile residence time on oil yield (in the temperature range of 375-525 ℃) with a p-value of 0.42 for the linear effect. Therefore, as the oil yield did not decrease with increasing volatile residence time, the results also indicated that char yield did not increase with a longer volatile residence time in this range.

From this discussion the conclusion can be made that the char yield will be very small (< 5 wt.%) and is consistent with ash and fixed carbon yields from proximate analysis, as long as the feedstock residence time is long enough to ensure complete conversion at the operating temperature (which should be above the minimum degradation temperature as indicated by TGA) and heating rate.

2.4.3.2 Gas yield

Both temperature and volatile residence time are known to affect the gas yield during pyrolysis. Higher temperatures are known to increase primary cracking and secondary reactions, the latter being especially promoted at longer volatile residence times, which result in increased gas production (as explained in Sections 2.2.2.3 and 2.2.2.5).

To investigate the effect of temperature on the gas yield, Liu *et al*. (2000) performed pyrolysis experiments with PS in a fluidised bed reactor in the temperature range of 450-700 ℃. It was found that the gas yield increased from < 0.4 to 3.5 wt.% when the temperature was increased from 450 to 700 ℃. Similar yields at 700 ℃ of 3.4 wt.% (in a semi-batch reactor) and < 2 wt.% (in a fluidised bed reactor) were reported elsewhere (Williams & Williams, 1997, 1999b). Therefore, these studies suggest that temperature has a small increasing effect on gas yield with less than 5 wt.% gas yield being expected even at the high temperature of 700 ℃.

Table 2.4 also references studies by Miandad *et al*. (2016b) and Shah and Jan (2014) in which higher gas yields of 16.1 wt.% and 20.4±0.72 wt.% respectively were obtained at 500 ℃. However, these studies calculated the gas yield by difference (i.e. gas wt.% = 100 wt.% - oil wt.% - char wt.%) and

Miandad *et al*. (2016b) reported to operate at a relatively high nitrogen flowrate of 30 L/min. This indicates that the high gas yields reported could be the result of entrained volatiles in the condensation system, instead of actual non-condensable gasses. This is different to the studies done by Williams and Williams (1997, 1999b) and Liu *et al.* (2000) (discussed in previous paragraph), who determined the gas yield using GC-analysis of the gas product with a calibrated method.

In terms of the effect of volatile residence time on the gas product yield, Williams and Williams (1997, 1999b) studied the pyrolysis of PS in a fluidised bed at 700 °C but at different volatile residence times in the heated zone of the reactor: 15s, and 25s respectively. The gas yields obtained were as follows for the different volatile residence times: < 2 wt.% at 15 s, and 3.41 wt.% at 25 s. Therefore, the effect of volatile residence time on the gas yield seems to be negligible in this range. Furthermore, as the temperature studied was high (700 °C), it strengthens the argument that volatile residence time either effects the gas yield only a little or not at all, as secondary cracking is expected to be more pronounced at higher temperatures.

Additionally, as was explained for the char yield (Section 2.4.3.1), for the study done by Mo *et al*. (2014), the volatile residence time was found to have a non-significant effect on the oil yield which then also indicates a non-significant effect on the gas yield in the range studied. Indeed, significant cracking of the oil product would have resulted in increased gas yield. This conclusion is also indicated by Park *et al*., 2003, who found an oil yield of 96.7 wt.% at a temperature of 480 °C and a very long volatile residence time of 33min after complete degradation, indicating a combined char and gas yield of 3.3 wt.%.

To summarise the insights gained from literature on gas yield during PS pyrolysis, it is indicated that temperature has a small increasing effect on gas yield and that volatile residence time has a small to non-significant effect up to 700 °C. This makes sense as the degradation mechanism (Section 2.4.2) suggests that the formed volatile compounds will predominantly contain at least one benzene ring, which is stable at temperature as high as 700 °C (Collard & Blin, 2014), making these compounds condensable at ambient conditions. Previous studies indicate that the gas yield can be expected to be less than 5 wt.% (as discussed above), while from a theoretical standpoint, based on the chemical structure of PS, it can be expected that the gas yield will be no more than 24 wt.%.

2.4.3.3 Oil/wax yield

The research consulted suggests the condensable fraction from PS pyrolysis is only oil and the formation of wax is not indicated (Mo *et al.*, 2014; Miandad *et al.*, 2016b). Therefore, from here on the condensable fraction will be referred to as the oil product instead of the oil/wax product. As the

three products from plastic pyrolysis are non-condensable gas, char, and an oil fraction, the oil fraction can be maximised by minimising the gas and char fractions. In Section 2.4.3.1 it was seen that the char yield is influenced by temperature, heating rate, and feedstock residence time. It was concluded that the char yield can be minimised by allowing enough feedstock residence time to ensure complete degradation of the PS at the specific temperature and heating rate. Generally during pyrolysis it is expected that the gas yield will increase significantly with increasing temperatures and longer volatile residence times, but from the studies discussed in Section 2.4.3.1, it was seen that temperature and volatile residence time had a small to insignificant effect on gas yield in the studied ranges, which were 450-700 °C and 15 s-33 min respectively. However, a smaller gas flow rate (resulting in longer volatile residence time) could be indicated as it would limit entrainment of condensable volatiles and allow efficient condensation.

From this discussion it would make sense, that to optimise oil yield during PS pyrolysis, the temperature, heating rate and feedstock residence time must be optimised. It is expected that as temperature and feedstock residence time increase, the oil yield will increase (because the char yield is decreasing due to more complete degradation) and at some point, reach a maximum or plateau point, after which it may start to decrease if sufficiently high temperatures are reached. This is confirmed by Park *et al.* (2003), who studied the oil yield evolution with temperature and feedstock residence time. In this study, PS samples of 200 g were pyrolyzed in a stirred semi-batch reactor in a temperature range of 350-480 °C and an intermediate heating rate of 116-160 °C/min. The study found that for temperatures greater than 400 °C, an oil yield plateau is reached in less than 30 min of feedstock residence time, with a maximum oil yield of 96.7 wt.% at 480 °C after approximately 15 min feedstock residence time.

Miandad *et al.* (2016b) performed experiments with 1 kg of PS sample in a semi-batch reactor and found that a temperature of 500 °C and a heating rate of 10 °C/min the degradation would be complete after 75 min of feedstock residence time (where the feedstock residence time was counted from when the first volatiles started to form). Different to the study by Park *et al.* (2003) (previous paragraph), was the slow heating rate (10 vs 116-160 °C/min) and the larger sample (1 kg vs 200 g) studied. The slower heating rate would result in slower degradation at lower temperatures and therefore a longer feedstock residence time would be needed for complete degradation. Additionally, as PS plastic melts, a larger sample would result in greater heat and mass transfer limitation and would therefore also require a longer feedstock residence time for complete degradation. Therefore, for smaller samples (< 200 g) and intermediate heating rates (> 100 °C/min), complete degradation could be achieved within 30 min for temperatures above 400 °C. For larger samples (> 1 kg), and low heating rates (10 °C/min), complete degradation could take up to 75 min for temperatures up to 500 °C.

Additionally, it was argued in Sections 2.4.3.1 and 2.4.3.2, that the char yield will be less than 5 wt.% after complete degradation and that gas yields of less than 5 wt.% have been found by various researchers. Therefore, the combined char and gas yield will be less than 10 wt.%, which would result in an oil yield of more than 90 wt.%. This high oil yield has indeed been achieved by various researchers (Williams & Williams, 1999b; Park *et al.*, 2003; Mo *et al.*, 2014), and from the discussion of the various literature studies, it is expected to be achieved at temperature greater than 400 ℃, intermediate to fast heating rates (100-1000 ℃/min), and with feedstock residence time long enough to ensure complete degradation.

2.4.4 Product quality and component distribution

This section discusses the composition of the oil and gas, and also investigates the quality of the products for fuel applications in terms of the HHV and other properties. Additionally, application of these products as fuel is considered.

The gas product is mainly composed of C_1-C_4 hydrocarbons including alkanes and alkenes, with the alkenes typically being more abundant than the alkanes (Williams & Williams, 1997, 1999b; Artetxe *et al.*, 2015). Williams and Williams (1997, 1999b) also reported the production of H_2 as part of the gas fraction which increased with increasing temperature. All the components in the gas fraction have an HHV greater than 45 MJ/kg as presented in Table 2.3, which makes the gas product valuable for its energy content as it is similar to the energy value in natural gas (López *et al.*, 2011). For instance, the heat produced from its combustion can be recycled back to the pyrolysis process (Williams & Williams, 1997; Angyal *et al.*, 2007). However, the gas yield is expected to be very low (< 5 wt.%) as previously discussed. The heat required for the pyrolysis of PS (including temperature change, melting, and reaction) was experimentally estimated by Brems *et al.* (2011) as 0.68 MJ/kg.

As for the oil fraction, most studies reported the predominant components as the aromatic compounds styrene, ethylbenzene, toluene, α-methylstyrene (with one benzene ring), and styrene dimers (with two benzene rings). These compounds constituted 82-93 % (by peak area) of the oil in the temperature range of 350-600 ℃ (Zhang *et al.*, 1995; Park *et al.*, 2003; Artetxe *et al.*, 2015). Various styrene dimers have been reported, such as 1,3-diphenyl propane, 1,2-diphenyl ethylene, and 1,1-diphenyl-1,3-butadiene (Artetxe *et al.*, 2015; Zhou *et al.*, 2016) among others.

Many researchers have studied the optimisation of the styrene yield from PS pyrolysis as styrene is by far the most abundant product, with yields of 40.00-81.54 wt.% being reported (Park *et al.*, 2003; Mo *et al.*, 2014; Artetxe *et al.*, 2015; Zhou *et al.*, 2016; Ojha & Vinu, 2015). Indeed, it is a valuable chemical as it is the monomer used in PS production. The styrene yield was found to increase and then

decrease as temperature and volatile residence time increased (Mo *et al*., 2014; Artetxe *et al*., 2015). The studies evidenced that at low temperatures (375-450 ℃) and short volatile residence times, the formation of styrene oligomers (dimer and trimer) were favoured. As the temperature and volatile residence time increased (to approximately 500 ℃), secondary cracking of the oligomers resulted in an increase in styrene yield. When the temperature and volatile residence time were further increased (500-600℃), there was lower selectivity towards styrene and increased proportion of toluene, ethylbenzene and α-methylstyrene (Mo *et al*., 2014). The maximum styrene yield of 64.52-81.54 wt.% has been found in the temperature range of 470-600 ℃ (Mo *et al*., 2014; Artetxe *et al*., 2015; Zhou *et al*., 2016; Ojha & Vinu, 2015).

The HHV of the oil, produced within the temperature range of 400-500 ℃, has been reported to be 37.85-42.59 MJ/kg (Miandad *et al*., 2016b), which is similar to that of the PS feedstock at 38.2-42.1 MJ/kg (Park *et al*., 2003; Diaz-Silvarrey & Phan, 2016) and slightly lower than that of conventional gasoline and diesel at 43.4-46.5 MJ/kg and 42.8-45.8 MJ/kg respectively (Sharuddin *et al*., 2016). The oil from PS pyrolysis has also been found to be similar to that of conventional diesel in terms of some other properties such as viscosity, density, freezing point and pour point (Miandad *et al*., 2016b). However, typically the properties of the oil for fuel applications were not reported as most studies focussed on the recovery of chemicals from PS via pyrolysis and not the production of fuel. As such, the influencing trends of operating parameters, such as temperature, on the oil properties for fuel applications, such as HHV, cannot be conclusively stated.

Even though the PS oil has a high HHV, it has some characteristics that would make it less valuable for fuel applications. Particularly, as stated in the previous paragraph, the oil is predominantly composed of aromatic compounds, which have an adverse effect on fuel quality as it is correlated with soot formation during combustion (Zetterdahl *et al*., 2017).

In addition, Williams and Williams (1999b) reported a polycyclic aromatic hydrocarbon (PAH) concentration in the oil of 0.08 wt.% at 500 ℃, which increased to 0.77 wt.% at 700 ℃, while Ojha and Vinu (2015) reported a PAH concentration (indene- and naphthalene derivatives, phenanthrene, and anthracene) of 0.78 wt.% at a temperature of 500 ℃, which increased to 4.73 wt.% at a temperature of 700 ℃ (10.86 wt.% yield at 800℃). This is important as some PAH's have been found to be carcinogenic (Williams & Williams, 1999b) and the SABS standard for diesel (SANS 342, 2006) specifies its maximum content in commercial grade diesel as 8 wt.% and therefore operating at a temperature higher than 700 ℃, can increase the risk of exceeding this limit. However, it is likely that in the studies mentioned here that some of the PAH were not detectable by GC, making these numbers minimum amounts that have been quantified.

Due to the high aromatic content, researchers have suggested blending of the pyrolysis oil with conventional fuel to make it more suitable commercially (Miandad *et al*., 2016b). Commercial gasoline is limited to 35 vol% aromatic compounds (SANS 1598, 2006). Commercial diesel and marine fuel diesel have been reported to have an aromatic concentration of 4 to 5 vol% and 20 to 30 vol% respectively (Zetterdahl *et al*., 2017).

Table 2.3: HHV of hydrocarbon gaseous compounds (Çengel & Boles, 2008; Engel and Reid, 2013)

Gaseous compound	HHV (MJ/kg)
H_2	141.80
Methane (CH_4)	55.53
Ethane (C_2H_6)	51.90
Ethylene (C_2H_4)	50.30
Acetylene (C_2H_2)	49.97
Propane (C_3H_8)	50.33
Propene (C_3H_6)	48.91
Butane (C_4H_{10})	49.15
1-Butene (C_4H_8)	48.44
Pentane (C_5H_{12})	49.00
1-Pentene (C_5H_{10})	47.76
Hexane (C_6H_{14})	48.31
Hexene (C_6H_{12})	47.50

Table 2.4: Results from literature studies on the pyrolysis of PS

Reactor	Temperature (°C)	Heating rate (°C/min)	Feedstock residence time (min)	Volatile residence time/ N$_2$ flow rate	Oil yield (wt.%)	Gas yield (wt.%)	Char yield (wt.%)	References
Semi-batch (1 kg sample)	400/450/500	10	75	54 s 30 L/min N$_2$ flow	76.0/80.8/78.7	8.0/13.1/16.8	16.0/6.1/4.5	Miandad *et al.* (2016b)
	450		60/75/120		79.0/80.8/80.7	11.9/13.1/14.1 (by difference)	9.1/6.1/5.3	
Semi-batch	345-525	10-40	NR	50-200 mL/min N$_2$ flow	60.84-91.68	NR	NR	Mo *et al.* (2014)
Stirred semi-batch (200 g sample)	350-480	116-160	< 5-55	33 min 30 mL/min N$_2$ flow	24.3-96.7	NR	NR	Park *et al.* (2003)
Semi-batch (15 g sample)	350	NR	3h	50 mL/min N$_2$ flow	80.1	NR	NR	Zhang *et al.* (1995)
Semi-batch	700	25	NR	25 s 0.2 L/min N$_2$ flow	83.77	3.41 (by GC-analysis)	3.50	Williams and Williams (1997)
Semi-batch (5 g samples)	500	NR	150	NR	78.07±0.64	20.40±0.72 (by difference)	1.53±0.61	Shah and Jan (2014)
Fluidised bed	500-700	NR	NR	< 15 s 34 L/min N$_2$ flow	79-90	< 2% (by GC-analysis)	negligible	Williams and Williams (1999b)
Fluidised bed (30 kg/h)	580	NR	NR	NR	89.5	9.9	0.6	Kaminsky *et al.* (2004)
Fluidised bed	450-700	NR	NR	0.3 s	97.6-90.2	< 0.04-3.54 (by GC-analysis)	NR	Liu *et al.* (2000)

NR = not reported.

The pressure is at atmospheric, the inert carrier gas is nitrogen, and no catalyst is used.

2.5 Pyrolysis of LDPE and PET multi-layer plastic packaging

In this section, the aspects relating to the pyrolysis of the LDPE/PET multi-layer are discussed. A typical example of packaging that is made from this multi-layer is the plastic film used to package dry dog food (personal communication with PlasticsSA).

2.5.1 Low density polyethylene (LDPE)

2.5.1.1 Feedstock characterisation

2.5.1.1.1 Structure

Polyethylene (PE) is formed from the polymerisation of the monomer unit, ethylene, as shown in Figure 2.6. Low density polyethylene (LDPE) is made of PE chains in a branched structure, giving it a low density, as opposed to high density polyethylene (HDPE), which has more tightly packed structure. Similar to polystyrene, LDPE is classified as both a thermoplastic and an addition polymer. It has a melting point of 115 °C (Callister & Rethwisch, 2011).
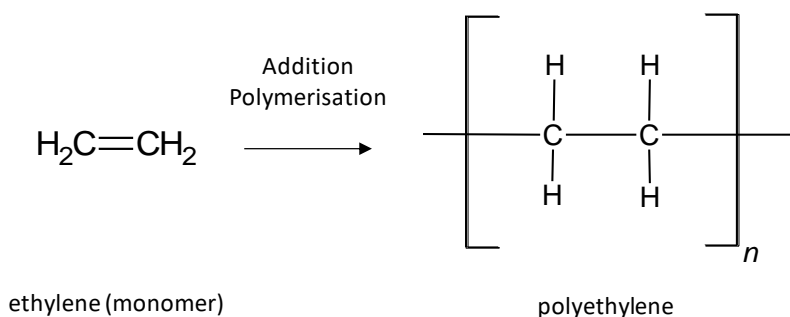
Figure 2.6: Polyethylene formed from the addition polymerisation of the ethylene monomer (adapted from Callister & Rethwisch (2011))

2.5.1.1.2 Ultimate, proximate and energy content analysis of LDPE

Properties of LDPE as reported by various studies are given in Table 2.5. Based on the structure of PE (Figure 2.6), pure LDPE will have a C-content of 85.7 wt.% and an H-content of 14.3 wt.%. Differences from pure LDPE composition as shown in Table 2.5 are due to additives (Diaz-Silvarrey & Phan, 2016) and possible contamination of the samples. However, according to Table 2.5, LDPE samples will still be largely of a hydrocarbon nature (> 95 wt.%), which makes it useful for its energy content, as confirmed by the HHV. The HHV of LDPE (43.1-46.6 MJ/kg) compares favourably with that of conventional gasoline, which has a HHV of 43.4-46.5 MJ/kg and with that of conventional diesel, which has an HHV of 42.8-45.8 MJ/kg (Sharuddin *et al*., 2016).

As with the proximate analysis of PS (Table 2.1), the results for LDPE in Table 2.5 are characterised by high volatile matter (> 99 wt.%) and low moisture, ash and fixed carbon contents, which is favourable for the conversion into an oil/wax product.

Table 2.5: Ultimate and proximate analysis, and energy value of LDPE

	Parameter	Value	References
Ultimate analysis (wt.%) dry, ash free basis	**C**	85.7 83.4-85.9	Based on pure LDPE structure (Park *et al.*, 2012; Diaz-Silvarrey & Phan, 2016; Gunasee *et al.*, 2017)
	H	14.3 14.0-16.3	Based on pure LDPE structure (Park *et al.*, 2012; Diaz-Silvarrey & Phan, 2016; Gunasee *et al.*, 2017)
	N	0.0 0.0-0.1	Based on pure LDPE structure (Park *et al.*, 2012; Diaz-Silvarrey & Phan, 2016)
	S	0.0 0.02-0.1	Based on pure LDPE structure (Li *et al.*, 1999; Park *et al.*, 2012)
	O*	0.0 0.0-0.5	Based on pure LDPE structure (Park *et al.*, 2012; Diaz-Silvarrey & Phan, 2016)
Proximate analysis (wt.%)	**Moisture**	0.0-0.3	(Park *et al.*, 2012; Diaz-Silvarrey & Phan, 2016)
	Volatile compounds	99.2-99.9	(Park *et al.*, 2012; Diaz-Silvarrey & Phan, 2016; Gunasee *et al.*, 2017)
	Ash content	0.0-0.1	(Park *et al.*, 2012; Diaz-Silvarrey & Phan, 2016; Gunasee *et al.*, 2017)
	Fixed carbon	0.0-0.8	(Park *et al.*, 2012; Diaz-Silvarrey & Phan, 2016; Gunasee *et al.*, 2017)
Energy value	**HHV (MJ/kg)**	43.1-46.6	(Park *et al.*, 2012; Diaz-Silvarrey & Phan, 2016; Gunasee *et al*., 2017)

*determined by difference

2.5.1.1.3 Thermal degradation behaviour

The TGA and DTG results for LDPE, as determined by various researchers, illustrate that LPDE degrades in a single step and the minimum temperature at which it will degrade is 390-411 ℃ (Table 2.6) with the maximum degradation rate occurring around 465-470 ℃.

Table 2.6: LDPE conversion behaviour determined by TGA

Heating rate (°C/min)	Temperature range (°C)	Maximum temperature (°C)	References
10	390-411 (start) 490 (end)	465-470	(Diaz-Silvarrey & Phan, 2016; Hujuri *et al*., 2008; Jayanarayanan *et al*., 2016)
20	410-500	480	(Diaz-Silvarrey & Phan, 2016)
40	415-510	500	(Diaz-Silvarrey & Phan, 2016)
50	447-567	503	(Aboulkas *et al*., 2008)

2.5.1.2 Degradation mechanism

LDPE follows a random scission, free radical mechanism involving initiation, propagation (intermolecular and intramolecular H-abstraction and β-scission), and termination reactions, which explains the wide range of compounds formed, as illustrated in Figure 2.7 (Aguado & Serrano, 1999; Faravelli *et al*., 1999; Williams & Williams, 1999a; Hujuri *et al*., 2010; Ahmad *et al*., 2015; Bockhorn *et al*., 1999).

These basic steps in the degradation mechanism can be used to describe the various products formed from the pyrolysis of LDPE. For example, after random scission to form two primary radicals (R_P), the primary radical can stabilise itself through intermolecular H-abstraction to form a more stable secondary radical (Rs) (Hujuri *et al*., 2010). This secondary radical can then undergo β-scission to either the left or right β-position of the free radical. β-scission to the right of the radical, as shown in Figure 2.7, will result in a shorter polymer with an unsaturated end and another primary radical. β-scission to the left, will result in a primary radical and the formation of hexene (Hujuri *et al*., 2010). The reaction pathways are highly influenced by temperature, which explains the formation of different products at different temperatures. However, the overall mechanism is described to favour the formation of alkenes over alkanes and dialkenes, which is reflected in the quantification of the volatiles by various researchers (Williams & Williams, 1999a; Bagri & Williams, 2002; Marcilla *et al*., 2009; Hujuri *et al*., 2010).

Aside from the random scission, free radical mechanism, secondary reactions of the aliphatic products involving cyclisation of the alkenes to form aromatic compounds via Diels-Alder reactions is reported (Williams *et al*., 1993; Li *et al*., 1999; Williams & Williams, 1999a).
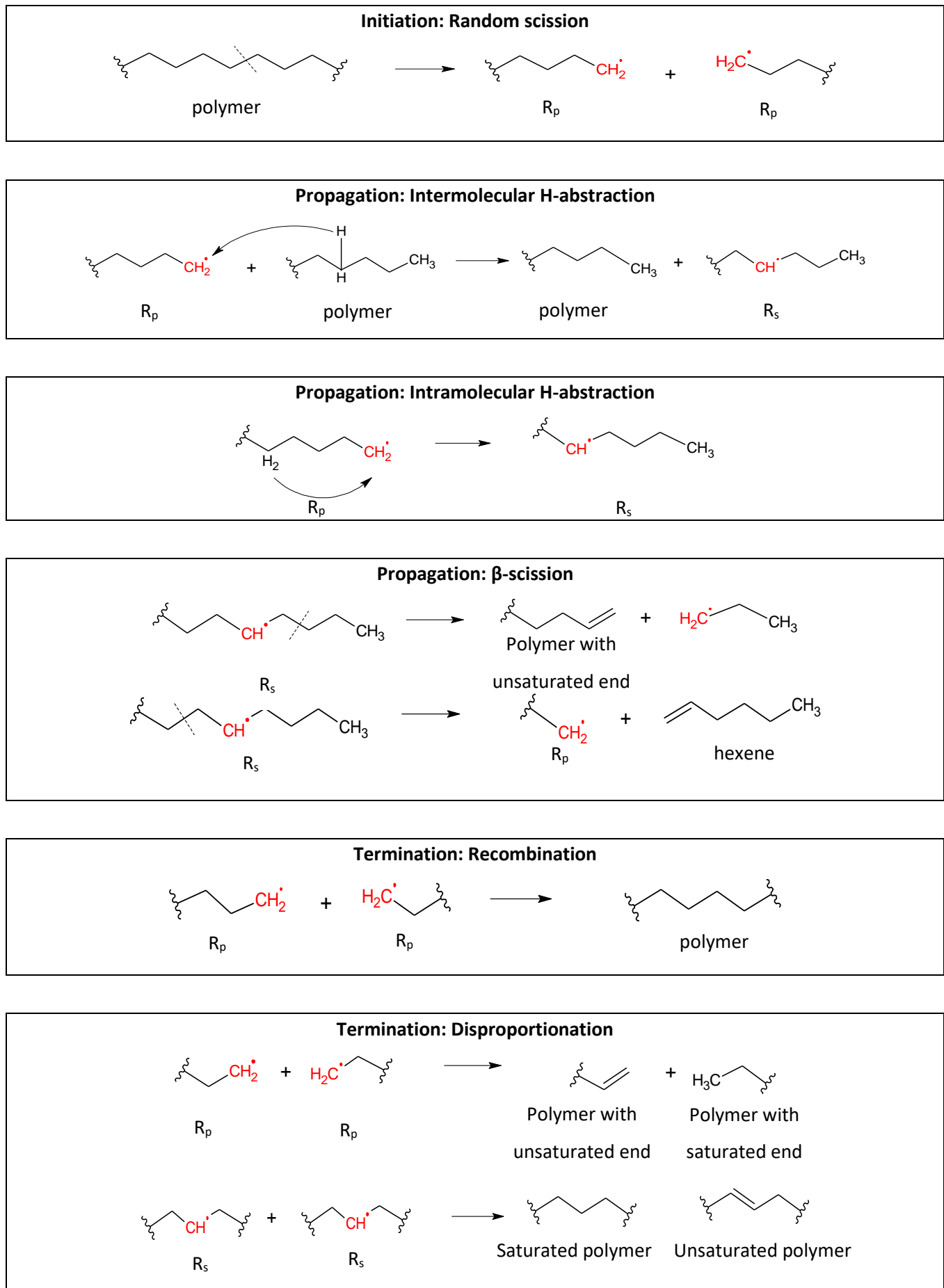
Figure 2.7: Reaction mechanism of LDPE, adapted from Hujuri *et al.* (2010) *and* Aguado and Serrano (1999) *(radical positions indicated in red)*

2.5.1.3 Effect of operating parameters on product yields

This section focusses on the effect that the operating parameters have on the product yields from LDPE pyrolysis. The discussion is based on results from various studies as summarised in Table 2.7 and the operating parameters that will be focussed on are pyrolysis temperature, heating rate, feedstock residence time and volatile residence time, which are the parameters most frequently studied. The aim of this discussion will be to identify trends in the effects of the operating conditions in order to suggest experimental ranges to be investigated for optimum oil or oil/wax yield. As for PS conversion, the discussion will focus first on the char and gas products, before investigating the optimisation of the yield of the oil or oil/wax fractions, the products of interest.

2.5.1.3.1 Char yield

The trends observed in the char yield during the pyrolysis of LDPE are similar to what was observed during the pyrolysis of PS. The char yield decreases as the conversion of the plastic feedstock progresses with very low char yields (< 1 wt.%) observed at the completion of the pyrolysis process (Williams & Williams, 1999; Marcilla *et al*., 2009; Gunasee *et al*., 2017).

Increased temperature and heating rate will result in faster degradation. Longer feedstock residence times will provide more time for degradation to occur, which will also result in a decreased char yield until full degradation is achieved. Park *et al*. (2002) studied the evolution of the oil/wax product between 440 and 500℃ and the time it takes for complete degradation of sample sizes of 50-200 g and found that the feedstock residence time required increased from 40 min to 132 min. While Gunasee *et al*. (2017) achieved full degradation (0.0 wt.% char yield) after 30 min feedstock residence time at a temperature of 550℃ when pyrolyzing samples of 20 g. The sample size is important in PE plastic pyrolysis as the plastic melts before it degrades, which means that larger sample sizes will have larger mass and heat transfer limitations. Therefore, it can be concluded that a feedstock residence time of 30 min will be sufficient to completely degrade smaller samples (±20 g as is typical during bench scale pyrolysis) at temperatures as low as 550 ℃, while for larger samples (50-200 g) and conversion at lower temperature, a longer feedstock residence time up to 132 min will be necessary.

2.5.1.3.2 Gas yield

Increased gas yield is generally observed at increased temperatures due to more intense cracking of the plastic feedstock (Gao, 2010). The effect of temperature on the gas yield due to primary cracking can be observed in the fast pyrolysis studies done by Williams and Williams (1999a) and Kaminsky *et al*. (2004) (Table 2.7). Williams and Williams (1999a) reported a gas yield increase from 10.8 to 71.4 wt.% with a temperature increase from 500 to 700 ℃, and even at 650 ℃ obtained a marked increase in gas yield to 40.1 wt.%. Kaminsky *et al*. (2004) reported a gas yield increase from 7.6 to 55.8 wt.%

with a temperature increase from 530 to 760 ℃. This indicates that the gas yield increases significantly with temperature. When targeting the oil/wax product, it would be recommended to convert PE at temperature lower than 550 ℃.

The effect of heating rate is expected to be related to the effect of the temperature, as a higher gas yield is expected at higher temperatures, higher heating rates will also facilitate higher gas yields due to increased reaction time at higher temperatures. This seems to hold true when comparing the slow pyrolysis study (semi-batch reactor) and the fast pyrolysis study (fluidised bed reactor) done by Williams and Williams (1997) and Williams and Williams (1999a) respectively. In the slow pyrolysis study, a gas yield of 15.0 wt.% was reported, while in the fast pyrolysis study a gas yield of 71.4 wt.% was reported, both at a temperature of 700 ℃. As the two studies had similar volatile residence times, the difference in gas yields is certainly due to the difference in heating rate (slow and fast respectively). Another work (Park *et al*., 2002) compared a conversion at a temperature of 440 ℃ (preheated reactor, indicating a very fast heating rate) and at a slow heating rate of 7 ℃/min (with final temperature of 440 ℃), while allowing enough feedstock residence time for both to reach complete degradation. For the isothermal experiment, the oil yield was 84.0 wt.%, while at a heating rate of 7 ℃/min the oil yield was 76.0 wt.% (indicating a gas yield increase of approximately 8 wt.%, if losses and char yields are assumed similar in both cases). Therefore, it can be concluded that the influence of heating rates on gas yields will be more pronounced for conversion at relatively high temperatures.

Increased volatile residence time is expected to result in increased gas production due to secondary reactions (cracking) of the primary volatiles. In the slow pyrolysis study performed by Gunasee *et al*. (2017), the volatile residence time was longer than the fast pyrolysis studies by other researchers such as Williams and Williams (1999a). The first study obtained a relatively high gas yield (29 wt.%) compared to the second study (21.4 wt.%) at the temperature of 550 ℃. The same as with the effect of heating rate, it is expected that there will be an interacting effect between volatile residence time and temperature, i.e. there will be a more pronounced increase in gas yield with increasing volatile residence time at higher temperatures than at lower temperatures.

2.5.1.3.3 Oil/Wax yield

During thermal pyrolysis of LDPE, the formation of a wax product in the condensable fraction has been reported by various researchers (Bagri & Williams, 2002; Kaminsky *et al*., 2004; Marcilla *et al*., 2009). The wax observed in the condensable fraction is due to the formation of larger hydrocarbon molecules with higher boiling points (Williams & Williams, 1999a). The wax complicates the handling of the condensable product and therefore its formation is not desirable.

Based on the structure of wax compounds (high molecular weight), the effect of the operating parameters on wax formation is anticipated to be the opposite to the effect on gas yield, with higher temperatures, higher heating rates, and longer volatiles residence times expected to result in a lower yield of wax. While many researchers reported the formation of wax in the condensable product, few reported how much was formed. Therefore, it is difficult to make a conclusion about the operating parameter ranges and trends in wax formation, based on the literature studies in Table 2.7. However, in one fast pyrolysis study done by Williams and Williams (1999a), it was reported that wax content in the condensable fraction decreased from 50.8 to 14.0 wt.% with a temperature increase from 500 to 700℃.

Williams and Williams (1999a) looked at the effect of temperature on the flowable oil yield during fast pyrolysis in a fluidised bed and found the optimum oil yield at 600 ℃ of 54.0 wt.%. While Kaminsky *et al*. (2004) did larger scale (30 kg/h) fast pyrolysis and obtained an oil yield of 50.3 wt.% at 530 ℃. As the reported maximum oil yield is quite low (< 55 wt.%), it is worthwhile to rather investigate the optimisation of the combined oil/wax yield. Similar to PS, to optimise the oil/wax product, the temperature must be decreased to a minimum point where complete degradation will occur at the feedstock residence time employed. As discussed in the char yield section (Section 2.5.1.3.1), for a feedstock residence time of 30 min and sample sizes of ±20 g (Gunasee *et al*., 2017), the temperature can be lowered to 550 ℃. At this low temperature (approximately 550℃), the heating rate and volatile residence time are not expected to have a large effect. As summarised in Table 2.7, the highest oil/wax yields were achieved by Williams and Williams (1999a), Bagri and Williams (2002) and Park *et al*. (2002) who investigated oil/wax yield at 500 ℃, with varying heating rates (fast and slow pyrolysis) and volatile residence times (with Park *et al*. (2002) even studying a very long volatile residence time of 80 min). These three studies found similar oil/wax yields in the range of 89-95 wt.%.

From this discussion, it can be concluded that the optimum oil/wax yield can be found in the range of 450-550℃ for a feedstock residence time of 30 min and that at this low temperature the effect of the heating rate and volatile residence time will be limited.

2.5.1.4 Product quality and component distribution

This section discusses the composition of the oil/wax and gas. Additionally, the HHV and use of these products as fuel are considered.

The gas fraction has been reported to be composed of C_1-C_6 hydrocarbons including alkanes and alkenes, with the alkenes being more abundant than the alkanes (Williams & Williams, 1997, 1999a; Bagri & Williams, 2002; Marcilla *et al*., 2009), with Faravelli *et al*. (1999) reporting an alkane/alkene ratio of 1:2. As with PS, the gas fraction is expected to have an HHV greater than 45 MJ/kg, based on its composition (Table 2.3) and the heat produced from its combustion can be recycled back to the

pyrolysis process (López *et al.*, 2011; Brems *et al.*, 2011). Brems *et al.* (2011) experimentally estimated the heat required (including temperature change, melting, and reaction) for pyrolysis in their study with polyethylene to be 0.26 MJ/kg.

The oil/wax product from pyrolysis of LDPE is typically composed of an aliphatic as well as an aromatic fraction (Li *et al.*, 1999; Williams & Williams, 1999a; Bagri & Williams, 2002; Marcilla *et al.*, 2009). The aliphatic fraction has been reported to have a wide distribution in the carbon number of the chain (as is expected from a random chain mechanism) of C_5-C_{57} (Williams & Williams, 1999a; Bagri & Williams, 2002; Marcilla *et al.*, 2009; Hujuri *et al.*, 2010), with C_7-C_{18} being considered oil (liquid) and C_{19}-C_{50} being considered wax. The aliphatic fraction mostly consists of alkanes, alkenes and alkadienes (Williams & Williams, 1999a; Bagri & Williams, 2002; Marcilla *et al.*, 2009; Hujuri *et al.*, 2010). As the upper limit of the hydrocarbon number in diesel fuel is typically C_{20} (Fahim *et al.*, 2010), the oil/wax from the pyrolysis of LDPE would need to undergo further processing such as fluid catalytic cracking (FCC) to make the fuel suitable at a commercial level (Wong *et al.*, 2015). The HHV of the oil/wax has been reported to be between 38.0 and 52.9 MJ/kg (Li *et al.*, 1999; Wiriyaumpaiwong & Jamradloedluk, 2017), making it comparable to that of commercial diesel and gasoline at 42.8-45.8 MJ/kg and 43.4-46.5 MJ/kg respectively (Sharuddin *et al.*, 2016).

An interesting trend in the carbon number distribution of the aliphatic fraction of the oil/wax has been observed, where at lower temperatures, the distribution was narrower and had a single maximum point at a lower carbon number of about C_{14} (Park *et al.*, 2002), meaning lower MW compounds were favoured. As the pyrolysis temperature increased (to approximately 460-490 ℃), the distribution size increased and with a maximum at a higher carbon number of about C_{19} (Park *et al.*, 2002; Marcilla *et al.*, 2009). A further increase in temperature resulted in two maximum points being formed, one at lower carbon number and one at a higher carbon number: In the temperature range of 495-520 ℃, the two maximum points were at C_{15} and C_{29}, and in the temperature range of 546-569 ℃, the two maximum points were at C_{11} and C_{35} (Marcilla *et al.*, 2009). This formation of the two maximum points has been attributed to secondary reactions of the intermediate carbon number chains (causing an increase in the shorter chains), but at temperatures that are not yet high enough to initiate secondary reactions in the larger chains, but high enough to cause them to become volatile (Marcilla *et al.*, 2009). As the temperature increased further (525-600℃), the maximum point again shifted toward the lighter fractions as the longer chains start to undergo secondary reactions to shorter chains (Williams &Williams, 1999a; Marcilla *et al.*, 2009).

The formation of aromatic compounds, including polycyclic aromatic hydrocarbons (PAH), have been reported by various researchers at higher temperatures (Li *et al.*, 1999; Williams & Williams, 1999a; Bagri & Williams, 2002; Marcilla *et al.*, 2009; Kaminsky, 2004). Williams and Williams (1999a)

reported that for fast pyrolysis in a fluidised bed reactor there were no aromatic compounds in the wax fraction formed in the temperature range of 500-700 ℃, and no aromatics formed in the oil fraction at temperature < 550 ℃. From 600 ℃ to 700 ℃ the aromatics started to increase significantly in the oil, and at 700 ℃ the oil fraction consisted of 25 wt.% aromatics including PAHs (Williams & Williams, 1999a). Other studies reported the detection of aromatics at lower temperature. Bagri and Williams (2002) found a very small amount of aromatics in the oil/wax fraction of 0.34 wt.% at 500 ℃, and (Demirbas, 2004) obtained 3.5 wt.% aromatics at 527 ℃. Li *et al*. (1999) found a similar increasing trend of the aromatic content in the oil/wax as temperature increased and at 750 ℃ determined an aromatic content of 15.63 wt.%. This increase in aromatic content with increasing temperature is attributed to secondary reactions at higher temperatures, in particular the aliphatic compounds undergoing Diels-Alder reactions to form aromatic compounds including PAHs (Li *et al*., 1999; Williams & Williams, 1999a). The presence of aromatics, especially PAHs, is undesirable in fuel as it causes incomplete combustion, forming toxic coking residue and aromatic (such as Benzene) and PAH emissions (Williams *et al*., 1993). PAH concentrations in air due to transport fuel emissions have been linked to a number of adverse health effects such as cardiopulmonary and lung cancer (Masri *et al*., 2018). Due to this, the content of aromatics in commercial fuels are controlled, with commercial diesel having a maximum PAH concentration of 8 wt.% (SANS 342, 2006), and commercial grade unleaded, metal free gasoline being limited to 35 wt.% total aromatics and 1 wt.% Benzene (SANS 1598, 2006). Therefore operating at a temperature < 550℃ would be desirable as it has been found that below this temperature, the aromatic content is less than 5 wt.% (Williams & Williams, 1999a; Bagri & Williams, 2002; Demirbas, 2004).

Table 2.7: Results from literature studies on the pyrolysis of LDPE

Reactor	Temperature (°C)	Heating rate (°C/min)	Feedstock residence time (min)	Volatile residence time/N$_2$ flow rate	Oil/wax yield (wt.%)	Gas yield (wt.%)	Char yield (wt.%)	References
Semi-batch	700	25	NR	25 s 0.2 L/min N$_2$ flow	84.25	15.02 (by GC-analysis)	0.00	Williams and Williams (1997)
Semi-batch	500	10	20	30 s	95	NR	negligible	Bagri and Williams (2002)
Semi-batch (320 mg sample)	569	5	104	150 mL/min N$_2$ flow	75.0	12.9 (by GC-analysis)	0.0	Marcilla *et al.* (2009)
Semi-batch (20 g sample)	550	10	30	128s	70	29 (by difference)	0	Gunasee *et al.* (2017)
Stirred semi-batch (50-200 g sample)	440-500	Isothermal reaction	40-132	< 80 min < 10 mL/min N$_2$ flow	84-94.3	NR	NR	Park *et al.* (2002)
Fluidised bed	500	NR	NR	15 s	43.9 oil/45.3 wax	10.8 (by GC-analysis)	0.0	Williams and Williams (1999a)
	550				43.2 oil/35.4 wax	21.4		
	600				54.0 oil/24.8 wax	24.2		
	650				47.8 oil/12.1 wax	40.1		
	700				24.6 oil/4.0 wax	71.4		
Fluidised bed (30 kg/h)	530	NR	NR	NR	50.3 oil/42.0 wax	7.6	1.8	Kaminsky *et al.* (2004)
	760				42.4 oil	55.8	0.1	
Rotary kiln	550-850	NR	NR	NR	65-35	28-65 (by GC-analysis)	8 - < 1	Li *et al.* (1999)

NR = not reported.

The pressure is at atmospheric, the carrier gas is nitrogen, and no catalyst is used.

2.5.2 Polyethylene terephthalate (PET)

2.5.2.1 Feedstock characterisation

2.5.2.1.1 Structure

Polyethylene terephthalate (PET) is formed from the polymerisation of terephthalic acid and ethylene glycol with the release of an H_2O molecule for every bond formed, making it a condensation polymer, as demonstrated in Figure 2.8 (Callister & Rethwisch, 2011). PET is also classified as a thermoplastic and it has a melting point of 265 °C (Callister & Rethwisch, 2011).
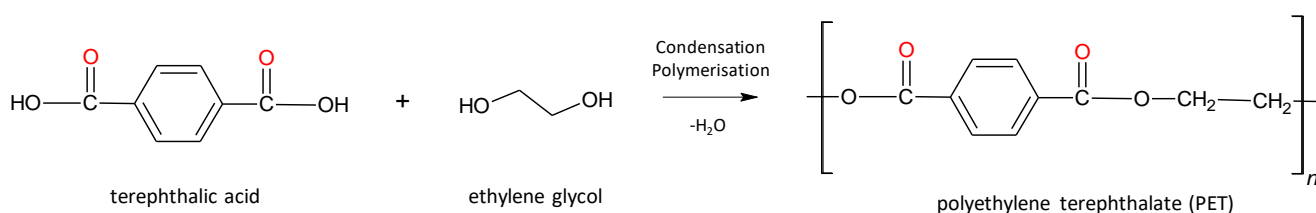
Figure 2.8: PET formed from the condensation (loss of H_2O) polymerisation of terephthalic acid and ethylene glycol (adapted from Callister and Rethwisch (2011))

2.5.2.1.2 Ultimate, proximate and energy content analysis of PET

In Table 2.8 the characterisation of PET, as determined by various researchers, is outlined in terms of composition and energy value. Based on the pure PET structure (Figure 2.8), the C, H, and O content will be 62.5, 4.2 and 33.3 wt.% respectively with no N and S. As with PS and LDPE, the observed differences from the pure structure are due to additives and other contamination. The presence of oxygen in the PET structure requires additional attention, as its pyrolysis conversion can cause the formation of oxygenated compounds, some of which can give acidic properties to the pyrolysis oil (Aguado & Serrano, 1999). Fuel acidity must be controlled in order to avoid equipment corrosion. The reported HHV of PET (22.9 MJ/kg) is significantly lower than that of LDPE (43.1-46.6 MJ/kg in Table 2.5), and an increased proportion will have a negative effect on the HHV of the multi-layer.

Compared to LDPE, PET has a much higher fixed carbon content (9.3-13.8 wt.% compared to 0.0-0.8 wt.%), which would explain the higher char yields (> 10 wt.%) that are typically observed during pyrolysis of PET (Çit *et al.*, 2010; Brems *et al.*, 2011; Chomba, 2018). However, the volatile matter is still more than 80 wt.%, and with the low moisture and ash content, this would make PET suitable for significant conversion to volatiles.

39

Table 2.8: Ultimate and proximate analysis, and energy value of PET

	Parameter	Value	References
Ultimate analysis (wt.%) dry, ash free basis	**C**	62.5 58.9-62.5	Based on pure PET structure (Brems *et al.*, 2011; Izzatie *et al.*, 2017)
	H	4.2 3.8-4.8	Based on pure PET structure (Brems *et al.*, 2011; Izzatie *et al.*, 2017; Singh *et al.*, 2019)
	N	0.0 < 0.1-0.3	Based on pure PET structure (Brems *et al.*, 2011; Izzatie *et al.*, 2017; Singh *et al.*, 2019)
	S	0.0 0.0	Based on pure PET structure (Singh *et al.*, 2019; Chen *et al.*, 2017)
	O*	33.3 23.5-36.9	Based on pure PET structure (Brems *et al.*, 2011; Izzatie *et al.*, 2017)
Proximate analysis (wt.%)	**Moisture**	0.0-0.2	(Izzatie *et al.*, 2017; Ganeshan *et al.*, 2018)
	Volatile compounds	87.4-99.2	(Izzatie *et al.*, 2017; Diaz-Silvarrey *et al.*, 2018; Ganeshan *et al.*, 2018)
	Ash content	0.1-3.0	(Izzatie *et al.*, 2017; Diaz-Silvarrey *et al.*, 2018; Ganeshan *et al.*, 2018)
	Fixed carbon	9.3-13.8	(Singh *et al.*, 2019; Chen *et al.*, 2017)
Energy value	**HHV (MJ/kg)**	22.9	(Diaz-Silvarrey *et al.*, 2018)

*by difference

2.5.2.1.3 Thermal degradation behaviour

The TGA results for the thermal degradation of PET (Table 2.9) shows that PET starts degrading at a temperature of 370-397 ℃, in a single step, with the maximum degradation rate point occurring in the range of 420-438 ℃. PET starts degrading at lower temperature than LDPE (minimum start temperature of 400 ℃) due to the C-O bond (where scission is initiated) in PET which has a lower bond dissociation energy than the C-C bond (where scission is initiated) in LDPE (Pek & Ghosh, 2015).

Table 2.9: PET conversion behaviour determined by TGA

Heating rate (°C/min)	Temperature range (°C)	Maximum temperature (°C)	References
10	370-397 (start) 450-490 (end)	420-438	(Hujuri *et al.*, 2008; Diaz-Silvarrey & Phan, 2018; Jayanarayanan *et al.*, 2016)
20	370-505	450	(Singh *et al.*, 2019)
50	405-500	460	(Brems *et al.*, 2011)
100	405-500	460	(Brems *et al.*, 2011)

2.5.2.2 Effect of operating parameters on product yields

Some studies reported the products from PET pyrolysis as char, gas, and a condensable fraction which appears to be solid (Artetxe *et al.*, 2010; Sogancioglu *et al.*, 2017; Singh *et al.*, 2019; Chomba, 2018). This is different from PS and LDPE where the condensable fraction is either liquid or wax. This solid is known to desublimate at very high temperatures (400 °C) (Brems *et al.*, 2011), which causes operating difficulties such as the blocking of downstream piping where the solids tend to condense, before reaching the condenser (Chomba, 2018).

2.5.2.2.1 Char yield

PET has been found to produce greater yields of char than other plastics such as LDPE, PS, and HDPE (Çit *et al.*, 2010; Singh *et al.*, 2019; Chomba, 2018; Pek & Ghosh, 2015). However, generally studies do not comment on the effect of the operating parameters on the char yield. Therefore, in this section, it will be attempted to describe them, based on pyrolysis results as summarised in Table 2.10.

In the study performed by Çit *et al.* (2010), PET was pyrolysed at temperatures of 400-700 °C, and the feedstock residence time was long enough to ensure that no more volatiles were formed. It was found that at a lower temperature (400 °C) more char was produced (16 wt.%) as opposed to higher temperatures (500-700 °C) where 11 wt.% was produced. This trend can be explained from thermal degradation behaviour studied using TGA. Inspection of the TGA curves suggest that the char formed undergoes further degradation after about 500-600 °C (Brems *et al.*, 2011; Diaz-Silvarrey & Phan, 2016; Diaz-Silvarrey *et al.*, 2018; Martín-Gullón *et al.*, 2001).

The effect of heating rate is indicated by the research performed by Brems *et al.* (2011) who studied the pyrolysis of PET in a fluidised bed reactor at a fluidising velocity that optimised the heating rate and a slower fluidising velocity that translated into a slower heating rate. This study found an increased char

yield (24 wt.%) at the slower heating rate than at the higher heating rate (16 wt.% char yield). However, this effect could also be due to longer volatile residence times at the slower fluidising velocity, which can also promote secondary reaction such as recombination and therefore increased char formation.

Volatile residence time increase would be expected to also lead to an increase in char formation. Singh *et al.* (2019) operated a semi-batch reactor by initially flushing with nitrogen and then performing the pyrolysis under a non-sweeping atmosphere (i.e. no nitrogen flow), which can be expected to result in a longer volatile residence time compared to an experiment operated under sweeping atmosphere conditions. This study obtained char yields of 24-21 wt.% in the temperature range of 400-600 °C. Diaz-Silvarrey *et al.* (2018) performed pyrolysis of PET in a similar temperature range (450-600 °C), but with a short volatile residence time of 20 s. This study obtained relatively lower char yields (15-12.5 wt.%) than Singh *et al.* (2019).

To summarise, the char formation mechanism during degradation of PET is not well understood, but it would seem that at lower temperatures (< 400 °C), PET can start degrading but conversion is not complete even for long feedstock residence time. Further, faster heating rates have been found to lead to smaller char yields in gram- and kilogram-scale experiments, while longer volatile residence times can lead to greater char yields due to secondary reactions. Finally, from the analysis of the different studies it can be expected that the char yield can be anywhere from 15-25 wt.%.

2.5.2.2.2 Gas yield

The gas yield profile follows a more straightforward trend than the char yield, and is similar to the trends observed with LDPE, where increased temperatures and longer volatiles residence times led to increased gas yields due to increased primary and secondary cracking. However, generally, PET pyrolysis results in greater yields of gas than other plastics due to the presence of oxygen in the polymer chain, producing oxygenated gaseous products such as CO and CO_2 (Singh *et al.*, 2019).

At the low temperature of 450 °C in a fluidised bed reactor (short volatile residence time), Brems *et al.* (2011), observed a gas yield of 16-18 wt.%. While, at the high temperature of 700 °C in a fluidised bed reactor, Williams and Williams (1997) obtained a much higher gas yield of 41.3 wt.%. In the semi-batch experiment under non-sweeping atmosphere (long volatile residence time) performed by Singh *et al.* (2019), the results at 400 °C and 600 °C were characterised by relatively higher gas yield (40 and 54 wt.% respectively), consistent with longer volatile residence times. Therefore, minimised gas yield would be promoted at lower temperatures (< 500 °C) and shorter volatile residence times (seconds as opposed to minutes). Based on PET structure and the stability of benzene rings on the investigated temperature range, a theoretical maximum gas yield of 56 wt.% would be expected.

2.5.2.2.3 Condensable yield

From the discussion on char and gas yields, it would seem that the condensable yield from PET pyrolysis can be maximised by operating at temperatures between 400 and 500 ℃. Additionally, longer volatile residence times (minutes) would promote cracking of the volatiles and a greater gas yield, at the expense of the condensable products. Finally, it seems that lower heating rates could limit PET degradation and minimise condensables yield.

The highest condensable yields were achieved by Çit *et al.* (2010) and Brems *et al.* (2011). Çit *et al.* (2010) achieved 57 wt.% condensable yield at 400 ℃ using a slow heating rate of 10 ℃/min but allowing enough feedstock residence time for complete degradation to occur. Brems *et al.* (2011) achieved a condensable yield of 58 wt.% at 450 ℃, using the fastest heating rate achievable in the fluidised bed reactor studied.

2.5.2.3 Product quality and component distribution

This section describes the composition of the three products, investigates the quality of the condensable fraction and the gas as fuel, and also considers the use of the char fraction.

The non-condensable gas product from PET pyrolysis has been reported to be mostly CO_2 and CO (due to the presence of oxygen in the polymer), as well as some C_1-C_4 alkenes, CH_4 and H_2 (Martín-Gullón *et al.*, 2001; Artetxe *et al.*, 2010; Brems *et al.*, 2011; Diaz-Silvarrey *et al.*, 2018; Williams & Williams, 1997). While the formation of gas such as CO or CO_2 will decrease the oil yield, such reaction will lead to deoxygenation of the condensable product, which could be beneficial in terms of fuel properties. The gas fraction can be burned to partially supply the energy needed for pyrolysis and can be used as an almost inert carrier gas (Brems *et al.*, 2011).

As the char product from PET pyrolysis is significant (when compared to LDPE and PS char), it is useful to look at its composition and possible use. Williams and Williams (1997) analysed the char for its elemental composition and ash content and found that the char was predominantly carbon (84.9 wt.%) with an ash content of 5.9 wt.%. Most researchers suggest that the upgraded char compares very well with commercially available activated carbon (Artetxe *et al.*, 2010; Brems *et al.*, 2011; Havelcová *et al.*, 2016). Brems *et al.* (2011) specifically studied upgrading the char by steam activation.

As for the condensable fraction, most researchers reported that it was composed predominantly of aromatic compounds, with benzoic acid as the major component (Artetxe *et al.*, 2010; Çit *et al.*, 2010; Brems *et al.*, 2011; Diaz-Silvarrey *et al.*, 2018). According to these reports, the yield of benzoic acid is in the range of 15.1-31.6 wt.%, depending on the operating conditions. The concentration of benzoic acid in the condensable fraction has been reported to be as high as 72.9 wt.% by Chomba (2018). The

formation of terephthalic acid has also been reported, with Brems *et al*. (2011) reporting a benzoic acid to terephthalic acid ratio of 10:1, while Chomba (2018) found concentrations of terephthalic acid as high as 51.6 wt.% in the condensable product. The benzoic acid and terephthalic acid content would account for the solid nature of the condensables and the problem of this solid fraction condensing early in a pyrolysis system, as terephthalic acid even starts to desublimate at the high temperature of 400 °C (Brems *et al*., 2011). Furthermore, the presence of PAHs have also been reported (Martín-Gullón *et al*., 2001), which as explained for LDPE and PS (Sections 2.4.4 and 2.5.1.4) is undesirable in fuel due to their toxicity. The HHV of the condensable fraction has been reported to be about 3 times lower than the oil/wax obtained from LDPE pyrolysis (Sogancioglu *et al*., 2017).

Table 2.10: Results from literature studies on the pyrolysis of PET

Reactor	Temperature (°C)	Heating rate (°C/min)	Feedstock residence time (min)	Volatile residence time/N_2 flow rate	Condensable yield (wt.%)	Gas yield (wt.%)	Char yield (wt.%)	References
Semi-batch (5.03±0.03 g samples with 3 wt.% catalyst)	450-600	45	10 min at final temperature	20 s	44-30 (optimum of 47 at 500 °C)	35.0-37.5 (by GC-analysis)	15.0-12.5	Diaz-Silvarrey *et al.* (2018)
Semi-batch	400-700	10	Until no more volatiles formed	30 mL/min N_2 flow	57-45	24-42 (by GC-analysis)	16-11	Çit *et al.* (2010)
Semi-batch (15 g samples)	410-550	5	30 min at final temperature	0.5 L/min N2 flow	33.9-32.3	29.3-47.8	36.8-19.8	Chomba (2018)
	410-550	25			30.5-39.7	30.8-44.0 (by difference)	38.6-16.3	
Semi-batch	700	25	NR	25 s 0.2 L/min N_2 flow	33.99	41.30 (by GC-analysis)	15.55	Williams and Williams (1997)
Semi-batch	400-600	20	NR	Non-sweeping atmosphere	32-25	40-54	28-21	(Singh *et al.*, 2019)
Fluidised bed (50 g samples)	450	Fast (fast mode) Slow (slow mode)	NR	Short (fast mode) Long (slow mode)	58-66 (fast mode) 55-65 (slow mode)	16-18 (by difference)	16 (fast mode) 24 (slow mode)	Brems *et al.* (2011)

NR = not reported.

Unless stated otherwise, the pressure is at atmospheric, the carrier gas is nitrogen, and no catalyst is used (unless specified).

2.5.3 Multi-layer considerations

The multi-layer investigated in this study typically has an LPDE layer of 130 µm and a PET layer of 12 µm (personal communication with supplier). Using the average densities reported for these plastics, this translates to a composition of 12 wt.% PET and 88 wt.% LDPE. Table 2.11 summarises the ultimate and proximate analysis and the energy value of the multi-layer as predicted by the literature values reported in Table 2.5 and Table 2.8 and a 12 wt.% PET layer. Due to the high LDPE content, the multi-layer is characterised by high C and H content, making it useful as a feedstock for hydrocarbon fuel production. Further, the O-content (4.0 wt.% theoretically) is significantly less than with the pure PET (33.3 wt.% theoretically), which reduces the adverse effects that oxygen can have on the quality of the produced oil/wax for fuel. Lastly, the HHV value (40.7-45.4 MJ/kg) is only slightly lower than that of pure LDPE (43.1-46.6 MJ/kg) and that of conventional gasoline and diesel (Sharuddin *et al*., 2016).

As with the proximate analysis of LDPE (Table 2.5), the results for the multi-layer in Table 2.11 are characterised by high volatile matter and low moisture, ash and fixed carbon contents, which is favourable for the conversion into volatiles.

Table 2.11: Ultimate-and-proximate analysis, and energy value of LDPE/PET multi-layer (based on 12 wt.% PET and literature values reported in Table 2.5 and Table 2.8)

	Parameter	Value
Ultimate analysis (wt.%) dry, ash free basis	**C**	82.8 (pure LDPE/PET) 80.5-83.1
	H	13.2 (pure LPDE/PET) 12.8-14.9
	N	0 (pure LDPE/PET) 0.0-0.1
	S	0 (pure LPDE/PET) 0.1
	O*	4.0 (pure LDPE/PET) 2.8-4.9
Proximate analysis (wt.%)	**Moisture**	0.0-0.3
	Volatile compounds	97.8-99.8
	Ash content	0.0-0.4
	Fixed carbon	1.1-2.4
Energy value	**HHV (MJ/kg)**	40.7-45.4

*by difference

In Sections 2.5.1 and 2.5.2 the literature available for the pyrolysis of individual LDPE and PET was reviewed and as the multi-layer is composed of predominantly LDPE, it is expected that the multi-layer will behave in a more similar manner to LDPE (as was observed with characterisation in Table 2.11), in terms of the product yields and quality for fuel applications. However, it has been found that when co-pyrolysis of different plastics are performed, some interaction effects can occur between the different types of plastic, which can affect the yield and quality of the products (Brems *et al*., 2011; Pek & Ghosh, 2015; Wong *et al*., 2015; Bockhorn *et al*. 1998). Interaction effects can be evidenced during the pyrolysis of the plastic mixture when the product yields deviate from the expected summed product yields from the individual plastics (Wong *et al*., 2015). When synergistic effects have been observed in other studies, it has been concluded that when one of the plastics degraded at a lower temperature it produced radicals that initiated earlier degradation of the other plastic(s) in the mixture and changed the conversion mechanisms (Wong *et al*., 2015).

Pek and Ghosh (2015) studied the kinetics of pyrolysis of a mixture of HDPE and PP (at varying compositions ranging from pure HDPE to pure PP) using TGA. The study demonstrated synergistic effects between the plastics from the TG and DTG curves, by noting earlier degradation of the mixed plastic compared to the pure plastic, two-step degradation of the mixed plastics at intermediate compositions, and faster maximum rates of degradation for the mixed plastics. This indicated the effect of the earlier degradation of PP compared to HPDE and the radicals formed from the PP pyrolysis initiating earlier degradation of the HDPE. Two research studies by Hujuri *et al.* (2008) and Jayanarayanan *et al*. (2016) investigated the effect of LDPE and PET mixing ratios in a mixture (where mixing ratios were defined by the researches in the range of 20-95 wt.% LDPE) on the thermal degradation kinetics. Hujuri *et al.* (2008) reported interaction between the two plastics as the raw kinetic data fitted an interacting model better than a non-interacting model the researchers had developed. Jayanarayanan *et al*. (2016) did not study a conclusion on interaction between the two plastics.

Aside from the synergistic effects on the thermal degradation behaviour observed from TGA, the synergistic effects can also influence the mechanisms of conversion (and therefore the product yields). Williams and Williams (1997) pyrolysed the six most common waste plastics (LDPE, HDPE, polypropylene, polystyrene, PVC, and PET) individually and as part of mixture (where LDPE and HDPE represented 62.5 wt.% and PET constituted 5.21 wt.%). The study observed interaction from the FTIR spectra of the oil pertaining to aromatic and oxygenated groups (increased amounts), that could not be explained from the pyrolysis of the individual plastics. A similar conclusion regarding the aromatic fraction was made by López *et al*. (2011), who studied a mixture of the same six plastics.

2.6 Effect of contamination

An important consideration in this study is the effect of contamination on the pyrolysis of the two plastic feedstocks. Contamination refers to both inorganic additives (fillers, plasticisers, stabilisers, colourants and others) used to enhance the properties of the plastic products and the organic contamination from contact with organic waste. This section will outline some of the literature available on the effect of contamination to shed light on the possible effects.

As stated previously, the polystyrene investigated in this study is the high-absorbent black punnet used to package raw meat. The major inorganic contaminant is expected to be the black colouring, as pure polystyrene is colourless (McKeen, 2014). The main organic contamination is meat juice, which is expected to be composed of mainly water, proteins and fat. The contamination is expected to be significant as the punnets are specifically designed to absorb the meat juice. The presence of water is very undesirable in pyrolysis feedstock as it affects the efficiency of the pyrolysis process and degrades the quality of the oil for fuel applications.

The presence of protein is expected to increase the amount of fixed carbon in the PS feedstock (Wei *et al*. (2018) reported a fixed carbon content of 14.84 wt.% from soybean protein), which will cause an increase in char yield and therefore a decrease in oil yield. Additionally, the presence of the protein will result in an increase in N and O content in the PS feedstock, as protein is partly composed of these elements (Yi *et al*., 2017). This could affect the quality of the oil for fuel applications, as oxygen presence will decrease its HHV and can make the oil acidic. (Wei *et al*., 2018). Nitrogen raises concern in terms of toxic emissions such as NO_x during combustion of the derived fuel oil (Aguado & Serrano, 1999). Apart from contributing a greater N, O, and fixed carbon content, the protein contamination in the feedstock is also expected to start degrading at a lower temperature than pure PS. For instance, Wei *et al*. (2018) reported that soybean protein started to degrade at approximately 220 ℃, compared to 369 ℃ for PS (with a heating rate of 20 ℃/min). Additionally, Kebelmann *et al.* (2013) investigated the thermal degradation of protein extracted from green microalgae and found that with a heating rate of 100 ℃/min, degradation started at approximately 250 ℃.

The gas fraction from protein pyrolysis has been found to contain CO_2, CO, ammonia (NH_3), and hydrogen cyanide (HCN) (Yi *et al.*, 2017; Wei *et al.*, 2018). The condensable product has been reported to include aromatics, alcohols, acids, nitriles, amines and amides, phenols, ketones, aldehydes, esters, and aliphatic compounds (Wei *et al*., 2018). The aromatic fraction was found to be the most abundant based on peak area with approximately 15% (Wei *et al*., 2018).

The multi-layer used in this study is composed of a white pigmented LDPE layer bound to a colourless PET layer with an organic adhesive and branded with ink. An adhesive that is commonly

used with LDPE/PET multi-layer films is ethylene-acrylic acid (Adhesive resins and tie layers, 2019). The organic adhesive layer can be expected to contribute to the oil/wax and gas products. The ink will be mostly inorganic, which will contribute a greater ash content and therefore more char product. The bags are specifically used to package dry dog food, which results in little contamination at the inside surface of the multi-layer. The dog food is expected to be composed of a combination of carbohydrates, protein and lipids as well as some micro-nutrients (vitamins and minerals). Such contamination will be characterised by an increase in the content of O, N and inorganic elements. Inorganic contamination, particularly metallic compounds have been reported to cause a catalytic effect during pyrolysis (López *et al.,* 2010).

Sogancioglu *et al.* (2017) compared the pyrolysis of washed and unwashed post-consumer plastic (collected from a waste recycling facility) in order to study the effect of contamination. The study focused on bench scale pyrolysis in a semi-batch reactor with waste HDPE, LDPE, PET, PP and PS in the temperature range of 300 to 700 °C. Characterisation of the waste plastics was not done, therefore conclusions about the nature of the contamination could not be drawn. The study reported that washing of the waste plastics led to lower oil product yields (about 10-20 wt.% lower) across all temperatures (i.e. contaminated plastics resulted in higher oil yields), however the reason for this was not discussed. Furthermore, the researchers found that washing did not result in a statistically significant difference in the HHV of the condensable product from LDPE, PET and PS.

2.7 Conclusions

2.7.1 Polystyrene single-layer

Polystyrene has been reported to have favourable properties in terms of the ultimate and proximate analysis for conversion via pyrolysis to an oil product with an HHV only slightly lower than diesel. It has been found to degrade in a single step starting in the range of 360-380 °C. From the literature studies it can be concluded that optimum oil yield from PS pyrolysis can be greater than 90 wt.%, that the minimal char yield is mostly dependent on the reaction being complete and can be expected to be less than 5 wt.% after complete degradation, while the gas yield was less than 5 wt.% even at temperature as high as 700 °C. The parameters that favour optimal oil yield are temperatures greater than 400 °C, provided the feedstock residence time is sufficient. Additionally, it was concluded that volatile residence times should be kept low to limit the entrainment of volatiles in the condensation system, especially as a longer volatile residence time was not observed to lead to significant increases in the gas yield.

In terms of the quality of the oil, the HHV was found to be 37.8-42.6 MJ/kg (only slightly lower than gasoline and diesel), but the influence of operating parameters cannot be conclusively stated. The oil

produced in the studies was predominantly aromatic with the main compounds being styrene, toluene, ethylbenzene, α-methylstyrene, and various styrene dimers. The high amount of aromatic content could be problematic in fuel applications, and therefore blending could be an option.

Finally, the contamination present in the PS feedstock is expected to be mainly meat juice which is composed of water and protein. Pyrolysis processing of pre-dried PS is recommended to avoid the presence of water in the oil product. The protein has the expected effect of earlier degradation (220 ℃ compared to pure PS at 369 ℃ at a heating rate of 20 ℃/min); a greater char yield due to higher fixed carbon content in the protein; and increased presence of N and O in the feedstock, which can lead to the formation of oxygenated compounds and NO_x when combusting the pyrolysis products.

Based on the reviewed literature, the limitations (to our knowledge) appear to be associated with the characterisation of the contamination; the comparison of product yields and quality of the oil from bench scale pyrolysis of clean and contaminated PS; the scale up of the bench scale process to pilot scale; and the operational difficulties associated with pilot scale pyrolysis of PS.

2.7.2 LDPE/PET multi-layer

As the multi-layer is predominantly composed of LDPE (around 88 wt.%), it can be expected that the pyrolysis process will be characterised by a behaviour similar to that of LDPE. Therefore, the conclusions drawn here are based mainly on the research relating to LDPE.

The characterisation of LDPE in terms of the ultimate, proximate and energy content analysis has indicated that LDPE has favourable properties for conversion via pyrolysis to an oil/wax product with a high HHV. Degradation of LDPE has been found to occur in a single step starting at 390-411 ℃. From the research studies examined, it has been concluded that to obtain the optimum oil/wax yield from LDPE pyrolysis, the lowest temperature that will ensure complete degradation, with a long enough feedstock residence time, must be found. The effect of heating rate and volatile residence has been found to be significant at higher temperatures (±700 ℃), but are not so pronounced at lower temperatures (±500 ℃). The optimal oil/wax yields have been found as 89-95 wt.%, and it is expected to be reached in the temperature range of 450-550 ℃ when using a feedstock residence time of 30 min. The char yield is expected to be very low after complete degradation (< 1 wt.%), which in the optimal range (for oil/wax yield) then translates to a minimal gas yield of 4-10 wt.%.

In terms of the quality of the oil/wax for fuel applications, the HHV has been found to be 38.0-52.9 MJ/kg (comparable to gasoline and diesel). The composition has been found to be mainly alkanes, alkenes and dialkenes, with the alkenes being the most abundant. The chain lengths of the compounds have been reported to be C_5-C_{57}, with C_7-C_{18} being considered oil (liquid) and C_{19}-C_{50} being considered

wax (solid). This means that for the product to be used as fuel, the waxy fraction will need to undergo further processing such as FCC to reduce the upper limit of the carbon number, so that it can be similar to that of diesel (upper limit of C_{20}). At temperatures greater than 550 °C, it has been found that the aromatic (including PAH) concentration in the oil/wax can increase significantly beyond 5 wt.%.

The effect of the presence of PET in the feedstock is that it will increase the fixed carbon content, which will result in a greater char yield. As PET contains oxygen, it will cause the formation of oxygenated compounds during pyrolysis and a decrease in the HHV of the condensable product. Pyrolysis of PET can also cause the formation of a solid organic fraction in the condensable product, which may result in pipe blockage due to early condensation.

Finally, the contamination in terms of the additives and packaging content (dry dog food), are expected to contribute to some changes in the organic and inorganic (ash) fractions of the feedstock respectively.

The likely limitation in literature, from this review, seem to be mainly the pyrolysis process of an LDPE/PET multi-layer. As mentioned in the review, two studies investigated the pyrolysis kinetics of LDPE and PET mixtures (where the mixing ratios were determined by the researchers). However, nothing, to our knowledge, is available regarding multi-layer pyrolysis, either with TGA, at bench scale, or at pilot scale. Furthermore, the effect of contamination on the product yields and quality of the condensable fraction does not seem to be well understood.

3 Key questions and objectives

The focus of this study is the pyrolysis of two types of waste plastic packaging. The first type of waste plastic packaging is a polystyrene single-layer and the second is an LDPE/PET multi-layer. The main goal of the study is to produce at pilot scale an oil/wax that can be used in fuel applications. To this end, the following key questions and objectives have been identified:

3.1 Key questions

1. What are the characteristics of the plastic composing the waste feedstocks in terms of composition (ultimate, proximate, contamination and plastic fraction amounts), energy content and thermal degradation behaviour?

2. At what conditions must the bench scale reactor be operated for optimum yield and quality of the oil/wax product for transport fuel applications?

3. What is the effect of contamination on the oil/wax yield and quality?

4. At what conditions must the pilot scale semi-continuous rotary kiln reactor be operated for optimum yield and quality of the oil/wax product?

5. In what type of application can the oil/wax product be used as fuel?

6. What are the major operational difficulties and solutions associated with the plastic feedstocks especially as pertaining to scale-up to the pilot scale reactor?

3.2 Objectives

1. Characterise the feedstock samples with and without contamination.

2. Perform pyrolysis experimentation at bench scale with clean and contaminated PS single-layer and LDPE/PET multi-layer and determine the yield and quality of the oil/wax product.

3. Scale up the bench scale results to a pilot scale rotary kiln reactor processing 1-5 kg/hr feedstock and determine the yield and quality of the oil/wax product.

4. Make recommendations as to whether the oil/wax can be used as fuel based on the quality assessment.

5. Identify the major operational difficulties and investigate solutions.

4   Methodology

To meet the study objectives, the experiments were organised as outlined below:

- Feedstock preparation: plastic feedstock size reduction, drying (in the case of the contaminated PS) and sub-sampling.

- Feedstock characterisation: ultimate, proximate and energy content analysis, feedstock degradation behaviour, contamination characterisation, and LDPE/PET fraction quantification in the case of the multi-layer.

- Bench scale pyrolysis: optimisation of the oil/wax yield at bench scale using a semi-batch induction heated reactor.

- Pilot scale pyrolysis: scale-up of bench scale optimised results to a pilot scale semi-continuous rotary kiln reactor.

- Product analysis: pyrolysis gas characterisation; energy analysis of the oil/wax products; and PS derived oil characterisation.

4.1   Feedstock source and preparation

4.1.1 Polystyrene single-layer plastic

The polystyrene plastic studied in this project is used in industry as black punnets packaging. Three different batches of this plastic were obtained:

1. A clean high-absorbent (pre-consumer) batch (obtained from Mpact in Paarl),

2. A contaminated high-absorbent (post-consumer) batch specifically used to package raw meat (collected from Waste Plan Recycling facility in Kraaifontein) to determine the effect of a high amount of meat juice contamination. It represented a "worst-case" scenario in terms of contamination.

3. A black contaminated densified (post-consumer) recycled batch from varying origins (obtained from New Earth Recycling in Cape Town). This batch is expected to be more representative of what would be collected in industry during post-consumer recycling.

The high-absorbent punnets are identified by the presence of holes, which increase their absorption properties for the specific purpose of absorbing meat juice. This type of punnet was selected as it was

considered as representing a "worst-case" scenario in terms of contamination. For instance, black punnets used to package fruits are expected to be less contaminated. It was determined that the high-absorbent batches were too light and bulky to be practical at pilot scale, specifically as it caused significant blockages in the feeding system of the pilot reactor. Consequently, a densified contaminated batch was used for the pilot study. This batch consisted of PS of varying origins (i.e. not just PS used to package raw meat) and had been densified by heating to 270 °C and then extruding the melt into cylindrical briquettes. Figure 4.9 compares 100 g of the high-absorbent and high-density PS. It is clear that the densification reduced the volume significantly. In order to increase the capacity of a pyrolysis process to make it more viable, densification appears as an attractive option.

Figure 4.9: Comparison of 100 g of high-absorbent and high-density PS

From each of the first and second batch (clean high-absorbent and contaminated high-absorbent), 1 kg of punnets was sub-sampled, using the cone and quarter method, to be used in bench scale testing. The 2 sub-samples of punnets were then cut by hand to particles of approximately 15×15×4 mm for bench scale testing. From each of the 2 sub-samples, 1 gram was sub-sampled and reduced in size to < 0.5 mm by cutting by hand for feedstock characterisation tests (ultimate, proximate, energy content and thermal behaviour analyses). Further preparation of the second batch of feedstock (contaminated high-absorbent) included drying in an oven at 70 °C (temperature lower than 100 °C was suggested elsewhere (Zhao *et al*., 2012) to prevent degradation of the PS) until all moisture had been removed (as meat juice contamination contains a lot of water) and then letting the plastic equilibrate to ambient moisture content.

The briquettes composing the third batch were reduced in size by first using a hydraulic band saw and then crushing to a final particle size of 5-15 mm, to be used in bench and pilot scale testing. 1 g was sub-sampled from the third batch and reduced to a particle size of < 0.5 mm in a ZM500 Retsch mill for feedstock characterisation tests.

4.1.2 LDPE/PET multi-layer plastic

The LDPE/PET multi-layer studied is used to make bags to package dry dog food. It consists of a clear PET layer of 12 µm and a white LDPE layer of 130 µm with an adhesive layer and ink in between (from personal communication with the supplier). Two batches of the multi-layer were used: a clean batch (pre-consumer) and a contaminated batch (post-consumer). The clean multi-layer was shredded with an industrial paper shredder and then further reduced in size using a rotating blade mill. The final particle size was approximately 5×5×0.142 mm for bench and pilot scale testing. For feedstock characterisation, 1 g was sub-sampled and reduced to a particle size of < 0.5 mm by cutting by hand. For the contaminated samples, the dry dog food pellets were milled in a ZM500 Retsch mill to particle size < 1.0 mm, and were added (to prevent loss of contamination during size reduction) to the clean samples so that the final samples consisted of 0.16 wt.% dry dog food contamination (which was determined as the amount of contamination present as explained in Section 4.2.5).

4.2 Feedstock characterisation

Four analyses were performed on the PS and LDPE/PET plastic feedstocks: ultimate composition, proximate analysis, energy content, and thermal degradation behaviour analysis.

4.2.1 Ultimate analysis

The ultimate analysis was performed with a Vario EL Cube elemental analyser from Elementar. The ultimate analysis quantified the amount of carbon (C), hydrogen (H), sulphur (S), and nitrogen (N). The oxygen content was then calculated as the difference of the organic fraction of the sample (i.e. on a moisture and ash free basis).

4.2.2 Proximate analysis

The proximate analysis was performed according to ASTM E1131 using thermogravimetric analysis with a TGA 5500 from TA Instruments. Samples were analysed with 2-6 repeats. The temperature protocol was as follows:

- Increase temperature by 50 ℃/min to 110 ℃ and isothermal at this temperature for 7 min under nitrogen flow (50 mL/min) to quantify moisture content.

- Increase temperature by 100 ℃/min to 900 ℃ and isothermal at this temperature for 5 min under nitrogen flow to quantify volatile matter content.

- Decrease temperature by 50 ℃/min to 525 ℃ and isothermal at this temperature for 5 min under oxygen flow (50 mL/min) to quantify the fixed carbon amount. The residue represented the

amount of ash in the sample.

4.2.3 Thermal degradation behaviour

Simulated pyrolysis of the plastic samples was performed using thermogravimetric analysis with a TGA 5500 from TA Instruments to characterise the thermal degradation behaviour of the plastic feedstocks. The temperature protocol was to heat the samples under nitrogen atmosphere from 50 ℃ to 600 ℃ with a heating rate of 10 ℃/min and the samples were analysed with 2-6 repeats. The resulting data was used to construct graphs of mass loss vs temperature and the derivative of the mass loss vs temperature (DTG). Important values, such as the onset, offset, and maximum temperature points were determined graphically.

4.2.4 Energy analysis

The energy value of the different plastic feedstocks was quantified as the higher heating value (HHV) determined by a bomb calorimeter (Cal2K Eco Calorimeter, model 2013). The analysis procedure was according to the ASTM standard D5865-11a and was performed in duplicate.

4.2.5 Contamination quantification

The amount of contamination present in the contaminated high-absorbent PS was quantified by weighing multiple clean punnets (clean high-absorbent PS) with a specific product identification number to determine the representative sample average mass. The punnets collected from Waste Plan recycling facility (contaminated high-absorbent PS) had the same product identification number as the clean punnets. These punnets were weighed before and after drying and equilibrating to ambient conditions to obtain the representative sample average mass. The difference in the average mass was taken as the contamination amount.

The contamination of the LDPE/PET multi-layer was determined by weighing some clean bags (from the supplier) and thereafter filling them with the dry dog food. After emptying the bags again, they were weighed once again, and the difference in the average mass (after contamination – before contamination) was taken as the mass of contamination.

4.2.6 LDPE and PET fraction quantification

The LDPE and PET amounts in the multi-layer plastic were determined from the derivative (DTG) curves established from TGA thermal degradation behaviour of the LDPE/PET multi-layer and of the DTG peaks from the individual LDPE layer and PET layer.

The LDPE and PET DTG peaks (signals) were found to overlap, therefore a deconvolution method was employed to separate the peaks. This was done in Matlab based on the resemblance of the peaks to skew Gaussian (normal) distributions and using code that was adapted from Curve fitting to get overlapping peak areas (2012). The method is summarised below:

- Estimate the mathematical model for individual peaks as stretched out Gaussian (normal) distributions with skewness (equation 4).

- Estimate the overlapping peak mathematical model as the sum of the individual model equations.

- Estimate the overlapping peak model parameters.

- Fit the estimated overlapping peak model using least squares regression.

- Extract the model parameters that relate to the individual peaks and replace them in the individual model equations to obtain the fitted mathematical models for the individual peaks.

The probability density function (pdf) of a skew-normal distribution can be given by the product of the pdf and the cumulative distribution function (cdf) of the standard normal distribution as in equation 1 (Figueiredo & Gomes, 2013):

$$pdf = f(y, \lambda, \delta, \alpha) = \frac{2}{\delta} \phi \left(\frac{y - \lambda}{\delta} \right) \Phi \left(\alpha \frac{y - \lambda}{\delta} \right) \qquad [1]$$

Where,

- ϕ is the pdf of the standard normal distribution.

- Φ is the cdf of the standard normal distribution.

- y is the random variable with the skew-normal distribution (which in this case would be temperature).

- λ is a location coefficient i.e. the location of the peak in terms of y.

- δ is a scale parameter i.e. the stretch of the distribution across y.

- α is a shape parameter i.e. the skewness of the distribution to the left or the right.

The pdf (ϕ) and cdf (Φ) of the standard normal distribution are given by equations 2 and 3:

$$\phi(x) = \frac{1}{\sqrt{2\pi}} e^{-\frac{1}{2}x^2} \tag{2}$$

$$\Phi(x) = \frac{1}{2}\left[1 + erf\left(\frac{x}{\sqrt{2}}\right)\right] \tag{3}$$

Where,

- x is the random variable with standard normal distribution.

- erf is an error function (built-in function in Matlab).

Equation 1 provides the pdf of a skew-normal distribution and it almost has the same shape as the DTG peaks. However, the pdf is restricted by the fact that the area under the pdf must be equal to 1. This is not the case with the DTG peaks and to overcome this restriction a fifth height parameter (h) was added to the equation in order to give it the capability to stretch out in the vertical direction. The final mathematical model (to model a single peak) which combines equations 1, 2, 3 and the height parameter is given in equation 4:

$$f(y, \lambda, \delta, \alpha) = \frac{2}{\delta}\left[\frac{1}{\sqrt{2\pi}} e^{-\frac{1}{2}\left(\frac{y-\lambda}{\delta}\right)^2}\right]\left[\frac{1}{2}\left(1 + erf\left(\frac{\alpha\frac{y-\lambda}{\delta}}{\sqrt{2}}\right)\right)\right] \times h \tag{4}$$

Once the peaks had been modelled, the area under the peaks were determined through numerical integration. As the DTG peaks represent the mass loss/temperature (wt.%/°C), the area under the peaks represent the mass loss (wt.%) due to the specific component in the sample (LDPE or PET). However, this information does not represent the actual composition of the multi-layer sample as the thermal degradation curves only account for the volatile fraction of the sample. Therefore, in order to determine the actual composition of the multi-layer in terms of the LPDE and PET fraction, calibration curves were constructed with the individual LDPE and PET layers.

The individual LDPE and PET layers were analysed in TGA at 2 different initial masses as summarised in Table 4.12, in duplicate. The DTG peaks were modelled with equation 4 and then numerically integrated to determine the area under the curve. Two calibration curves, one for each of the individual LDPE and PET layers, were then constructed as given in Figure 4.10 and Figure 4.11. An adequate linear fit to the calibration data is evident for both LDPE and PET from the R^2-values of 1 and 0.996 respectively.

The area under the deconvoluted peaks from the multi-layer DTG curve were then compared to the calibration curves to obtain the masses of the LDPE and PET layers in the multi-layer.

Table 4.12: Individual LDPE and PET calibration initial masses

Sample	Initial mass (mg)	
	LDPE	PET
1	12.43	7.56
2	12.35	7.61
3	36.72	10.91
4	36.81	11.09
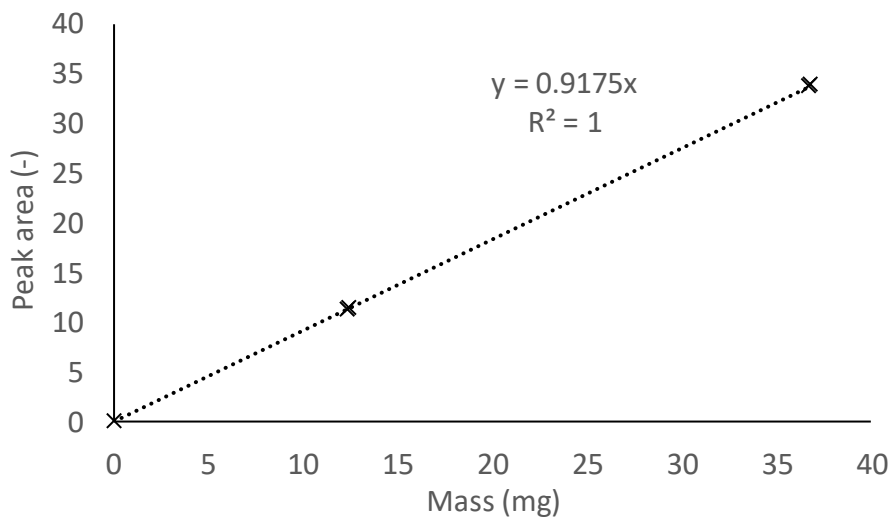
Figure 4.10: LDPE calibration curve
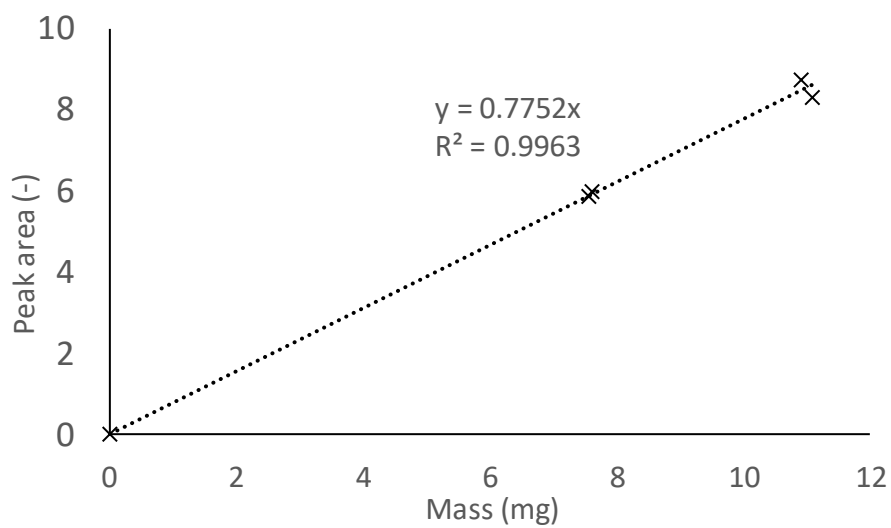
Figure 4.11: PET calibration curve

59

4.3 Bench scale pyrolysis

This section describes the bench scale pyrolysis experimental set-up and the design of experiments used for the optimisation study.

4.3.1 Bench scale pyrolysis experimental set-up

For both the PS and LDPE/PET plastic feedstocks, a gram-scale semi-batch reactor that was inductively heated was used to perform the bench scale pyrolysis tests. However, the condensation systems employed differed for the two plastic feedstocks as shown in Figure 4.12 (PS system) and Figure 4.13 (LDPE/PET system). The different condensation system for the LDPE/PET pyrolysis facilitated better separation of the wax and oil products, while the condensation for the PS pyrolysis did not require such addition as only oil was produced.

Figure 4.12 illustrates the set-up that was utilised for the PS pyrolysis tests. The PS samples (10.00±0.01 g) were placed in a Pyrex sample boat, that was placed in the middle of the stainless-steel reactor. The reactor had an inner diameter of 97 mm and a length of 445 mm. The heating of the reactor was via induction with the current being varied in the electrical coils to maintain the desired heating rate and final temperature. Nitrogen was used as the inert carrier gas and was supplied from a gas bottle upstream from the reactor. The flowrate of the nitrogen was controlled with an Alicat Scientific flow controller (model: MC-10SLPM-D/5M). Downstream from the reactor, the condensation system consisted of two stainless steel shell-and-tube condensers with a condensation pot in between. The shell-and-tube condensers were cooled with circulating water at 8 °C, with the first condenser having a counter-current flow and the second condenser having a co-current flow (as illustrated in Figure 4.12). The condensation pot was immersed in solid CO_2 (-78.5 °C). The final component after the second condenser was an electrostatic precipitator (ESP) which was set to 10 kV. The ESP ensured condensation of potential condensable volatiles remaining in the gas stream. The gas that exited the ESP was collected with Tedlar bags in 2-3 min increments to be analysed as described in Section 4.5.1.

Figure 4.13 presents the bench scale set-up used for the LDPE/PET multi-layer plastic experiments with LDPE/PET samples of 30.00±0.01 g being pyrolyzed during each test. The set-up is the same as was used for PS, but with a different condensation system: after the volatiles exited the reactor, they were condensed in a condensation pot at atmospheric temperature. From there, the remaining volatiles were condensed in 4 glass condensers that were immersed in solid CO_2 (-78.5 °C) and then the remaining entrained volatiles were captured with the ESP before the gas was collected in Tedlar bags in 2-3 min increments for analysis. This condensation system allowed better separation of the wax formed during LDPE and PET pyrolysis from the flowable oil formed, with most of the wax collecting in the atmospheric pot and the oil collecting in the 4 cooled condensers. However, this system did not ensure

perfect separation of the wax and oil.
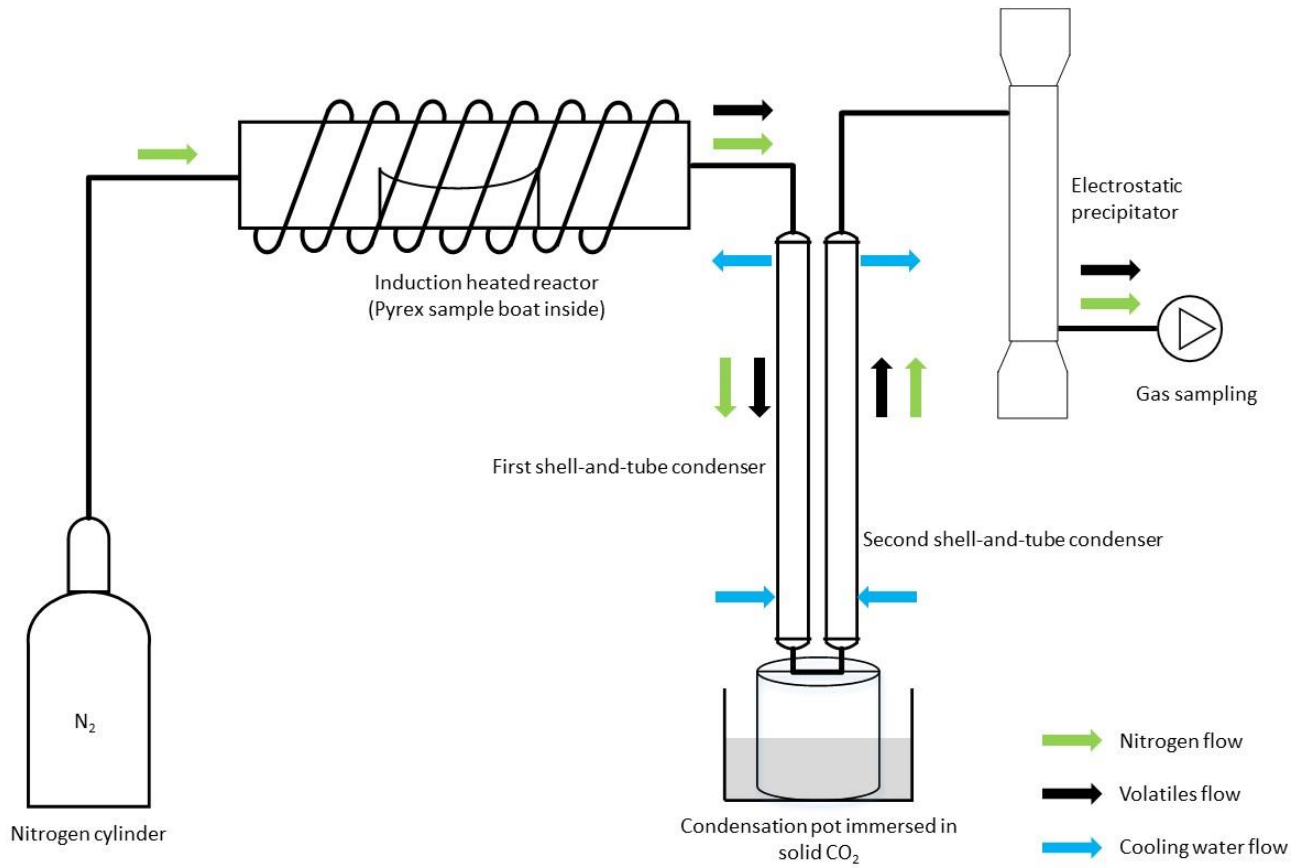
Figure 4.12: Schematic of bench scale pyrolysis system with condensation system employed for PS experiments
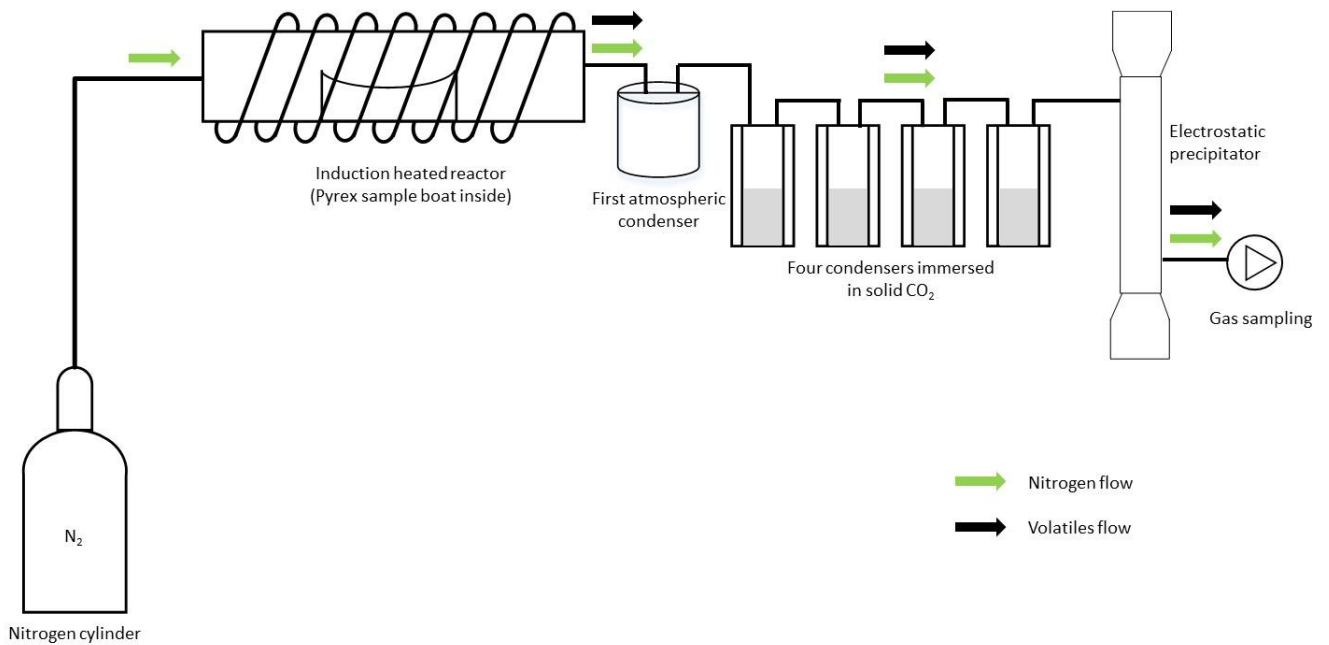
Figure 4.13: Schematic of bench scale pyrolysis system with condensation system employed for LDPE/PET experiments

4.3.2 Product yields determination

The product (oil/wax, char, and gas) yields were determined using equations 5 to 7. The gas yield was also determined using the gas characterisation and equation 13 described in Section 4.5.1.

$$Oil/wax\ yield\ (wt\%) = \frac{m_{after} - m_{before}}{m_{sample}} \times 100\% \qquad [5]$$

$$Char\ yield\ (wt\%) = \frac{m_{residue}}{m_{sample}} \times 100\% \qquad [6]$$

$$Gas\ yield\ (wt\%) = 100\% - Oil\ yield - Char\ yield \qquad [7]$$

Where,

- m_{after} is the mass of all the set-up components where oil/wax product was condensed (condensers, connecting pipes, and ESP) after the pyrolysis experimental run.

- m_{before} is the mass of all the set-up components where oil/wax product was condensed before the pyrolysis experimental run.

- $m_{residue}$ is the mass of the residue left in the sample boat after the pyrolysis experimental run.

- m_{sample} is the mass of the original plastic sample.

4.3.3 Bench scale pyrolysis design of experiments

This section explains how the experiments were organised for the bench scale pyrolysis to meet the objective of optimising the oil/wax yield.

4.3.3.1 Polystyrene single-layer plastic

As stated in Section 4.1.1, three batches of the polystyrene plastic were studied: a clean high-absorbent batch, a contaminated high-absorbent batch specifically used to package raw meat, and a contaminated high-density batch. The design of experiments at bench scale was organised as follows:

- Preliminary experiments to determine the effect of the nitrogen flow rate with 0.5 L/min and 2.0 L/min being compared.

- 2-Factor factorial design with clean high-absorbent PS, with temperature and heating rate as factors to optimise the oil yield. The temperature range was 450-550 °C and the heating rate range was 25-200 °C/min, with 3 centre point runs at 500 °C and 112.5 °C/min. These factors were chosen for the study as temperature is considered the most important parameter during

pyrolysis (López *et al*., 2011; Sharuddin *et al*., 2016) and the effect of heating rate is not clear as very few studies include it as a variable.

- 3 Repeats with the contaminated high-absorbent PS at conditions determined from the factorial design to determine the effect of contamination.

- 2 Repeats with the contaminated high-density PS at conditions determined from the factorial design to compare this batch with the high-absorbent batches.

- The feedstock residence time was kept constant at 30 min and the nitrogen flow rate was kept constant at 0.5 L/min (giving a volatile residence time of 3 min 17 s in the heated zone).

4.3.3.2 LPDE/PET multi-layer plastic

For the LPDE/PET multi-layer, a clean and a contaminated version was tested, as explained in Section 4.1.2. As temperature has been found in literature to be the factor with the major effect (López *et al*., 2011; Sharuddin *et al*., 2016), it was the only factor that was optimised for. The optimisation was performed with the clean multi-layer in the range of 475-700 °C with 2 repeats at each temperature. Similar to the PS design, 2 repeats with the contaminated multi-layer, at the optimised conditions from the clean multi-layer experimental runs, were performed. The feedstock residence time was kept constant at 30 min and the nitrogen flow rate was kept at 0.5 L/min.

4.4 Pilot scale pyrolysis

The pilot scale set-up is illustrated in Figure 4.14. The plastic feedstock was dropped into the feed hopper and was then deposited into the feeding pipe via gravity by the action of two pneumatic valves. The first valve opened, dropping the feedstock to the second valve and then closed where-after the second valve opened to drop the feedstock into the feeding pipe in front of the motorised feeding cylinder. This double valve action was employed to limit the escape of volatiles through the feed hopper and limit the introduction of oxygen in the reactor. The motorised cylinder then pushed the plastic feedstock into the stainless-steel reactor. The reactor was electrically heated in a furnace and rotated continuously. The rotation of the reactor coupled with baffles on the inside wall of the reactor ensured the forward motion of the feedstock and the solid residue in the reactor. The solid residue exited the reactor and gathered in the char pot (from where it could be recovered), which was heated to 270 °C to mitigate the condensation of heavier MW compounds in the char pot. The volatiles formed in the reactor were swept out by the flow of nitrogen (1.0 L/min). The volatiles left the reactor and were swept past the char pot into an exit pipe heated at 270 °C to prevent condensation of the volatiles in the pipe. From there the volatiles entered the condensers, the first of which was at ambient temperature. Condensers 2,

3 and 4 were counter-currently cooled with cooling water with an initial temperature of 8 °C. The condensable fraction of the volatiles could be recovered at the end of the test in the four condensers. After the condensers, the non-condensable gasses were extracted with a vacuum pump to reach one of the two water filled gas towers (which allowed the quantification of the volume of gas) and then vented. Gas samples were taken with Tedlar bags from the gas sampling point after the fourth condenser for composition analyses (Section 4.5.1).
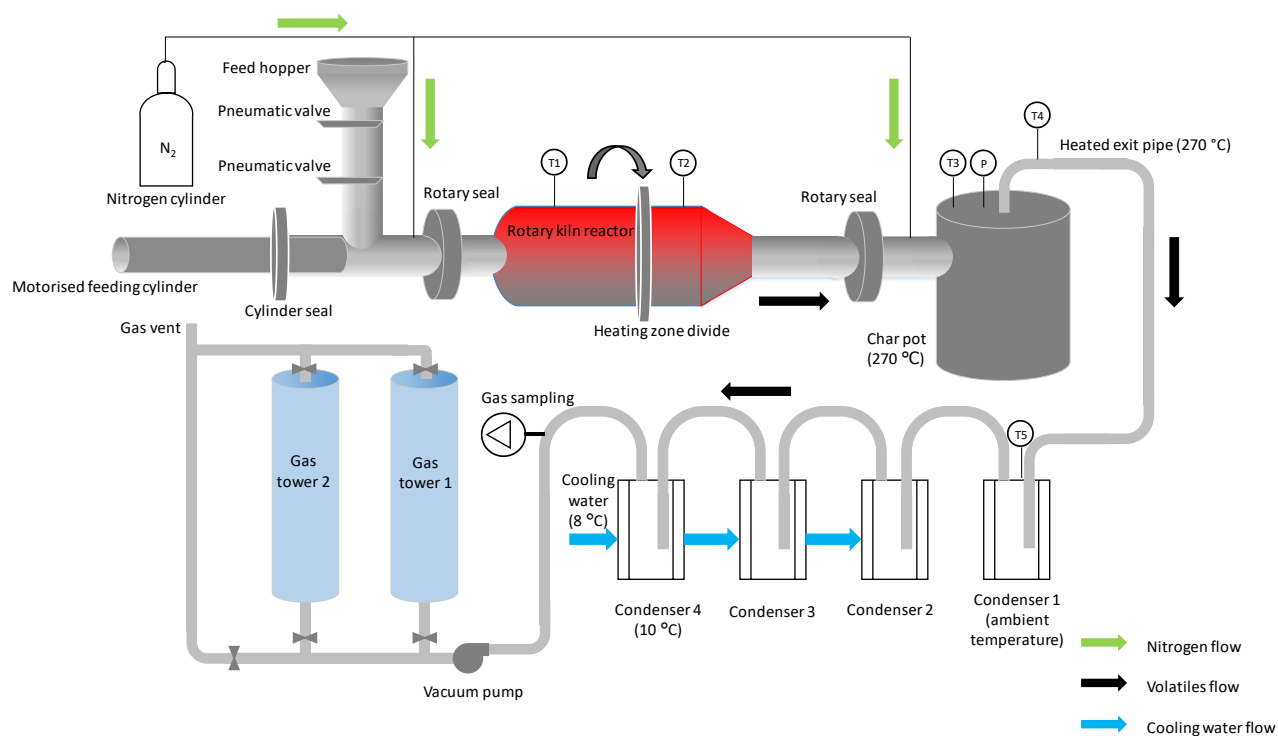
Figure 4.14: Simplified schematic of pilot scale experimental set-up

4.5 Product analysis

This section explains how the products from bench and pilot scale pyrolysis were analysed to determine the composition and some properties related to fuel applications.

4.5.1 Gas composition characterisation and energy estimation of gas

The gas sampled with Tedlar bags, was analysed for its molecular composition via gas chromatography using a Compact GC 4.0 from Global Analyser Solutions. The instrument employs three columns and detectors that were calibrated to quantify different gaseous compounds: A flame ionisation detector (FID) to analyse for C_3-C_6 hydrocarbons; a thermal conductivity detector (TCD) to analyse for C_2 hydrocarbons and CO_2, and a second TCD to analyse for H_2, N_2, O_2, CO and CH_4.

The analysis determined the volume% of the different compounds in the gas sample in a Tedlar bag. Using this information and the nitrogen flow rate, the weight% yield of the gas could be determined.

64

Equation 8 was used to determine the volume of compound i in the tedlar bag sample, based on the nitrogen flow rate used, the sampling time, and the concentration of nitrogen in the sample. The moles of compound i could then be determined by assuming ideal gas behaviour, where 1 mole of ideal gas is equal to 22.4 L of the gas, as in equation 9. The moles of compound i was then converted to the mass of compound i by multiplying by the molecular mass of compound i, as in equation 10. The total mass of compound i evolved during the experiment was then calculated as the sum of compound i in all the sample bags (equation 11). The total mass of gas evolved during the pyrolysis experiment was obtained by summing all compounds i evolved during the experiment. Finally, the gas yield was determined as the mass of gas over the mass of plastic sample tested (equation 12).

$$V_{i,bag} = \frac{V\%_i}{V\%_{N_2}} \times \dot{V}_{N_2} \times t_{sampling} \tag{8}$$

$$n_{i,bag} = \frac{V_{i,bag}}{22.4} \tag{9}$$

$$m_{i,bag} = \text{n}_{i,bag} M_i \tag{10}$$

$$m_{i,experiment} = \sum m_{i,bags} \tag{11}$$

$$Gas\ yield\ (wt.\%) = \frac{m_{gas}}{m_{sample}} \times 100 \tag{12}$$

Where,

- $V_{i,bag}$ is the volume of compound i (L) in the sample bag.

- $V\%_i$ is the volume % of the compound i in the sample bag as determined with the GC instrument (vol%).

- $V\%_{N_2}$ is the volume % of nitrogen in the sample bag as determined with the Compact GC (vol%).

- $\dot{V}_{N_2}$ is the volumetric flow rate of the nitrogen (L/min) used to purge the reactor.

- $t_{sampling}$ is the time that the gas was sampled (min) in the bag.

- $n_{i,bag}$ is the moles of compound i in the sample (mol).

- $m_{i,bag}$ is the mass of compound i in the sample (g).

- M_i is the molecular mass of compound i (g/mol).

- $m_{i,experiment}$ is the total mass of compound i evolved during the experiment (g).

- m_{gas} is the total mass of non-condensable gas formed during the pyrolysis experiment (g). Obtained by summing the mass of all gas compounds evolved during the experiment.

- m_{sample} is the mass of the plastic sample pyrolysed (g).

The energy content of the gas was calculated from the composition of the gas in terms of the calibrated gaseous compounds and the theoretical HHV of these compounds (Table 2.3). From this result, the gross energy recovered in the gas product from the plastic feedstock was calculated as in equation 13.

$$Gross\ energy\ recovered\ (\%) = \frac{(HHV_{gas})(Gas\ yield)}{HHV_{feedstock}} \qquad [13]$$

4.5.2 Energy analysis of oil/wax products

The energy value of oil/wax was quantified as the higher heating value (HHV) determined by a bomb calorimeter (Cal2K Eco Calorimeter, model 2013). The analysis procedure was according to the ASTM standard D5865-11a performed in duplicate. For the PS derived oil, representative samples from the condensation pot at bench scale and the 4 condensers at pilot scale were tested. For the multi-layer derived oil/wax, representative samples of the oil and wax were tested, and it is worth noting that the HHV of the wax showed non-significant differences from the oil samples. The gross energy recovered in the oil/wax from the plastic feedstock was determined using equation 14:

$$Gross\ energy\ recovered\ (\%) = \frac{(HHV_{oil/wax})(Oil/wax\ yield)}{HHV_{feedstock}} \qquad [14]$$

4.5.3 Polystyrene derived oil composition characterisation

The oil product from the pyrolysis of PS was analysed for its composition in terms of the most abundant compounds as determined from literature. These compounds are styrene, toluene, ethylbenzene, α-methylstyrene, and styrene dimer (Zhang *et al*., 1995; Park *et al*., 2003; Mo *et al*., 2014; Artetxe *et al*., 2015).

The instruments used to do the qualitative and quantitative analysis of these compounds were a Hewlett Packard 5890 Series II gas chromatographer (GC) coupled with a Hewlett Packard 5973 mass-spectrometer (MS) from Agilent Technologies. The column was a Zebron ZB-1701 capillary column with 60 mm length, 0.25 mm ID and 0.25 µm film thickness. The carrier gas was Helium with a purity of 99.999% at a flow rate of 1.3 mL/min. The samples were injected at a split ratio of 1:70 and the

temperature program employed was as follows:

- Isothermal at 45 ℃ for 10 min.

- Temperature increase to 100 ℃ at a heating rate of 2 ℃/min.

- Temperature increase to 260 ℃ at a heating rate of 7 ℃/min.

- Isothermal at 260 ℃ for 24 min.

The oil samples were prepared by weighing 40 µL of the oil sample and diluting it with 2 mL Acetone (purity of 99.8%) and 1 mL internal standard (IS) solution. The IS used was 2-Octanol diluted with Acetone to have a concentration of 3.041 mg/mL. The final concentration of the IS in all the samples was constant at 1.014 mg/mL

Calibration of the instrument for the compounds was performed at five different concentrations as summarised in Table 4.13. The concentration of the IS in the standard solutions was kept constant at 1.014 mg/mL. The calibration curves were constructed as the ratio of the concentration of the compound to that of the IS and compared to the ratio of the signal area of the compound (based on specific fragmentation ions) to that of the IS.

Table 4.13: Calibration standard concentrations of PS derived oil compounds

Compound	Concentration (mg/mL)				
	Standard 1	**Standard 2**	**Standard 3**	**Standard 4**	**Standard 5**
Styrene	15.120	7.457	3.678	2.237	1.103
Toluene	1.493	0.737	0.363	0.221	0.109
Ethylbenzene	2.033	1.003	0.495	0.301	0.148
α-Methylstyrene	2.887	1.437	0.716	0.356	0.177
Dimer (1,4-diphenyl butane)	2.040	1.006	0.496	0.302	0.149

Many different styrene dimer species have been reported in literature such as 1,3-diphenylpropane, 1,2-diphenylethylene, and 1,1-diphenyl-1,3-butadiene (Section 2.4.4). As some of the dimer species are not commercially available, a semi-quantitative method was employed whereby one commercially available dimer species (1,4-diphenyl butane) was calibrated for to approximate the entire range of dimers. The calibration curve of 1,4-diphenyl butane is illustrated in Figure 4.15 where the signal areas (using the total ion chromatogram) and concentrations of the dimer are compared to that of the IS to

obtain a straight line fit with R^2-value of 0.99. To obtain the concentration of dimers in the PS pyrolysis oil samples, the areas of the signals around the retention time of 1,4-diphenylbutane (57.35 min) were added and compared with that of the IS standard and finally, the total concentration of the dimer species was estimated using the calibration curve in Figure 4.15 and the concentration of the IS in the sample.
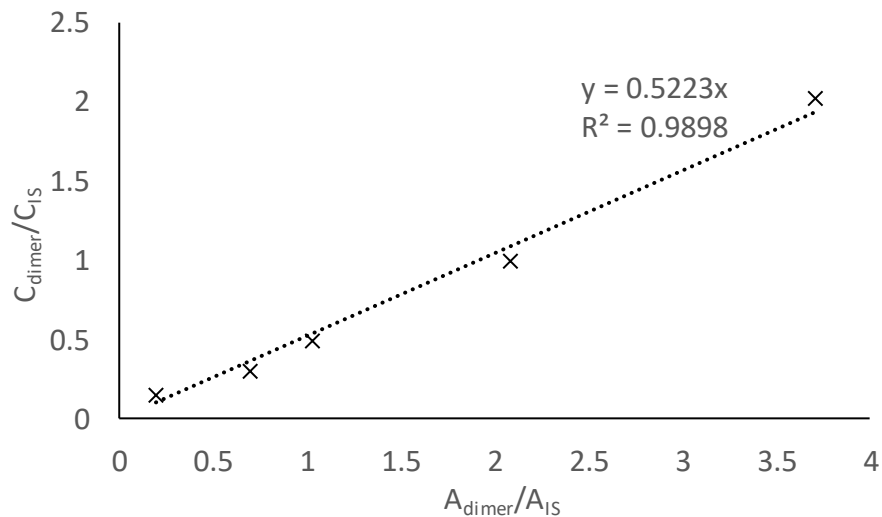
Figure 4.15: Calibration curve for 1,4-diphenyl butane (styrene dimer)

4.5.4 Fuel properties

Samples of the oil/wax produced at pilot scale were tested for their fuel properties at Intertek, Cape Town. Below is summarised the properties tested, and the standard test methods used:

- Distillation behaviour: ASTM D86

- Ash content: ASTM D482

- Pour point: ASTM D97

- Density at 15 °C: ASTM D4052

- Sulphur content: ASTM D4294

- Kinematic viscosity at 40 °C: ASTM D445

- Flash point: ASTM D93

5 Results and discussion

This section is organised by firstly considering the PS feedstock characterisation and bench scale testing in Sections 5.1 and 5.2. Following this is the discussion regarding the feedstock characterisation and bench scale testing of the LDPE/PET multi-layer in Sections 5.3 and 5.4. Lastly, the results from the pilot scale testing of both the PS and the multi-layer are presented and discussed in Sections 5.5.1 and 5.5.1.5 respectively, with major operational difficulties associated with pilot scale pyrolysis being considered in Section 5.6.

5.1 Polystyrene feedstock characterisation

Three different batches of PS feedstock were used in this study (as described in Section 4.1.1): a clean high-absorbent batch, a contaminated high-absorbent batch (to test the effect of a high amount of meat juice contamination), and a contaminated high-density batch (to be used in the pilot reactor). This section provides the characterisation of these three batches in terms of the ultimate and proximate analysis, the energy content of the PS feedstock as the HHV, the amount of contamination present, and the thermal degradation behaviour.

5.1.1 Polystyrene composition, energy content and impact of contamination

Table 5.14 summarises the results from ultimate, proximate and HHV analysis of the three PS feedstock batches and compares them with the literature values as was previously outlined in Table 2.1.

Table 5.14 shows that the clean high-absorbent batch compared well with what was expected from literature, as most literature studies were also performed with clean plastics. However, a slightly higher value can be seen with the sulphur and ash content, which indicates the presence of more additives used in the processing of this type of PS punnet. The overall analysis suggests that this plastic is favourable for conversion into a hydrocarbon condensable product via pyrolysis with its high C and H content ($>$ 99 wt.%), high volatile matter ($>$ 96 wt.%), its low moisture ($<$ 0.2 wt.%), fixed carbon ($<$ 2 wt.%) and ash content ($<$ 2 wt.%), and its HHV of 37.2±0.8 MJ/kg, which is about 13% below the range for commercial diesel (42.8-45.8 MJ/kg).

Table 5.15 sets out the contamination amount in the contaminated high-absorbent PS in terms of the total contamination, moisture from contamination (assuming that only moisture was removed during drying) and the dry contamination left when the PS punnets had been dried and left to settle to ambient moisture content, as explained in Section 4.1.1. It is clear that the majority of the contamination was due to moisture. Moisture contamination represented around 46.5 wt.% of the wet contaminated

punnets, while the dry contamination represented about 8.9 wt.%. Therefore, drying of this type of contaminated feedstock is essential for the pyrolysis process, as high amounts of moisture cause inefficient heating during pyrolysis and result in significant amount of water in the oil fraction, which degrades the quality of the oil for fuel applications. For the final feedstock used in the bench scale experiments (i.e. the dried punnets that have settled to ambient moisture content), the total dry contamination was 15.9±1.3 wt.%.

Comparison of the clean and contaminated high-absorbent batches supplies information on the effect of the contamination (predominantly meat juice) on the fuel characteristics of the feedstock as summarised in Table 5.14 (where the results for the contaminated high-absorbent PS are based on the dried/settled feedstock). A significant decrease in C content was balanced by an increase in the N and O content (approximately 3 wt.%). The basic units of protein, amino acids, can have an O:N mass ratio in the range of 0.6-4.6, based on the structure of the 20 commonly occurring amino acids (Daintith, 2008). The average O:N mass ratio in the contaminated high-absorbent PS from Table 5.14 was 3.98 and is therefore in the range expected from contamination composed mostly of protein.

The slightly higher fixed carbon content observed for the contaminated vs the clean high-absorbent PS (higher by approximately 1 wt.%) in Table 5.14 can also be attributed to the presence of proteins (Wei *et al.*, 2018). It means that a slightly greater minimum char yield and therefore a decreased oil yield can be expected. The moisture content of the dried contaminated PS was approximately 0.19 wt.% higher than for the clean PS, but still quite low and within the ranges reported in literature (0.3-1.4 wt.%). It indicates that following drying, some moisture was adsorbed under ambient conditions, due to the polarity of the contamination component. Overall, the results in Table 5.14 indicate that the dried contaminated high-absorbent plastic is suitable for pyrolysis when targeting a hydrocarbon rich oil yield, with its high C and H content (> 95 wt.%), high volatile matter (> 95 wt.%), with low moisture (< 0.4 wt.%), fixed carbon (< 3 wt.%) and ash content (< 2 wt.%). Its HHV of 37.6±0.2 MJ/kg was found to be similar to that of clean PS and slightly lower than that of commercial diesel, making it favourable for a pyrolysis process to produce fuel oil.

The contaminated high-density PS is the batch that was used during pilot scale testing (as explained in Section 4.1.1). As can be seen in Table 5.14, it had a similar composition in terms of the ultimate analysis to that of the contaminated high-absorbent PS, but with a lower N content (0.18 wt.% compared to 0.65 wt.%). The lower N content makes sense as the contaminated high-density batch was a mixture of black PS from varying origins (i.e. not just the punnets used to package raw meat), thus a lower content of protein was expected. Table 5.14 shows that the contaminated high-density batch contained a higher amount of sulphur-compound-contamination (0.52 wt.% compared to 0.13 and 0.15 wt.% for the two high-absorbent batches). It means that in the context of combustion application (of the feedstock

or pyrolysis-derived products), this feedstock will be the source of less NO_x and more SO_x emissions. It is worth noting that the N- and S-contents are below that of coal at about 1.4 and 1.5 wt.% respectively (Caillat & Vakkilainen, 2013). In terms of the proximate analysis (Table 5.14), the contaminated high-density PS had a high volatile matter content (> 95 wt.%) and low fixed carbon (< 0.3 wt.%) and moisture content (< 0.1 wt.%), making it favourable for conversion to an oil product via pyrolysis. Additionally, the contaminated high-density PS had a significantly higher ash content (3.27±1.38 wt.% in Table 5.14) than the other PS batches, which indicated more inorganic contamination, which could result in a possible catalytic effect, as has been reported by López *et al.* (2010). The HHV of this batch at 39.8±0.3 MJ/kg was similar to the high-absorbent batches.

Table 5.14: Characterisation in terms of ultimate, proximate, and energy contents of PS for the three different feedstock batches

	Parameter	Literature Value	Clean high-absorbent	Contaminated high-absorbent	Contaminated high-density
Ultimate analysis (wt.%) dry, ash-free basis	**C**	92.3 (pure PS) 89.5-92.7	92.16±0.05	88.97±0.63	87.62±2.09
	H	7.7 (pure PS) 7.2-8.5	7.69±0.03	7.64±0.04	7.67±0.36
	N	0 (pure PS) 0.0-3.0	< 0.03 (LOD)	0.65±0.14	0.18±0.05
	S	0 (pure PS) 0.0	0.13±0.04	0.15±0.06	0.52±0.00
	O*	0 (pure PS) 0.0-0.5	< 0.1	2.59±0.50	4.26±1.92
Proximate analysis (wt.%)	**Moisture**	0.30-1.4	0.11±0.00	0.30±0.06	0.09±0.01
	Volatile compounds	98.5-99.6	96.84±0.22	95.68±0.01	96.40±1.32
	Ash content	0.0	1.58±0.18	1.77±0.10	3.27±1.38
	Fixed carbon	0.2-1.5	1.47±0.04	2.25±0.03	0.24±0.05
Energy value	**HHV (MJ/kg)**	38.2-42.1	37.22±0.79	37.64±0.23	39.82±0.30

*by difference; LOD = limit of detection

Table 5.15: Total, moisture, and dry contamination of contaminated high-absorbent PS

	Amount (wt.%)
Total contamination (based on wet punnets)	55.4±10.0
Moisture contamination (based on wet punnets)	46.5±10.7
Dry contamination (based on wet punnets)	8.9±1.3
Dry contamination (based on dried punnets under ambient conditions)	15.9±1.3

Clean punnets mass (based on 40 punnets) = 6.1±0.2 g

Contaminated wet punnets (based on 36 punnets) = 13.7±9.5 g

5.1.2 Thermal degradation behaviour

Figure 5.16 illustrates a comparison of the thermal degradation behaviour of the three PS feedstocks, as determined with TGA at a heating rate of 10 °C/min. The clean high-absorbent PS started to degrade at about 370 °C, reached the maximum degradation rate at 435 °C (maximum rate of 30 wt.%/min) and ended at about 480 °C. This is consistent with literature values that reported the start, maximum, and end temperature ranges as 360-380 °C, 400-430 °C, and 420-480 °C respectively (Diaz-Silvarrey & Phan, 2016; Park *et al*., 2003). The contaminated high-absorbent PS had the same maximum degradation point and end temperature as the clean high-absorbent PS, but the degradation of the contaminated high-absorbent PS started at an earlier temperature (approximately 250 °C), which is consistent with the presence of proteins. Indeed, protein has been reported to start degrading in the range of 220-250 °C (Wei *et al*., 2018; Kebelmann *et al.,* 2013). Except for the earlier degradation of the protein contamination, the clean high-absorbent and contaminated PS samples behaved almost identically, which indicates insignificant interaction effects at TGA scale between the pure PS and the contamination, and the absence of any significant catalytic effect from the contamination. The high-density PS started to degrade earlier (at about 350 °C) and had a lower maximum degradation temperature (425 °C) than the clean high-absorbent PS feedstock. This difference could be due to a catalytic effect from the inorganic contamination (this batch had the higher ash content, Table 5.14) or a more degraded structure of the PS plastic, which could be the consequence of the thermal treatment endured at 270 °C during densification.
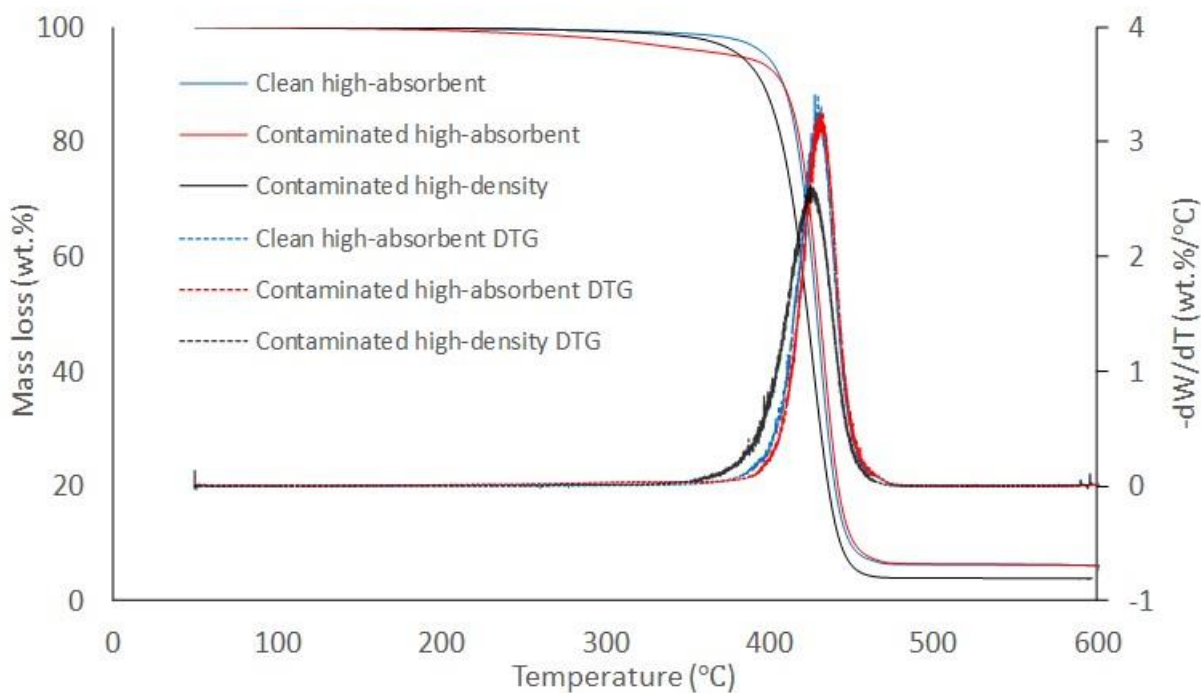
Figure 5.16: Thermal degradation behaviour of the three PS feedstocks. Heating rate = 10 ℃/min

5.2 Bench scale pyrolysis of polystyrene

This section presents the results obtained from the bench scale pyrolysis of the PS feedstock, where the main goal was to optimise the yield of the oil product and to determine its quality in terms of the HHV and composition. The polystyrene bench scale testing was organised as follows:

- Preliminary testing to determine the effect of the nitrogen flow rate on entrainment of condensable volatiles in the gas stream.

- Optimisation of the oil yield from the pyrolysis of the clean high-absorbent PS with temperature and heating rate as influencing factors.

- After optimisation with the clean PS, the optimised conditions were used to assess the influence of contamination in the 2 contaminated batches i.e. the contaminated high-absorbent with meat juice ("worst case scenario") and the contaminated densified batch.

The section is organised by first presenting the results from the tests as outlined above. Thereafter, the energy and composition of the oil and gas products are presented.

5.2.1 Preliminary nitrogen flow rate tests

Figure 5.17 illustrates the effect of nitrogen flowrate on the yield of products from the pyrolysis of PS. Typically, with biomass and most of the plastic feedstock, a higher flowrate, which translates to a shorter volatile residence time, would be expected to cause an increase in oil yield and a corresponding decrease in gas yield, as it limits secondary reactions (Parku, 2019; Chireshe, 2019). However, what is important to notice in Figure 5.17 is the opposite trend, observed as a decrease in oil yield (approximately 30 wt.% decrease) at the higher flowrate of 2.0 L/min compared to 0.5 L/min. This decrease in oil yield was interpreted as a consequence of incomplete condensation, as described in other works (Chomba, 2018). It is likely that some condensable volatiles were entrained in the carrier gas stream and exited the condensation system with the non-condensable gasses. This is reflected in the calculated gas yield (which was here determined by difference: 100% - oil yield - char yield), which reached values up to 44 wt.% at the higher nitrogen flowrate. Based on the chemical structure of PS, the theoretical maximum gas yield is 24 wt.% (Section 2.4.2). Therefore, it is clear that some condensable volatiles were entrained with the non-condensable gasses. The oil yield at the flow rate of 0.5 L/min was 92±4 wt.%, which is close to the optimum oil yield reported in literature (Section 2.4.3.3). Therefore, the flowrate of 0.5 L/min appeared suitable and was not further optimised. Additionally, these preliminary tests confirmed that the pyrolysis of PS yields only oil, gas and char, with no wax formation being observed, as reported elsewhere (Mo *et al.*, 2014; Miandad *et al.*, 2016b). The oil was mostly collected in the condensation pot (Figure 4.12).
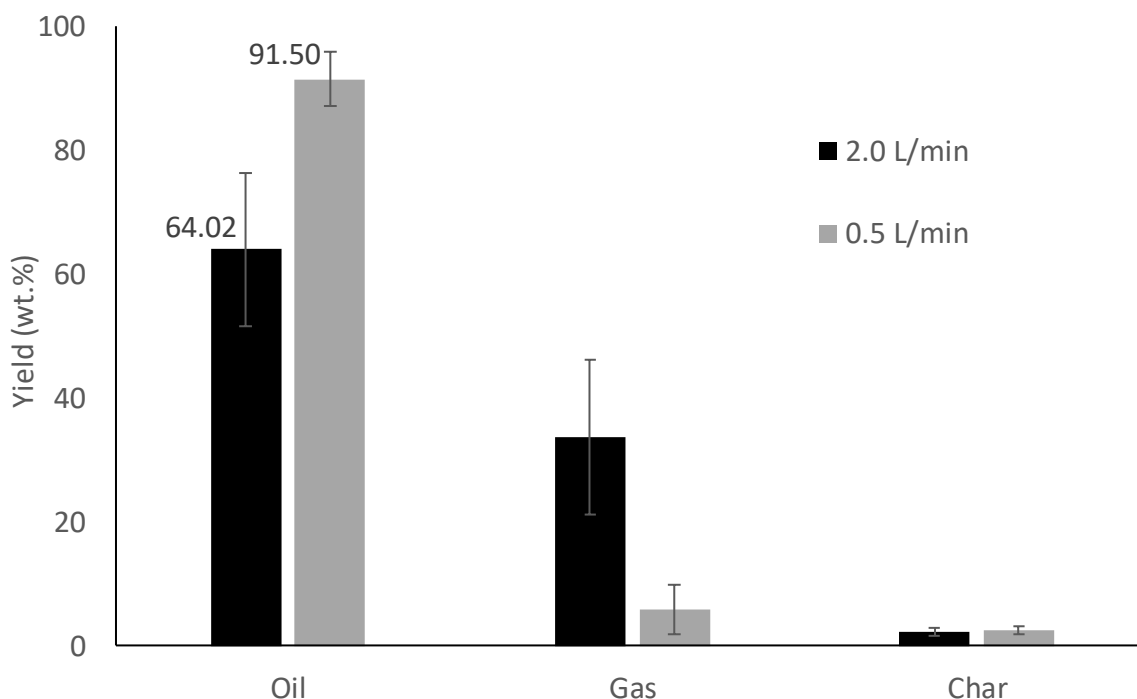
Figure 5.17: Effect of nitrogen flowrate on product yields at 500 ℃ and an intermediate heating rate (approximately 200 ℃/min)

5.2.2 Optimisation of oil yield from clean high-absorbent PS

Statistical optimisation of the oil yield when pyrolyzing the clean high-absorbent PS at bench scale was done using a 2-factor factorial design of experiments. The factors investigated were temperature in the range of 450-550 °C and heating rate in the range of 25-200 °C/min. The mass balance closure was greater than 94 wt.% for all experimental runs. Table 5.16 presents the ANOVA results for this design and it can be seen that the heating rate and interaction (between temperature and heating rate) effects were non-significant with p-values of 0.54 and 0.89 ($\gg$ 0.05) respectively. It confirmed that, on the studied range, heating rate did not significantly affect the oil yield. The temperature effect, with a p-value of 0.08, was significant at a 92% confidence interval. Ignoring the non-significant heating rate and interaction effects yielded the ANOVA results for temperature alone, as presented in Table 5.17. This confirmed the significant effect of temperature with an increased confidence of 98%.

Table 5.16: ANOVA for 2-factor statistical design for bench scale pyrolysis of clean high-absorbent PS

	SS	df	MS	F	p
Temperature (°C)	9.67	1	9.67	7.14	0.08
Heating rate (°C/min)	0.64	1	0.64	0.47	0.54
Interaction	0.03	1	0.03	0.02	0.89
Error	4.06	3	1.35		
Total	14.4	6			

Table 5.17: ANOVA for 2-factor statistical design with insignificant effects ignored for bench scale pyrolysis of clean high-absorbent PS

	SS	df	MS	F	p
Temperature (°C)	9.67	1	9.67	10.21	0.02
Error	4.74	5	0.95		
Total	14.41	6			

Figure 5.18 presents the residuals of the ANOVA model graphically in order to test the assumptions related to ANOVA. Figure 5.18a proves that the residuals are normally distributed with a straight-line trend through the origin. Figure 5.18b shows the trend in the residuals with time (i.e. the run order as the experiment progressed) and suggests that with time the residuals decreased. However, this does not conclusively prove dependence on time as the centre points are the important points to analyse residuals (as the centre points provide the variance necessary to make inferences about deviation from the mean) and as there are only three centre points, an increasing or decreasing trend like this could easily be obtained. A closer look at the centre point residuals shows that the first two (case number 1 and 2) have

positive deviation from the model, while the third centre point (case number 6) displays negative deviation, which created the decreasing trend but did not conclusively prove dependence on time. Figure 5.18c displays the effect of the predicted oil yield values on the residuals, and looking at the centre points, it can be seen that the data is reasonably unstructured, suggesting constant variance (homoscedasticity).
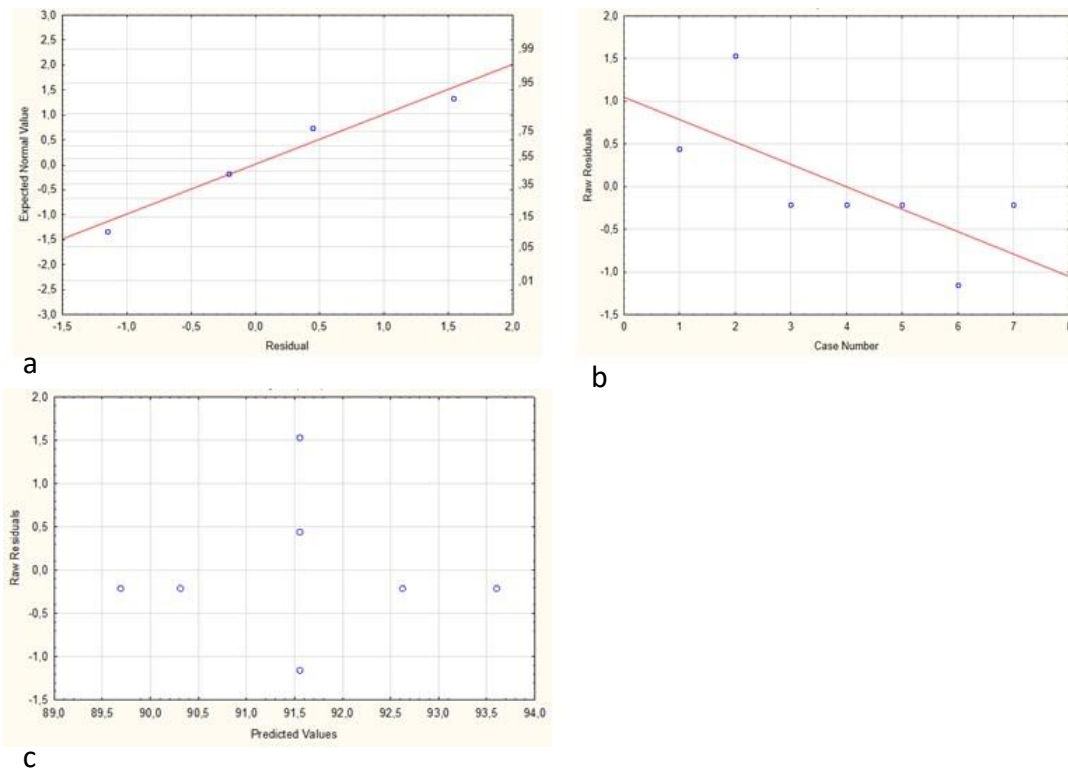
Figure 5.18: ANOVA model (clean high-absorbent PS oil yield optimisation at bench scale) adequacy check with residuals. a) normal probability of residuals; b) residuals vs run order/time (case number); c) residuals vs model predicted (oil yield) values

Figure 5.19 graphically presents the response surface of the temperature and heating rate effect on the oil yield. The figure illustrates that as temperature increased from 450 to 550 ℃, the oil yield increased from about 90 to 93 wt.%. The linear relationship between temperature and oil yield suggests that the oil yield would keep increasing beyond 550 ℃ (the upper limit of the temperature range studied). However, a factorial design of experiments can only estimate a linear model and the adjusted R^2-value is 0.44, meaning that the linear model does not fit the data well.
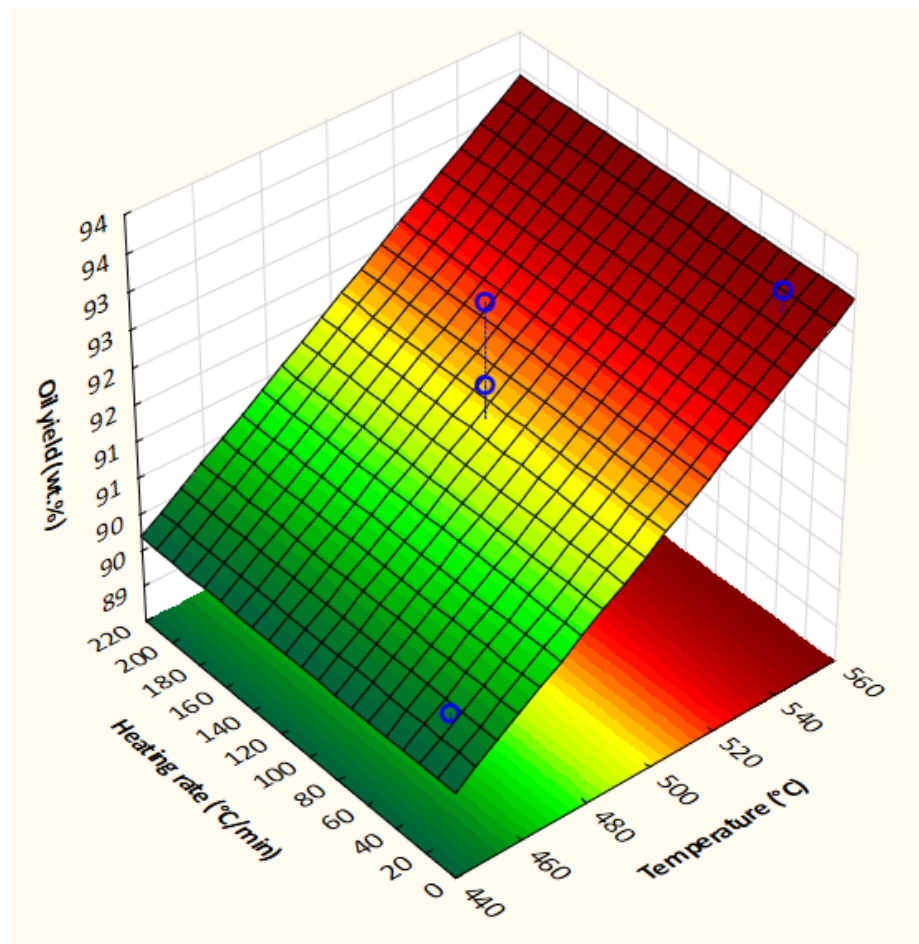
Figure 5.19: Response surface of 2-factor factorial design of clean high-absorbent PS at bench scale

To further investigate the relationship between temperature and oil yield at temperatures higher than 550 °C, an additional data point was generated at 600 °C. The effect of temperature on the oil yield, with this additional data point is illustrated in Figure 5.20. The oil yield increased from 89.8±0.4 to 91.8±1.4 wt.% as temperature was increased from 450 to 500 °C, which from literature can be expected to be balanced by a decrease in char yield, due to more complete degradation at higher temperature (Miandad *et al.*, 2016). To test this expectation the effect of temperature on the char yield is shown in Figure 5.21. A slight (non-significant) decrease in char yield as temperature increased can be observed. However, the decrease in char yield was too little to explain the increase in oil yield. This is especially observable from 450 to 500 °C, where the char yield decrease was an average of 0.07 wt.%, while the oil yield increased by approximately 2 wt.%. A look at the mass balances shows that the closure was less at 450 °C than at 500 °C by about 2 wt.%, which would account for the oil yield increase.

At pyrolysis temperatures between 500 and 600 °C, a significant difference in the oil yield data points is not evident (p-value of 0.49), but rather a plateauing (second-order effect) of the data is observed in Figure 5.20. This shows that the optimum point in oil yield is probably in this region. As oil yields in this region were similar (from 91.8±1.4 to 93.2±1.4 wt.%), it was considered that there was no need to investigate other temperatures in this range. Higher temperatures were not tested because converting PS

at such high temperatures would likely affect the energy efficiency of the process negatively and it would probably result in little to no improvement in oil yield. The assumption that higher temperatures (beyond 600 °C) would not result in greater oil yields can be supported by looking at Figure 5.21, which illustrates the effect of temperature on the char and gas yields. The char yield was less than 5 wt.% and decreased only slightly for temperatures greater than 450 °C (0.2 wt.% decrease from 450 to 550 °C), suggesting that full degradation was being achieved, as has been found by other studies such as Williams and Williams (1997, 1999b), Kaminsky *et al*. (2004), Shah and Jan (2014), and Miandad *et al*. (2016b). Furthermore, a slight increase in gas yield can be observed as the temperature increased (increase of 0.42 wt.% from 450 to 550 °C) due to more intense primary and secondary cracking at the higher temperatures. These insights, together with the plateau observed in Figure 5.20, suggest that beyond 600 °C, the oil yield could start to decrease.

From this discussion, it appeared that the maximum oil yield was 93.2±1.4 wt.% at 600 °C. However, at 450 °C, the oil yield was 89.8±0.4 wt.%, suggesting only a slight increase in oil yield (3.4 wt.% increase) with increase in temperature. Therefore, as running an industrial process at lower temperature would save on energy expenditure, while still achieving a reasonably good oil yield, the option to operate this process at 450 °C cannot be dismissed.
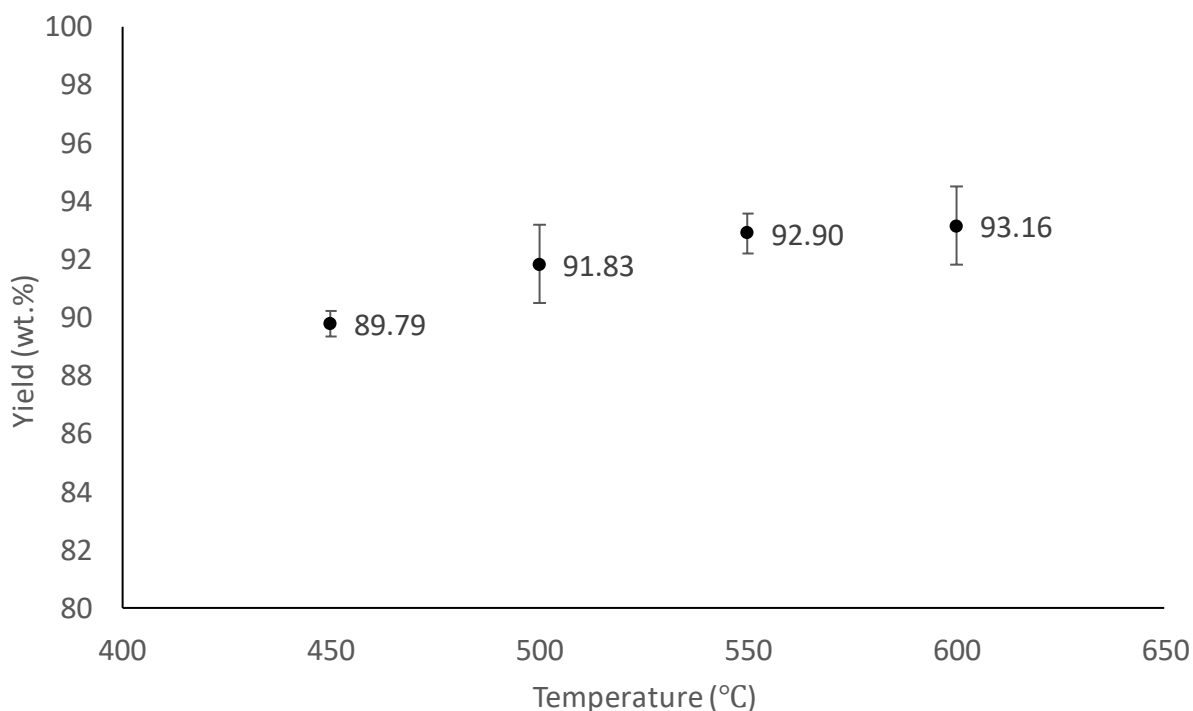
Figure 5.20: Effect of temperature on oil yield for bench scale pyrolysis of clean high-absorbent PS
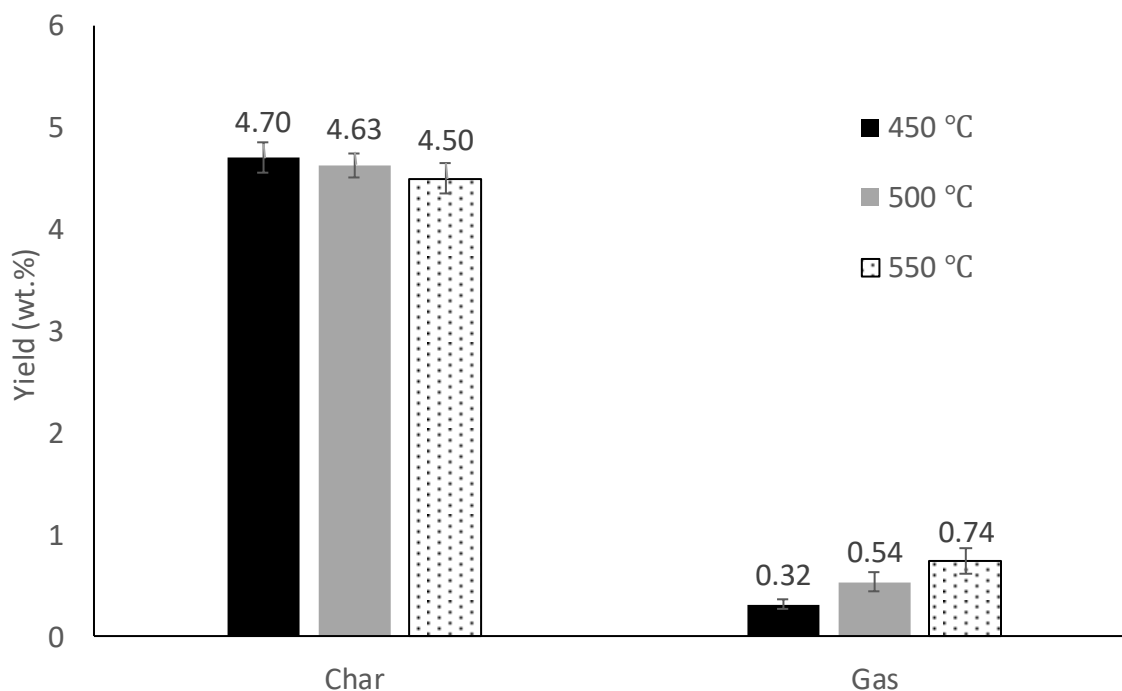
Figure 5.21: Effect of temperature on char and gas yields from bench scale pyrolysis of clean high-absorbent PS

5.2.3 Comparison of clean and contaminated PS in terms of product yields

To investigate the effect of contamination on the pyrolysis oil yield, the contaminated high-absorbent PS was tested at bench scale at 450 °C. The results are presented in Figure 5.22. A contamination of around 16 wt.% had the effect of decreasing the oil yield from 89.8±0.4 wt.% (clean PS) to 83.4±1.2 wt.% (an average decrease of 7.3 wt.% in comparison with the clean PS). The decreased oil yield was balanced by an increased char and gas yield (combined average increase of 6.3 wt.%). This increase in char and gas yield was to be expected from the ultimate and proximate analysis (Table 5.14), which evidenced a higher fixed carbon and oxygen content from the meat juice contamination. The oxygen in protein has been found to result in the formation of oxygenated gaseous products during pyrolysis by Wei *et al*. (2018) and therefore the increased gas yield was to be expected (Wei *et al.*, 2018).

The high-density PS behaved more similarly to the clean high-absorbent PS than to the contaminated high-absorbent PS in terms of product yields with an oil yield of 90.7±3.1 wt.% at 450 °C (Figure 5.22). This makes sense as the origin of this batch was not limited to only the PS punnets used to package raw meat, but included punnets used to package various other products such as fruits and vegetables. Additionally, the thermal treatment at 270 °C during the densification process could have resulted in partial degradation of the contamination fraction. As such the contamination in the contaminated high-density PS is expected to be less than that in the contaminated high-absorbent PS.
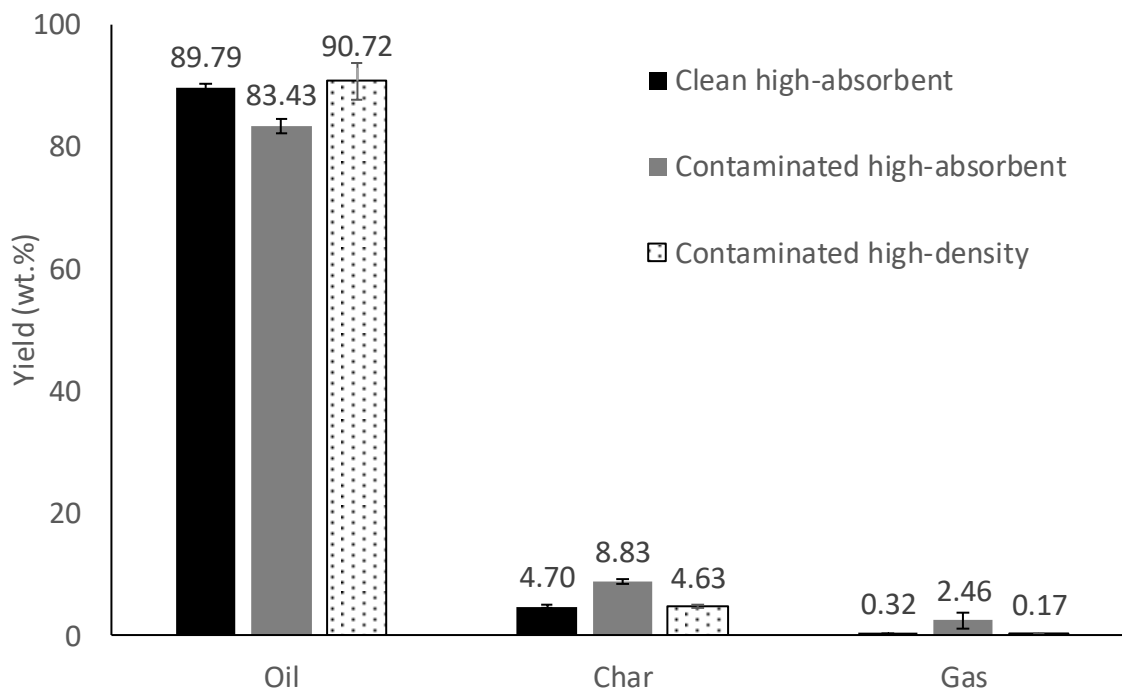
Figure 5.22: Product yields from bench scale pyrolysis of the three PS feedstock batches at 450 ℃

5.2.4 Energy analysis and composition of the oil

The HHVs of the oils obtained from the tests planned in the context of the 2-factor factorial design using the clean high-absorbent PS, were measured. A representative sample of the oil formed in the condensation pot (Figure 4.12) was used for the analysis. It was found that neither temperature nor heating rate had a significant effect on the HHV with p-values of 0.34 and 0.77 respectively. Across the entire studied range, the HHV of the oil was in the average range of 41.61-42.81 MJ/kg.

Figure 5.23 presents the HHV of the oils obtained from pyrolysis of the three different PS batches at 450 °C. No significant differences were detected, with the average HHV of all three being in the range of 42.5-43.4 MJ/kg. This is on the higher end of the range reported in literature of 37.85-42.59 MJ/kg (Miandad *et al*., 2016b). Additionally, conventional gasoline and diesel have HHV in the range of 43.4-46.5 MJ/kg and 42.8-45.8 MJ/kg respectively (Sharuddin *et al*., 2016). Therefore, the PS derived oils from all three of the batches were similar to diesel and gasoline in terms of the energy value. The oil from all three batches had higher HHV than the PS feedstocks (average of 37.2-39.8 MJ/kg in Table 5.14), probably due to the removal of the inorganic fraction (which forms part of the char product) during pyrolysis. Consequently, the gross energy recovered was greater than 95%.
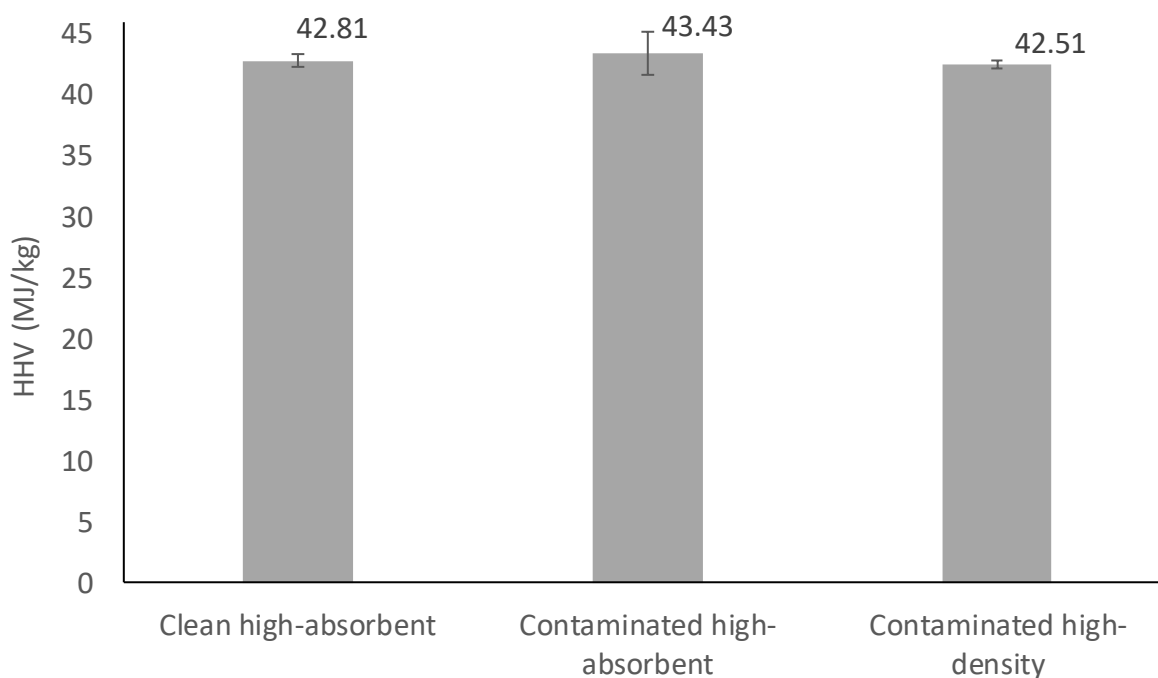
Figure 5.23: HHV analysis of PS pyrolysis oils for the three batches of PS (obtained at pyrolysis temperature of 450 ℃)

The oils from the bench scale pyrolysis of the clean high-absorbent PS were analysed for their composition in terms of styrene, toluene, ethylbenzene, α-methylstyrene, and styrene dimer content as explained in Section 4.5.3. These compounds have been found to be the most abundant products from PS pyrolysis (Zhang *et al*., 1995; Park *et al*., 2003; Mo *et al*., 2014; Artetxe *et al*., 2015).

The total concentration of these compounds was for all the tested conditions (data not shown), which proved that the feedstock was significantly depolymerised and confirmed the oil composition was predominantly aromatic.

The styrene yield is a point of interest as styrene monomer is used for polystyrene manufacturing, and therefore its recovery is considered here as a side interest to the main goal of oil recovery for fuel applications. Temperature and heating rate had a non-significant effect on the styrene yield and the yields of the other four compounds with p-values greater than 0.10. Some studies have reported that styrene yield increased as temperature increased and then decreased again, with the studied temperature ranges being about 375 to 600 °C (Mo *et al.*, 2014; Artetxe *et al.*, 2015). The non-significant trends observed in the compound yields could be because the temperature range studied in this experiment (450-550 °C) was too narrow. The average yield of the compounds produced in the oil across all studied conditions are summarised in Table 5.18. It can be seen that styrene was the most abundant compound with a yield of 48.3±6.1 wt.%, which is consistent with other research, but lower than the maximal range of 64.52-81.54 wt.% that has been reported (Mo *et al*., 2014; Artetxe *et al*., 2015; Zhou *et al*., 2016; Ojha & Vinu, 2015), due to the fact that this study did not focus on styrene optimisation.

Table 5.18: Average yield of compounds in the oil product from pyrolysis across all tested temperature and heating rate conditions

Compound	Yield (wt.%)
Styrene	48.3±6.1
Ethylbenzene	1.4±0.9
Toluene	2.2±1.1
α-Methylstyrene	2.3±1.1
Styrene dimer	12.4±1.8

5.2.5 Gas composition and energy content

Table 5.19 presents the composition and the HHV of the gas produced from the 3 different PS feedstocks at a pyrolysis temperature of 450 ℃. It is important to note that the values given in Table 5.19 are for the concentration of the component in the gas fraction produced. As it was seen in Figure 5.22, the yield of gas was very little (< 3 wt.%), meaning that the actual amount and yield of the gas components evolved were quite small. All three of the plastic feedstocks produced gas fractions consisting of C_2-C_4 hydrocarbons, H_2 and CO_2, with no CO, CH_4, and C_5 to C_6 hydrocarbons being detected. C_2-C_4 hydrocarbons had been detected by other studies too (Williams & Williams, 1997, 1999b; Artetxe *et al*., 2015). The production of CO_2 and H_2 have also been reported by Williams and Williams (1997, 1999b).

The production of CO_2 was unexpected given the low oxygen content determined from ultimate analysis, especially for the clean batch (Table 5.14). Parku (2019) explained the production of CO_2 during the pyrolysis of polypropylene (which also does not contain oxygen in its structure) as evolving from some O_2 still left in the reactor after purging with nitrogen. Indeed, in this study, some O_2 was still remaining in the reactor after purging. Experiments were started when O_2 concentration was measured at less than about 3 wt.%.

The CO_2 yield, evolved from the contaminated high-absorbent PS, increased by about 2 wt.% (data not shown), which was to be expected due to the greater O content observed with the ultimate analysis (Table 5.14), presumably from protein contamination. This correlates with the increased gas fraction yield from this PS batch (Figure 5.22) of approximately 2 wt.%, which was explained as the increased formation of oxygenated gaseous products such as CO_2. It also explains the much lower HHV (6±3 MJ/kg compared to 20±6 MJ/kg) of the gas from this PS batch compared to the clean batch as CO_2 is inert during combustion.

Table 5.19 shows that the gas from the contaminated high-density PS had the highest HHV of 27±5 MJ/kg (due to its higher H_2 and lower CO_2 content). However, because of the low gas yield achieved

from this feedstock (0.17±0.01 wt.%), it produced less energy per mass of feedstock (0.05±0.00 MJ/kg feedstock) compared to the contaminated high-absorbent PS (0.15±0.04 MJ/kg feedstock).

Table 5.19: Gas composition and energy value from the pyrolysis of PS at 450 ℃

	Clean high-absorbent	Contaminated high-absorbent	Contaminated high-density
H_2 (wt.%)	4.38±0.11	0.81±0.36	9.72±1.21
CO (wt.%)	nd	nd	nd
CH_4 (wt.%)	nd	nd	nd
CO_2 (wt.%)	68.56±7.35	89.04±5.67	63.69±6.34
C_2 (wt.%)	10.38±9.14	2.56±1.54	9.52±2.28
C_3 (wt.%)	9.95±0.81	4.86±2.51	12.47±3.31
C_4 (wt.%)	6.73±0.99	2.72±1.31	4.60±0.46
C_5 (wt.%)	nd	nd	nd
C_6 (wt.%)	nd	nd	nd
HHV (MJ/kg gas)	19.70±5.68	6.19±3.18	27.05±4.74
HHV (MJ/kg feedstock)	0.06±0.01	0.15±0.04	0.05±0.00

nd = not detected; C_i = hydrocarbons containing i atoms of carbon

5.3 LDPE/PET multi-layer feedstock characterisation

The LDPE/PET multi-layer was investigated at clean and contaminated conditions. This section provides the characterisation of the clean and contaminated LDPE/PET multi-layer in terms of the amount of PET and LDPE in the multi-layer, the ultimate and proximate analysis, the energy content of the multi-layer feedstock as the HHV, the amount of contamination present, and the thermal degradation behaviour.

5.3.1 Multi-layer LDPE and PET fraction

In order to determine the amount of PET and LDPE in the clean multi-layer sample, a deconvolution technique (as described in Section 4.2.6) was applied to the multi-layer DTG data. Figure 5.24 depicts the DTG data and deconvolution graphically. It can be seen that the DTG data of the multi-layer ("Multi-layer raw data") had two overlapping peaks. The first smaller peak (observed as a shoulder in the data) represented the PET degradation and the second larger peak represented the LDPE degradation. The DTG data was modelled using equation 4 in Section 4.2.6 and illustrated in Figure 5.24 as "Multi-layer model". It can be seen that the mathematical model described the raw data well. Integration of the deconvoluted LDPE and PET peak signals provided area values that could be used to calculate the mass

of the LDPE and PET layers (from the calibration curves, Figure 4.10 and Figure 4.11, in Section 4.2.6) in the sample and therefore the weight percentages. Following this method and subtracting the significant ash content in the LDPE layer from the white colouring (determined as 4.73 ± 0.09 wt.%), the composition of the LDPE/PET multi-layer was calculated as 76.6 ± 2.6 wt.% LDPE (pure) and 18.6 ± 2.5 wt.% PET (pure). Further details on the composition of the clean multi-layer in terms of the ultimate and proximate analysis are considered in the following section.
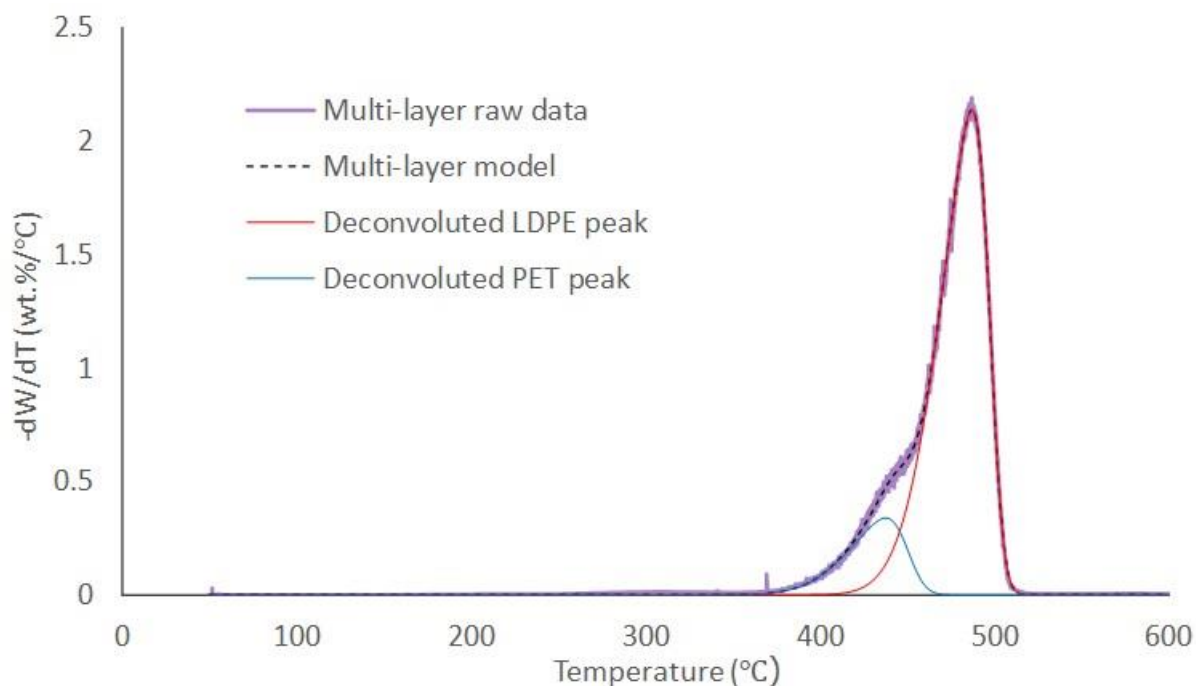
Figure 5.24: Deconvolution of LDPE/PET multi-layer DTG data

5.3.2 LDPE/PET multi-layer composition, energy content and impact of contamination

Table 5.20 summarises the ultimate and proximate analysis, and the HHV of the clean and contaminated multi-layer batches. The experimental results are compared to what is expected from literature, based on values reported for single LDPE and PET, when the LDPE and PET fractions are taken as the experimentally determined 76.6 and 18.6 wt.% respectively (as calculated in Section 5.3.1).

Table 5.20 shows that the oxygen content in the experimental results of the multi-layer was significantly lower than what was predicted using values from LPDE and PET in literature (2.75 ± 0.37 wt.% compared to 4.38-7.26 wt.% oxygen). This suggests that the deconvoluted PET peak as shown in Figure 5.24 (used to determine the fraction of 18.6 wt.% of PET in the multi-layer) may not have been obtained from pure PET but rather a combination of PET and another component (possibly the adhesive used to bind the two layers together). A common adhesive used in LDPE/PET multi-layer binding is ethylene-acrylic acid (Adhesive resins and tie layers, 2019), which has been reported to degrade in

similar temperature range as PET (Liu & Zhang, 2011). This means that the PET composition was likely overestimated, and therefore it can be assumed that the PET layer represented less than 18.6 wt.%.

If the proximate results (Table 5.20) for the clean multi-layer are compared with the literature predicted values, it can be seen that the ash content was significantly higher (4.89±0.07 wt.% compared to 0.02-0.64 wt.% ash), which can be assumed to be due to the inorganic content in the multi-layer, introduced particularly for the colouring. Further insight into the ash content can be observed in Table 5.21, which presents the proximate analysis results of the individual LDPE and PET layers, following separation of the layers. From these results, it is clear that the inorganic fraction was essentially found in the LDPE layer (4.73±0.09 wt.% ash), which indicates that most of the inorganic content in the multi-layer was from the white ink used to colour the LDPE layer.

Comparison of all the characterisation results (ultimate, proximate and energy content) for the clean and contaminated multi-layer, in Table 5.20, reveals that there were no significant differences. This makes sense as the quantification of the dry dog food contamination determined that it constituted an average of only 0.16 wt.%. Overall, the multi-layer samples were predominantly hydrocarbon in nature (> 95 wt.%), with a high amount of volatile matter (> 93 wt.%). This makes it favourable to be converted to a hydrocarbon oil/wax during pyrolysis. Additionally, the clean and contaminated multi-layer had similar HHVs in the range of 40.7-41.2 MJ/kg, which is comparable to that of commercial diesel 42.8-45.8 MJ/kg (Sharuddin *et al*., 2016).

Table 5.20: Ultimate and proximate analysis, and energy value of clean and contaminated LDPE/PET multi-layer

	Parameter	Literature value (based on 18.6 wt.% PET)	Clean	Contaminated
Ultimate analysis (wt.%) dry, ash-free basis	**C**	77.29 (pure LDPE/PET) 74.86-77.44	81.92±0.23	80.91±0.85
	H	11.74 (pure LDPE/PET) 11.43-13.38	15.22±0.12	14.72±0.48
	N	0 (pure LDPE/PET) 0.02-0.13	< 0.1 (LOD)	0.44±0.44
	S	0 (pure LDPE/PET) 0.08	0.03±0.03	0.08±0.08
	O*	6.2 (pure LDPE/PET) 4.38-7.26	2.75±0.37	3.85±0.75
Proximate analysis (wt.%)	**Moisture**	0-0.27	0.05±0.01	0.06±0.02
	Volatile compounds	92.27-95.00	93.19±0.08	93.33±0.16
	Ash content	0.02-0.64	4.89±0.07	4.83±0.11
	Fixed carbon	1.74-3.18	1.88±0.02	1.78±0.05
Energy value	**HHV (MJ/kg)**	37.28-45.53	40.72±0.40	41.18±0.13

*by difference; LOD = limit of detection

Table 5.21: Proximate analysis (wt.%) of individual LDPE and PET layers

	LDPE layer	PET layer
Moisture	0.04±0.00	0.10±0.01
Volatile compounds	95.11±0.09	86.79±0.01
Ash content	4.73±0.09	0.00±0.00
Fixed carbon	0.12±0.00	13.11±0.01

5.3.3 Thermal degradation behaviour

The thermal degradation behaviour results for the clean and contaminated multi-layer are presented in Figure 5.25 at a heating rate of 10 °C/min. The clean and contaminated samples behaved identically, which again indicated the minor effect of the contamination. Degradation started at about 390 °C and

the sample was completely converted at approximately 520 ℃. From the DTG curves, two overlapping signal peaks can be observed. The first smaller peak is observed as a shoulder before the larger peak. The larger peak occurred at a temperature of about 490 ℃. These two signals were from the PET and LDPE degradation respectively. The start temperature was consistent with what has been reported for pure PET of 370-397 ℃ (Hujuri *et al.*, 2008; Jayanarayanan *et al.*, 2016; Diaz-Silvarrey *et al.*, 2018). The peak from the LDPE degradation occurred at a higher temperature compared to reported values of 465-470 ℃ (Hujuri *et al.*, 2008; Diaz-Silvarrey & Phan, 2016; Jayanarayanan *et al.*, 2016).
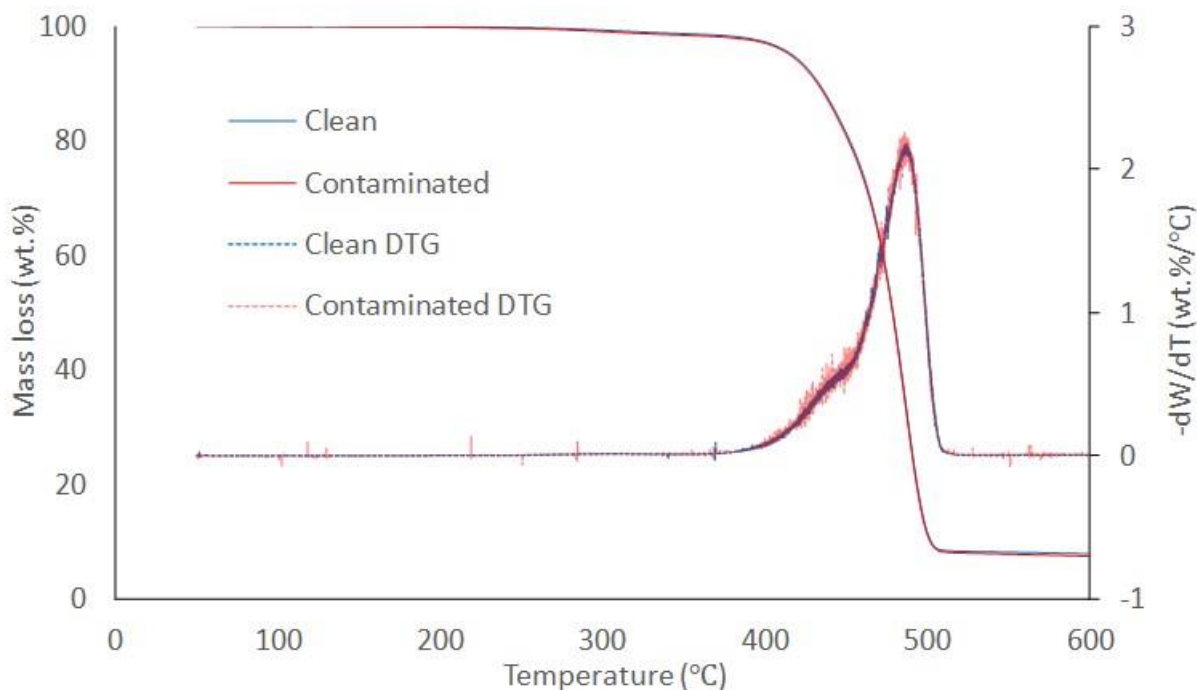
Figure 5.25: Thermal degradation behaviour of clean and contaminated LDPE/PET multi-layer. Heating rate = 10 ℃/min

As the effect of the contamination could not be observed in the thermal degradation behaviour curves of the contaminated multi-layer (Figure 5.25), the thermal degradation of the dry dog food contamination was also studied and compared to the multi-layer curves as in Figure 5.26. The goal was to investigate whether the degradation of the dry dog food contamination could have been obscured by the main plastic component peaks. It is clear from Figure 5.26 that the dry dog food would have degraded much earlier than the multi-layer and that the main peak would not be obscured by the plastic DTG peaks. Therefore, the absence of a peak related to dog food contamination in Figure 5.25 was due to the amount of the contamination being too little (0.16 wt.%) to be observed compared to the DTG peaks from the plastic components.
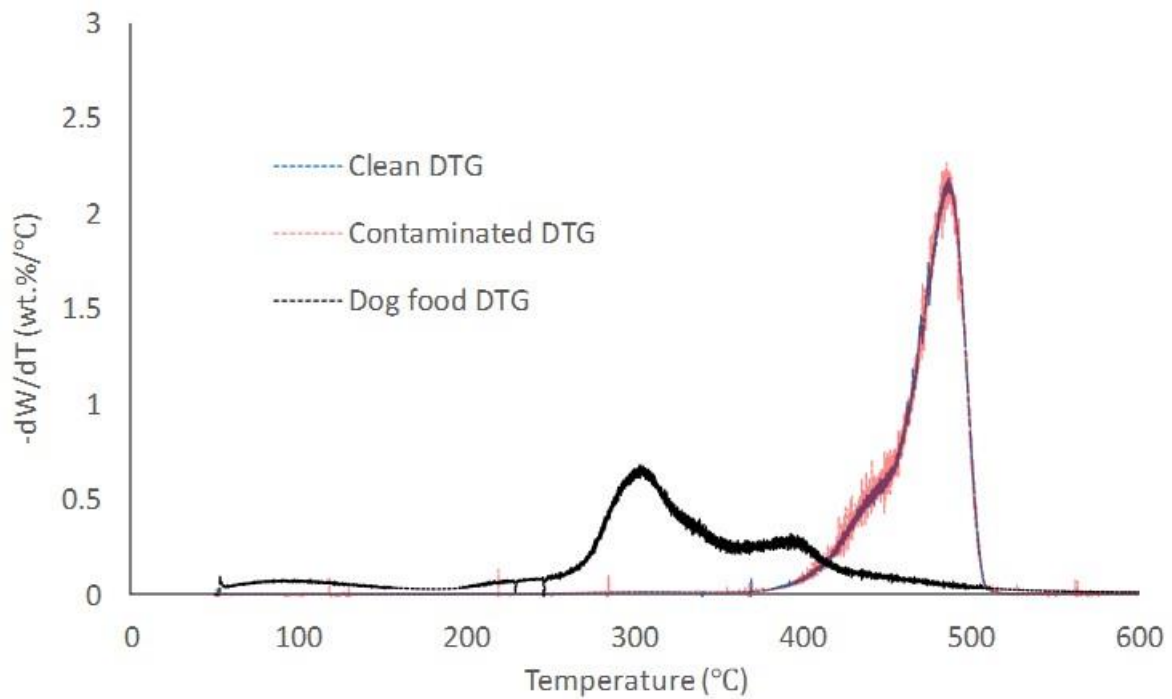
Figure 5.26: DTG of clean and contaminated LDPE/PET multi-layer compared with DTG of dry dog food

To investigate whether interaction occurred between the LDPE and PET layers, Figure 5.27 was constructed. In Figure 5.27 DTG data from the thermal degradation behaviour of individual LDPE and PET were added in the proportion of 81.4 wt.% LDPE (LDPE layer including white colouring) and 18.6 wt.% PET to construct the simulated multi-layer data. This was compared to the raw data from the thermal degradation behaviour of the multi-layer. Interaction between components can typically be observed when the mixed plastic reacts differently to what would be expected from the summed behaviour of the individual plastic constituents (Wong *et al.,* 2015). As can be seen, the two curves compared quite well, indicating that there was limited interaction between the LDPE and PET layer.
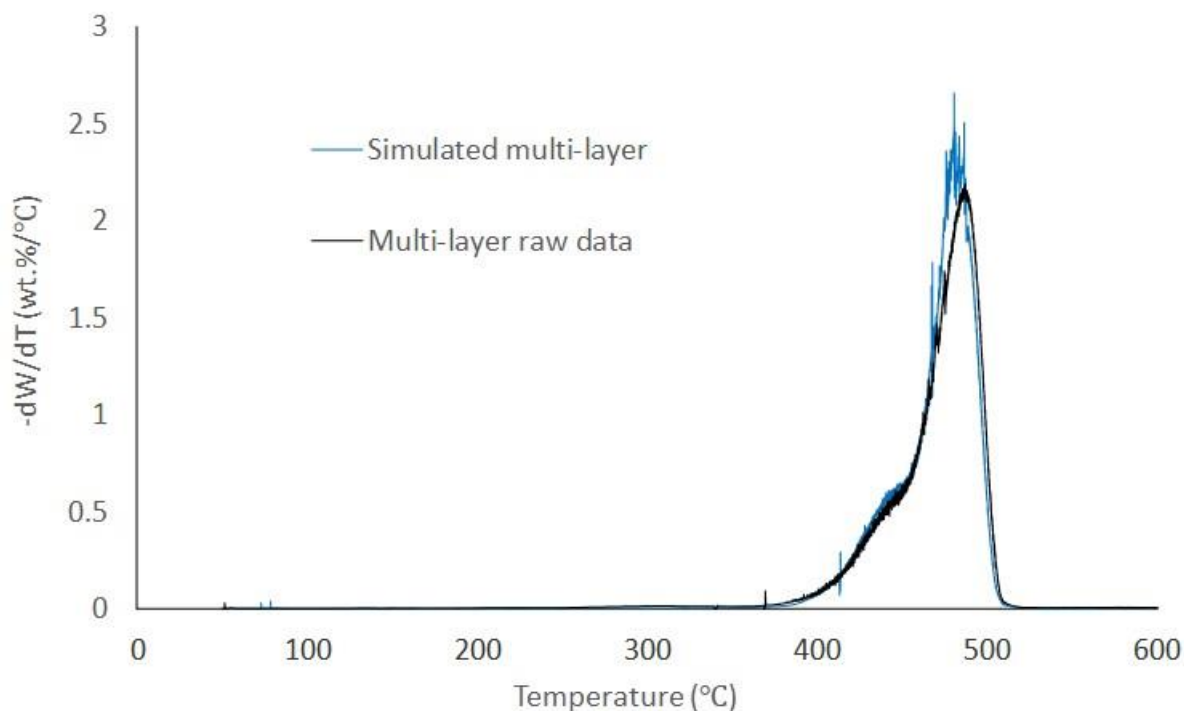
Figure 5.27: Comparison of DTG of the raw multi-layer data and simulated multi-layer data from the summation of the individual LDPE and PET data

5.4 Bench scale pyrolysis of LDPE/PET multi-layer

The LDPE/PET multi-layer was tested at bench scale by optimising temperature for the oil/wax yield from the pyrolysis of the clean multi-layer. The effect of contamination was then tested by pyrolyzing the contaminated multi-layer at the optimum conditions, as determined from the clean multi-layer optimisation. Finally, the energy value of the oil/wax and the gas, as well as the composition of the gas were determined.

5.4.1 Optimisation of oil/wax yield from clean LDPE/PET multi-layer

The temperature range investigated during the bench scale optimisation study of the clean multi-layer was 475-700 °C, with duplicate runs. Only the effect of temperature was studied as it has been found in literature to be the factor with the greatest effect (López *et al*., 2011; Sharuddin *et al*., 2016). The bench scale set-up is illustrated in Figure 4.13. It was observed during collection of the pyrolysis products, that wax formed in the outlet of the reactor and in the first atmospheric condenser. An oil fraction was collected from the four condensers (cooled with solid CO_2) after the atmospheric condenser. It was observed that some oil also condensed in the atmospheric pot with the wax (especially at higher temperatures) and therefore the separation of the oil and wax fractions was not perfect. However, the condensation system was always assembled in a similar way, in order to allow reproducibility and comparison of the results at different temperatures. The mass balance closure for all the experiments was greater than 89 wt.%.

Table 5.22 presents the ANOVA for the experimental design with oil/wax yield as the dependent variable. With a p-value of 4.0×10^{-6}, it is clear that the temperature had a significant effect on the oil/wax yield.

Table 5.22: ANOVA for single factor (temperature) experimental design for bench scale pyrolysis of clean LDPE/PET multi-layer

	SS	df	MS	F	p
Temperature (°C)	2726.07	5	545.21	141.46	4.0×10^{-6}
Error	23.12	6	3.85		
Total	2749.20	11			

Figure 5.28 illustrates the residuals in the data to determine whether the assumptions related with the ANOVA model hold true. Figure 5.28a. proves that the residuals were normally distributed with a straight line fit through the origin. Figure 5.28b tests whether the residuals were independent from time (i.e. the run order as the experiments progressed) and suggests a mostly random spread of the residuals and therefore independence from time, which means influences such as instrument calibration drift were not evident (Montgomery, 2013). Figure 5.28c shows a structureless spread of the residuals with the predicted values of the oil yield, confirming that the variance was constant (homoscedasticity) (Montgomery, 2013) and therefore the assumptions hold true.
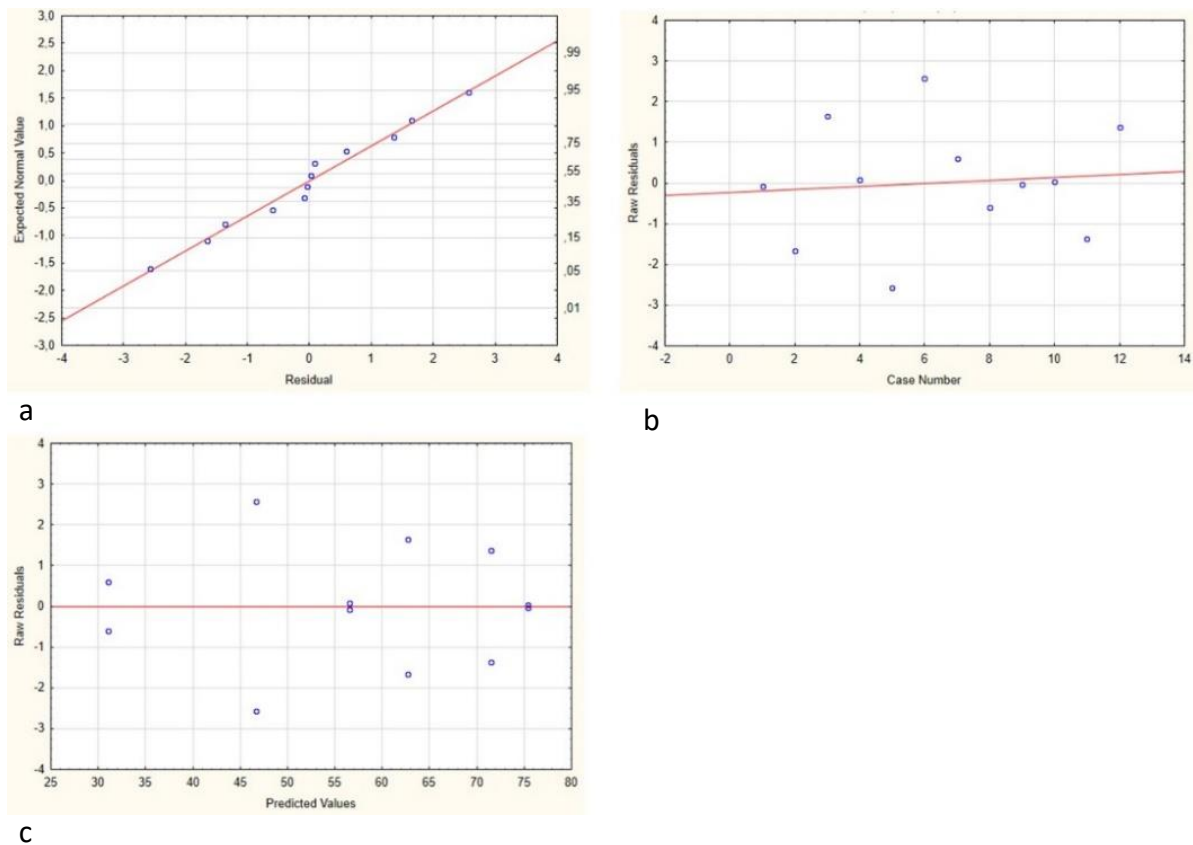
Figure 5.28: ANOVA model (clean multi-layer oil/wax yield optimisation at bench scale) adequacy check with residuals. a) normal probability of residuals; b) residuals vs run order/time (case number); c) residuals vs model predicted (oil/wax yield) values

The oil/wax yield experimental results are graphically illustrated in Figure 5.29, along with the yields of the separate oil and wax. The oil/wax yield was found to increase from 71.55±1.94 to 75.37±0.04 wt.% with a temperature increase from 475 to 500 °C (reaching the optimum point at 500 °C) and then decreased significantly by about 6 to 16 wt.% for every 50 °C increase in temperature up to 700 °C. The flowable oil yield in Figure 5.29 shows an overall increasing trend (9.92 to 16.44 wt.%) with an increase in temperature (475 to 700 °C), which was due to more cracking of wax compounds to produce lighter compounds at higher temperatures. Temperatures higher than 700 °C were not tested (the potential aim of testing at higher temperatures would have been to further increase the oil yield) as they would negatively affect the energy efficiency of the process, but also because literature indicated that above 700 °C the formation of PAH could be significant (Li *et al.*, 1999; Williams & Williams, 1999a). The low oil yield (< 17 wt.%) drove the decision to rather optimise for the oil/wax yield (as discussed above), instead of optimising for the oil yield (even though the oil is preferable to wax from an ease of handling point of view).
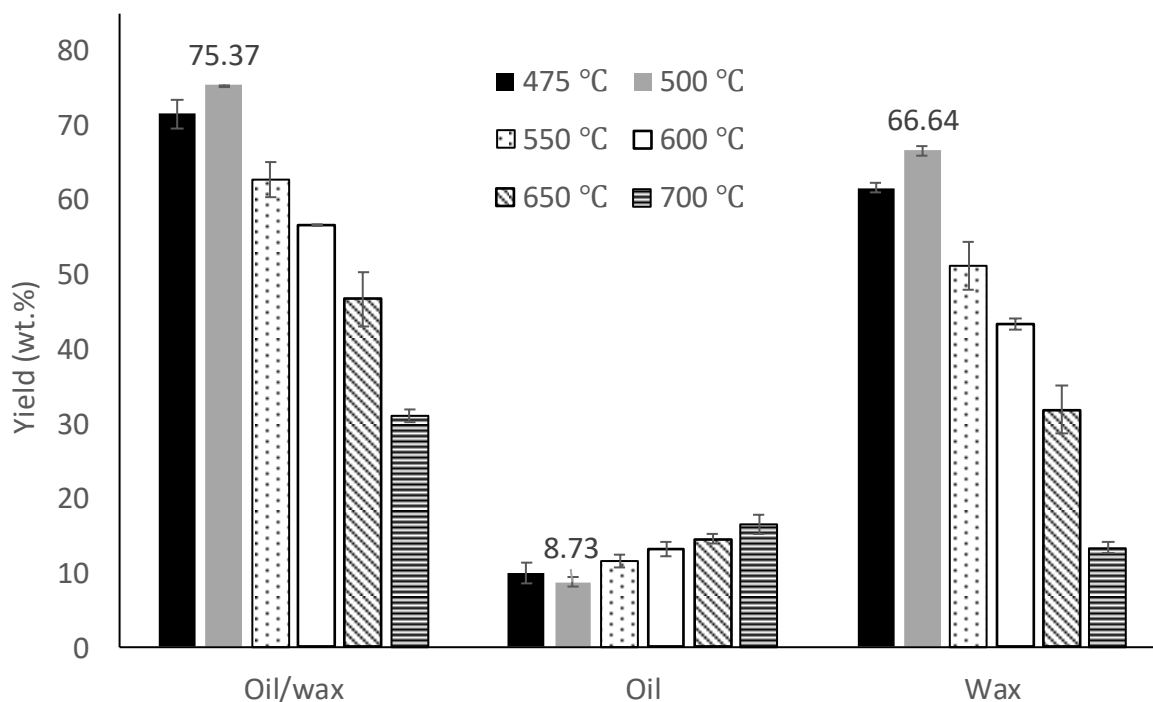
Figure 5.29: Effect of temperature on the oil/wax and the separate oil and wax yields

To investigate the effect of temperature further, Figure 5.30 was constructed, which illustrates the char and gas yield trends. It can be seen from Figure 5.30 that the char yield was significantly higher (10.58±1.01 wt.%) at the lowest temperature of 475 ℃, likely due to incomplete degradation (this is consistent with results obtained by Park *et al.* (2002)). When the temperature was increased to 500 ℃, the char yield decreased to 8.22±0.07 wt.%. This 2.36±1.08 wt.% decrease in char yield accounts for the 3.82±1.98 wt.% increase in oil/wax yield at 500 ℃, when compared to 475 ℃. When the temperature was increased further beyond 500 ℃, the char yield decreased only slightly and reached 7.33±0.00 at 700 ℃. The small decrease in char yield (< 1 wt.%) as temperature increased from 500 to 700 ℃, indicates that complete degradation was being reached for temperatures from 500 ℃ and higher. The char yield results were between values obtained for LDPE (< 1 wt.% when pure, thus < 6 wt.% when taking ash content into account) and PET (11 wt.%) in literature (Çit *et al.*, 2010; Gunasee *et al.*, 2017), supporting the expectation that the presence of PET would contribute to significant char production.

Figure 5.30 shows that the gas yield increased significantly from 550 ℃ upward to 700 ℃ (due to increased primary and secondary cracking), which explains the decrease in oil/wax yield after 550 ℃. At the optimum temperature of 500 ℃, a gas yield of 7.93±0.80 wt.% was obtained. This correlates well with literature results obtained for LDPE pyrolysis, with gas yields of approximately 7 to 11 wt.% being reported at a temperature of about 500 ℃ (Williams & Williams, 1999a; Kaminsky *et al.*, 2004).

In summary, the maximum oil/wax yield of 75.37±0.04 wt.%, from the pyrolysis of the LDPE/PET multi-layer at bench scale, was achieved at 500 ℃. At this temperature there was a char yield of 8.22±0.07 wt.%, a gas yield of 7.93±0.80 wt.%, and a separate oil and wax yield of 8.73±0.61 wt.% and 66.64±0.65 wt.% respectively.
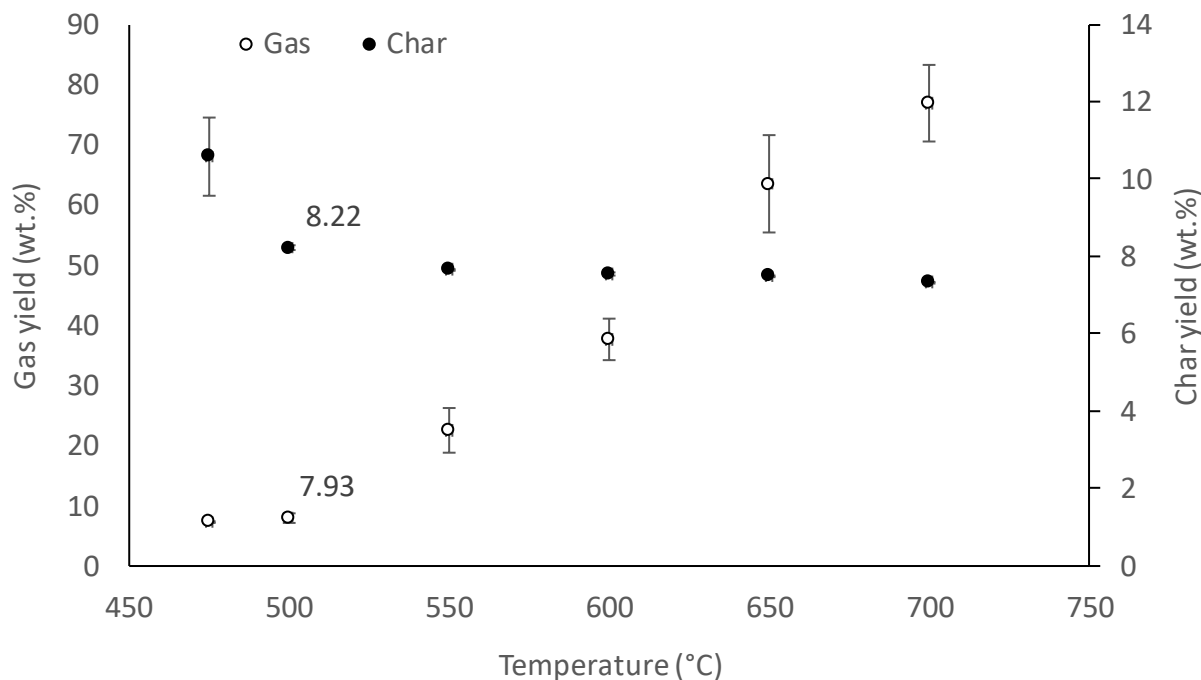
Figure 5.30: Effect of temperature on char and gas yields from bench scale pyrolysis of clean LDPE/PET multi-layer

5.4.2 Comparison of clean and contaminated LDPE/PET multi-layer in terms of product yields

Figure 5.31 graphically compares the product yields from the contaminated multi-layer with the yields from the clean multi-layer obtained at the condition of 500 ℃ (as selected in the previous section). An important difference is the higher oil yield (12.56±1.61 wt.% compared to 8.73±0.61 wt.%) and lower wax yield (58.89±1.64 wt.% compared to 66.64±0.65 wt.%) obtained from the contaminated compared to the clean multi-layer. Conversion of the contamination into oil could have contributed to oil yield increase. However, the amount of contamination determined, of 0.16 wt.% average, was too little to account for the 3.83 wt.% increase in oil yield. Therefore, it must be assumed that there were some interactions between the plastic and the contamination. In particular, the inorganic part of the dry dog food contamination could have had a catalytic effect that caused increased cracking of the wax. López *et al.* (2010) also found that inorganic contamination, particularly metallic compounds, caused a catalytic effect during pyrolysis. Catalytic effect was not indicated in the characterisation of the multi-layer feedstocks in terms of thermal degradation behaviour, where it was observed that the clean and contaminated samples behaved similarly. This was probably due to the catalytic effect being more pronounced at bench scale (where volatiles go through the particle bed to escape the sample boat

resulting in greater secondary reactions) compared to the small scale used for TGA characterisation (where only the primary mechanism can usually be observed).

Also, of interest is the decreased oil/wax yield (decrease of 3.92±0.07 wt.%) observed in Figure 5.31 for the contaminated multi-layer, which is balanced by an increased gas yield (increase of 2.37±1.95 wt.%). This indicates the increased cracking of heavier volatiles to lighter non-condensable volatiles, which is typical of catalytic cracking of the volatiles (as observed in various other studies such as Shah *et al.* (2010) and Gao (2010)), comforting the assumption of a catalytic effect of the contamination. The char yield, as presented in Figure 5.31, was 8.22±0.07 and 7.98±0.07 wt.% for the clean and contaminated multi-layer respectively, showing that contamination caused a slight decrease in char yield.

In summary, the contaminated multi-layer produced an oil/wax yield of 71.45±0.03 wt.% (3.92 wt.% less than the clean multi-layer at 500 °C), higher flowable oil (12.56±1.61 wt.%) and gas (10.31±1.14 wt.%) yields, and a lower wax yield (58.89±1.64 wt.%). These effects of the contamination on the product yields have been concluded to be due to a possible catalytic effect from the inorganic fraction of the contamination.
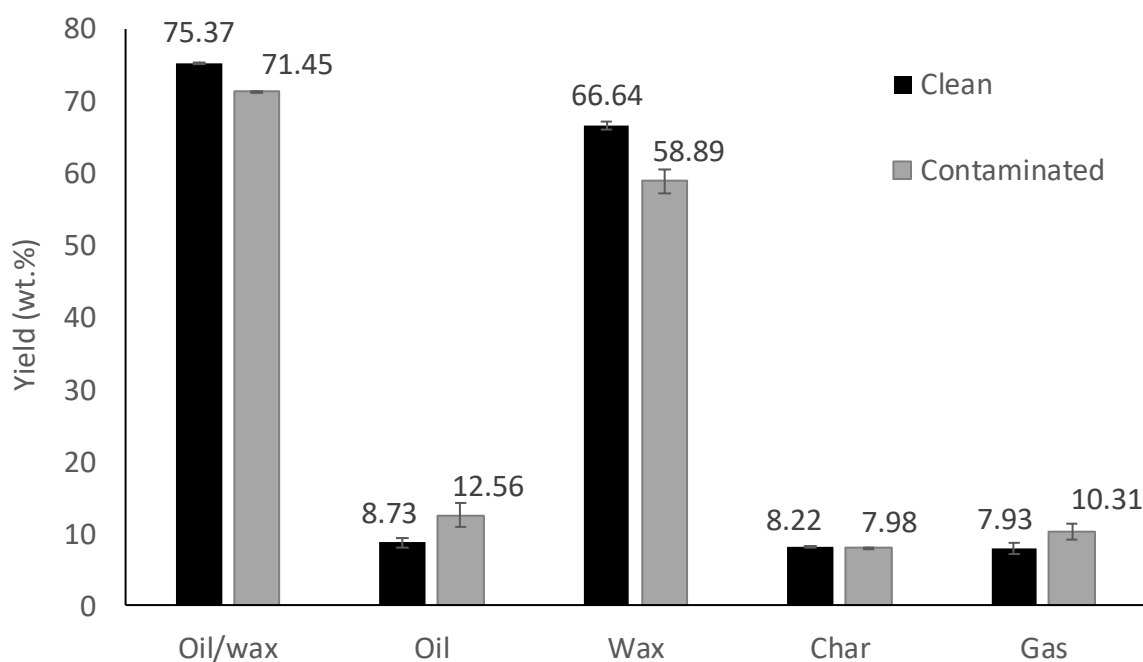
Figure 5.31: Product yields for bench scale pyrolysis of clean and contaminated LDPE/PET multi-layer at 500 °C

5.4.3 Energy analysis of the oil/wax

The HHV of the oil/wax products obtained from the pyrolysis of the clean and contaminated multi-layers were determined. The HHV analysis was performed on a representative sample of the oil/wax product formed in all 5 of the condensers (Figure 4.13). In Figure 5.32, the effect of temperature on the HHV of the oil/wax from the clean multi-layer is illustrated. Additionally, the HHV of the oil/wax from the contaminated multi-layer at a pyrolysis temperature of 500 ℃ is provided for comparison. The figure indicates that temperature did not have a significant effect on the HHV of the oil/wax (p-value of 0.23). Only at 700 ℃, it was found that the HHV was significantly lower (40.65±2.03 MJ/kg compared to the range of 43.72-44.78 MJ/kg at temperatures 475 to 650 ℃), which could be due to the increased production of aromatics (from Diels-Alder reactions) at this high temperature as also described by other researchers (Li *et al*., 1999; Williams & Williams, 1999a; Bagri & Williams, 2002; Marcilla *et al*., 2009; Kaminsky, 2004).

In Figure 5.32, contamination was also seen to have an non-significant effect on the HHV with a value of 45.15±0.13 MJ/kg compared to 44.24±1.24 MJ/kg for the oil/wax from the clean multi-layer at the temperature of 500 ℃. The gross energy recovered in the oil/ from the multi-layer plastic at the optimum temperature of 500 ℃, for the clean and contaminated was 81.9±1.7% and 78.3±0.3% respectively. Less energy was recovered from the contaminated multi-layer derived oil/wax (compared to the clean) due to the smaller oil/wax yield (71.45±0.03 wt.% compared to 75.37±0.04 wt.%) obtained from the contaminated multi-layer as illustrated in Figure 5.31.
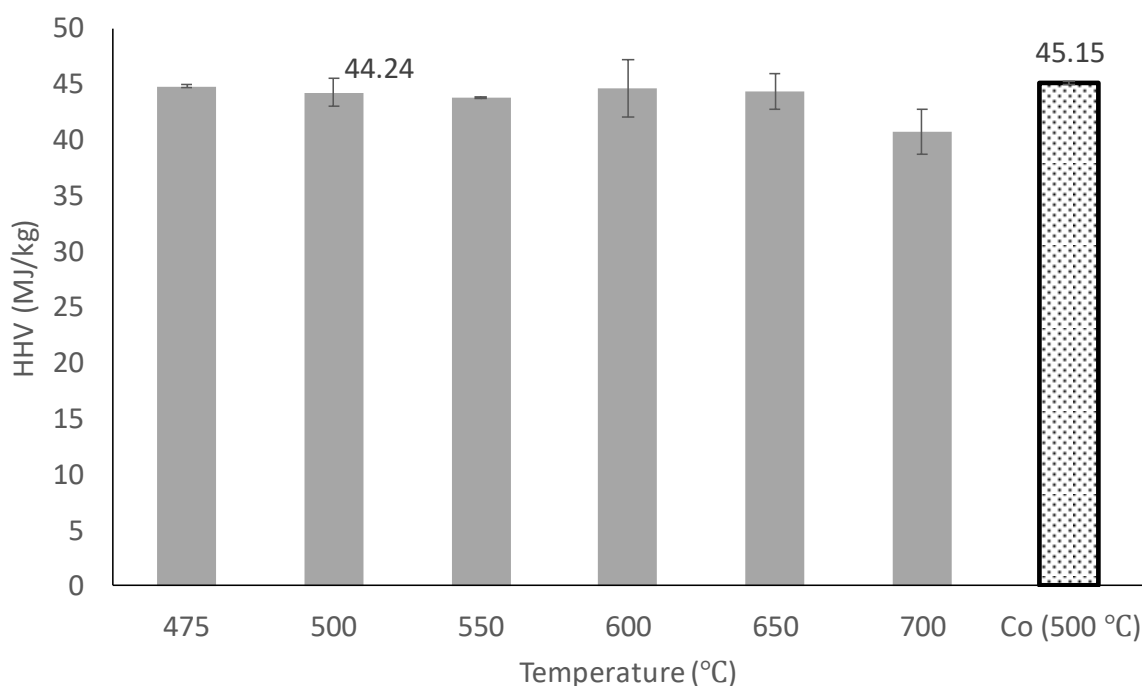
Figure 5.32: Effect of temperature on the HHV of the oil/wax from pyrolysis of clean and contaminated (Co) LDPE/PET multilayer at bench scale

5.4.4 Gas composition and energy value

The gas composition and the calculated HHV of the gas produced at 500 ℃ are summarised in Table 5.23. The gas from the clean and contaminated multi-layer consisted of C_1-C_5 hydrocarbons, as well as CO, CO_2 and H_2. These gaseous compounds have been reported for the pyrolysis of LDPE and PET by various other researchers such as Williams and Williams (1997, 199a), Marcilla *et al*. (2009) and Brems *et al.* (2011). Table 5.23 shows that pyrolysis of the contaminated (compared to the clean) multi-layer resulted in the increased production of lighter compounds such as CH_4 and C_2, C_3 and C_4 hydrocarbons (with a combined average increase of 9.5 wt.%). This could be due to the possible catalytic effect from the inorganic fraction of the contamination as explained in Section 5.4.2. The increase in the lighter hydrocarbons was balanced by a 9.2 wt.% decrease in CO and CO_2 concentration. The greater hydrocarbon content (and less CO and CO_2 content) explains the increased energy value of the gas produced from the contaminated multi-layer of 38.7±0.8 MJ/kg compared to the gas obtained from the clean multi-layer of 34.4±0.6 MJ/kg.

Table 5.23: Gas composition and energy value at a pyrolysis temperature of 500 ℃

	Clean	**Contaminated**
H_2 (wt.%)	0.35±0.00	0.13±0.01
CO (wt.%)	8.29±0.10	6.72±0.42
CH_4 (wt.%)	8.39±0.19	9.54±0.19
CO_2 (wt.%)	26.15±0.71	18.49±0.48
C_2 (wt.%)	22.02±0.49	25.41±0.56
C_3 (wt.%)	28.47±0.27	31.55±0.65
C_4 (wt.%)	6.16±0.25	8.01±0.04
C_5 (wt.%)	0.18±0.03	0.16±0.01
C_6 (wt.%)	nd	nd
HHV (MJ/kg gas)	34.38±0.64	38.69±0.79
HHV (MJ/kg feedstock)	2.73±0.01	3.99±0.01

nd = not detected; C_i = hydrocarbons containing i atoms of carbon

5.5 Pilot scale pyrolysis

Bench scale testing of PS with temperature and heating rate as input factors, proved that only temperature had a significant effect. The multi-layer was tested at bench scale with only temperature as input factor based on reports that temperature is the most influential parameter (Sharuddin *et al*., 2016). Therefore, the pilot scale experiments attempted to scale-up the optimised temperature conditions from bench scale by investigating ranges including the optimised temperature points.

5.5.1 Polystyrene single-layer

As stated previously, the high-density PS feedstock was used in scale-up testing in the pilot reactor. This was due to operational problems associated with the un-densified PS (i.e. the high absorbent batches), which are further discussed in Section 5.6. Additionally, the high-density PS batch was a more representative sample of what would be collected in industry. This section describes the results from the pilot scale pyrolysis of the contaminated high-density PS, which include the product yields as a function of temperature, the energy and composition of the oil, certain fuel quality properties of the oil product, and lastly the energy value and composition of the gas product. The average processing rate of the high-density PS at pilot scale was 2.3±0.6 kg/h.

5.5.1.1 Product yields

From the bench scale experiments, it was determined that the maximum oil yield was achieved around 550-600 °C. However, from 450 to 600 °C there was only a 3.4 wt.% increase in oil yield, which prompted the decision to also consider 450 °C as the use of such temperature to run the process at is likely to save on energy requirements. Therefore, the pilot scale experiments were tested at a minimum of 450 °C. Final temperature points tested at pilot scale were 450, 500 and 550 °C. Some important observations were made during pilot scale testing with PS, as follows:

- At the end of the experiment, the product in the char pot was collected. This product was observed to be a black mass (Figure 5.33), with some parts being hard and dry and other parts being very viscous and sticky. The hard, dry parts resembled what had been observed in the sample boat at bench scale when the PS plastic had melted, but not degraded, and then cooled again. Therefore, this part was considered to be undegraded PS. The sticky part was assumed to be heavy MW volatiles that had condensed (earlier than expected) in the char pot. The presence of char was not observed, which was assumed to be because it was mixed in with the black mass and could not be seen. In the rest of the document this black mass in the char pot is described as the residue.

- Most of the oil produced condensed in the first ambient temperature condenser (Figure 4.14). Typical distribution of the oil in condensers 1 to 4 is shown in Figure 5.34.

- Some volatiles were observed to escape at the feeding point. Additionally, when the feeding cylinder moved forward to push the PS sample into the reactor, the pressure in the reactor increased and this caused small amounts of volatiles to escape at the cylinder and 2 rotary seals (see schematic of the reactor, Figure 4.14).
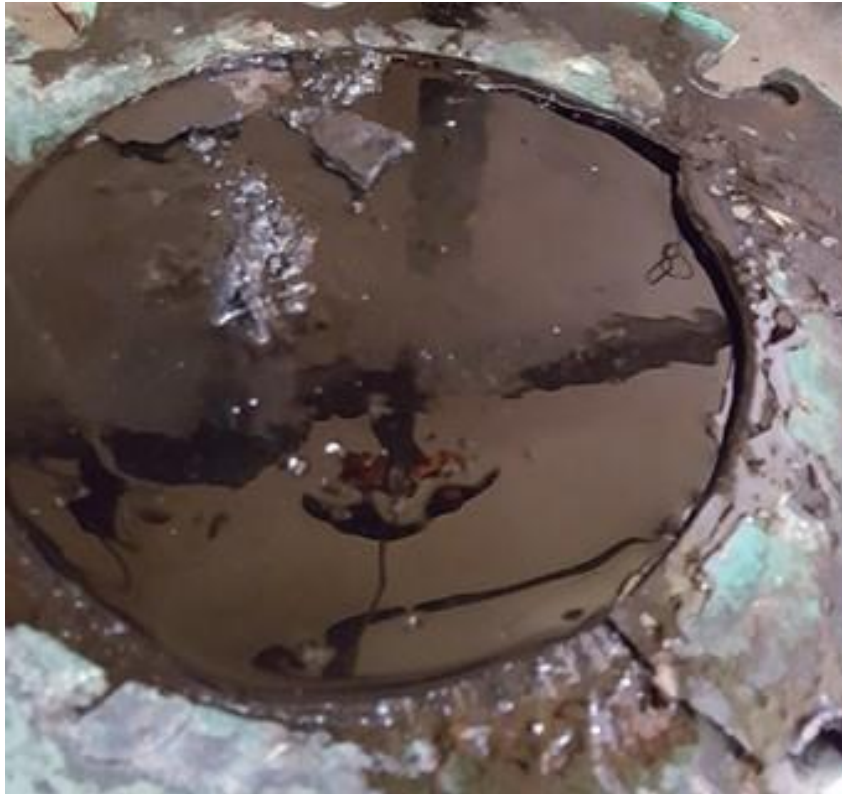
Figure 5.33: Typical residue in char pot from PS processing at pilot scale

Figure 5.34: Typical distribution of PS derived oil in pilot scale condensers 1 to 4 (as shown from left to right)

The average mass balance closure for all the experiments was found to be 85.3±0.9 wt.%, which was about 10 wt.% lower than what was achieved at bench scale. This lower mass balance closure is due to greater losses at pilot scale, specifically due to volatile losses at the feeding point and seals as described previously. Losses were also due to condensation of oil in some parts of the pilot scale set-up that could not be weighed and therefore, could not be included in the mass balance.

Table 5.24 presents the ANOVA for the temperature effect in the investigated range and, with a p-value of 0.0022, the temperature was found to have a significant effect.

Table 5.24: ANOVA for single factor (temperature) statistical design for pilot scale pyrolysis of contaminated high-density PS

	SS	df	MS	F	p
Temperature (℃)	251.70	2	125.85	87.78	0.0022
Error	4.30	3	1.43		
Total	256.00	5			

The ANOVA model was tested for its adequacy in Figure 5.35. Figure 5.35a shows that the residuals are normally distributed and Figure 5.35b does not show a strong dependence of the residuals on time. Figure 5.35c indicates the residuals have constant variance and therefore the data are homoscedastistic.

a

b

c
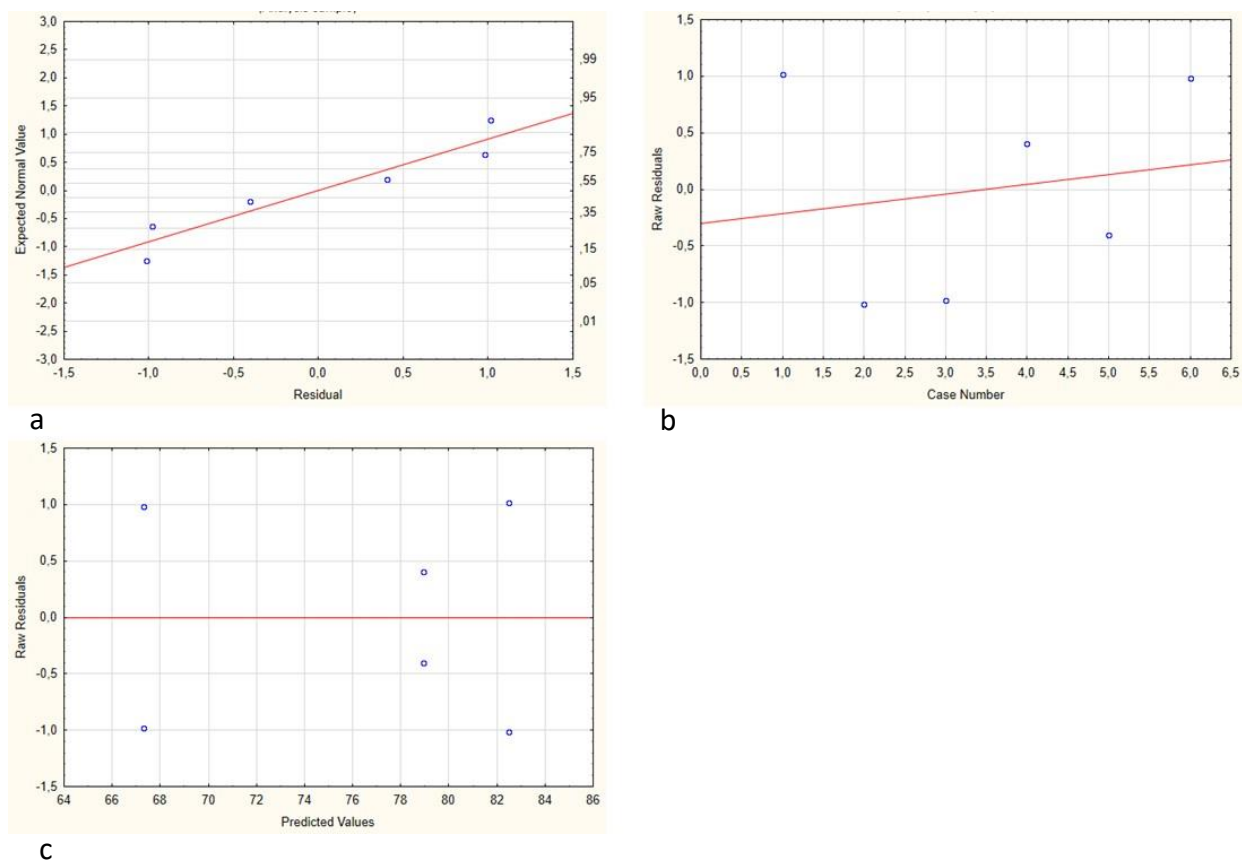
Figure 5.35: ANOVA model (contaminated high-density PS oil yield at pilot scale) adequacy check with residuals. a) normal probability of residuals; b) residuals vs run order/time (case number); c) residuals vs model predicted (oil yield) values

The resulting oil yields as a function of the pilot reactor temperature are illustrated in Figure 5.36. A more significant trend can be observed than was the case at bench scale (Figure 5.20). The more significant trend is probably because of shorter feedstock residence times at pilot scale, due to the melted PS flowing through the reactor at a fast rate. This reason translated to more undegraded PS collected in

the char pot (as will be discussed in the following paragraphs) in the studied temperature range than what was obtained at bench scale. This meant that when the temperature was increased at pilot scale, there was more potential for increased oil yield.

Figure 5.36 shows that at pilot scale the oil yield started to plateau at 550 ℃, while at bench scale the plateau had started at 500 ℃. The oil yield increased from 67.3±1.4 to 78.9±0.6 wt.% when the temperature increased from 450 to 500 ℃. A further temperature increase from 500 to 550 ℃ caused the oil yield to increase but only by 3.6 wt.% to 82.5±1.4 wt.%. At the temperature of 550 ℃ the oil yield obtained at bench scale (with the clean high-absorbent PS) was an average of 92.9 wt.%. Therefore, there is a decrease in oil yield when scaling up to pilot scale of about 10 wt.%. This decrease in oil yield can be attributed to the lower mass balance closures observed at pilot scale as discussed earlier.
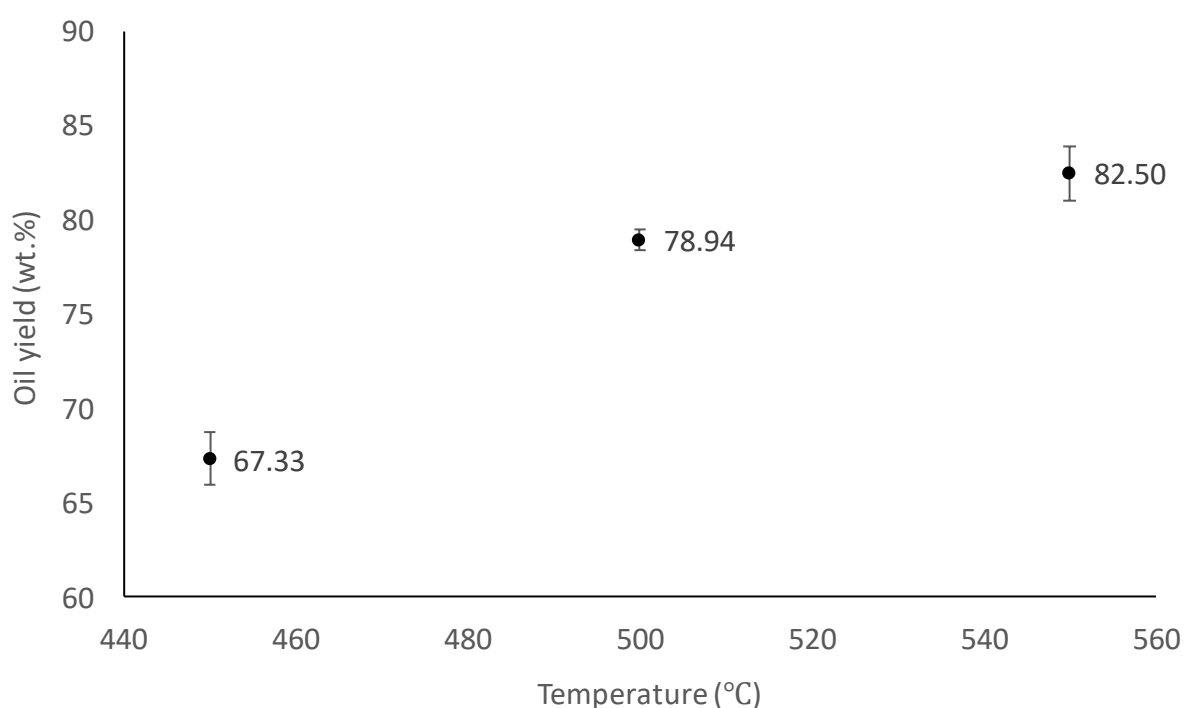
Figure 5.36: Effect of temperature on oil yield of pilot scale pyrolysis of contaminated high-density PS

To investigate the effect of temperature on the product yields further, the gas and residue yields as a function of the reactor temperature are presented in Figure 5.37. The gas yield can be seen to increase from 0.16±0.07 to 0.35±0.09 wt.% as temperature increased from 450 to 550 ℃ as more intense primary and secondary cracking occurred to yield non-condensable gasses. However, the gas yield overall remained very low (< 0.5 wt.%) in this tested range, as was also the case at bench scale (< 1 wt.% gas yield). The low gas yields are also consistent with the low yields (< 5 wt.%) that have been reported in literature (Williams & Williams, 1997, 1999b; Liu *et al.*, 2000). At 450 ℃, the residue yield was observed to be high (17.6±2.8 wt.%), compared to char yields at bench scale (< 5 wt.%). This was interpreted as a consequence of the undegraded melted plastic that flowed through the reactor at a rate

that reduced the feedstock residence time below what was required for complete degradation. Increasing the temperature caused significant reduction in the residue yield, with only 3.1±1.2 wt.% being produced at 550 °C. Based on this result, it was expected that increasing the temperature beyond 550 °C would not have caused a significant increase in oil yield (< 5 wt.%). Therefore, higher temperatures were not considered. This low yield of the residue is desirable not only from the perspective that it resulted in a higher oil yield, but also from a handling perspective, as it was very difficult to deal with and clean. The high MW condensable fraction of the residue was very viscous and had a sticky toffee like consistency. From this point of view, 550 °C seems like the most desirable temperature for pilot scale operation. However, at 500 °C the residue yield of 5.8±0.7 wt.% is not much higher than at 550 °C. Therefore, a future techno-economic analysis will be necessary to confirm whether the small increase in oil yield (only 3.6 wt.%) can justify the increase in temperature from 500 to 550 °C.
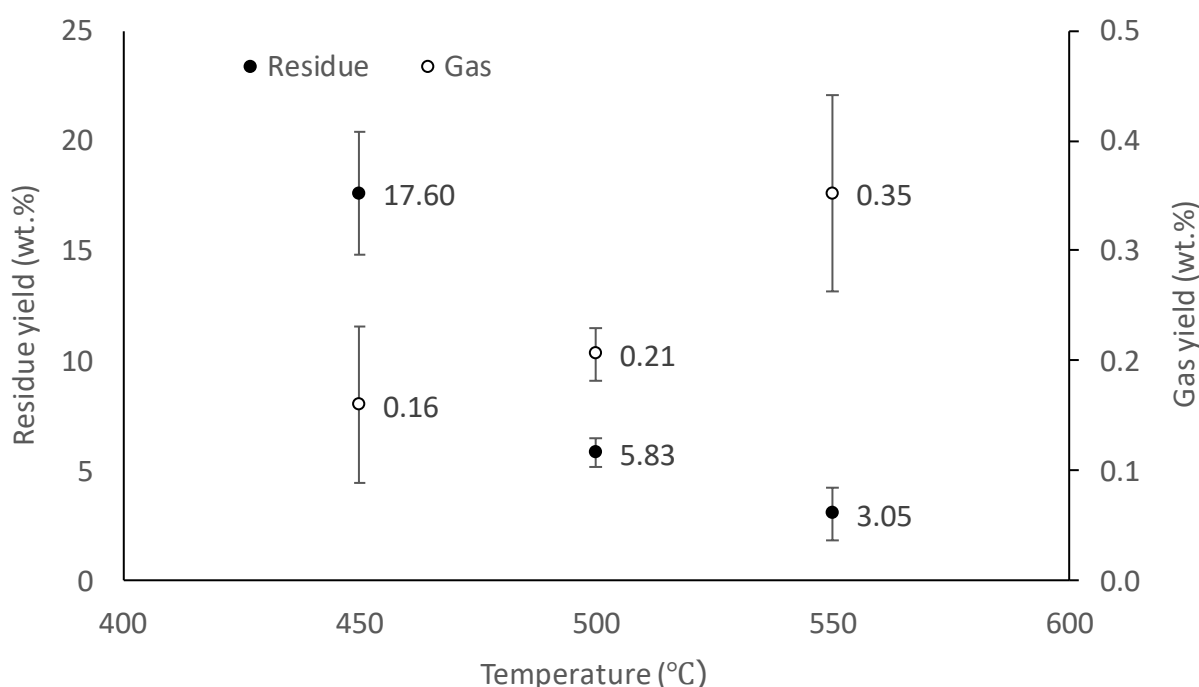
Figure 5.37: Effect of temperature on residue and gas yield of pilot scale pyrolysis of contaminated high-density PS

5.5.1.2 Energy analysis and composition of the oil

The HHV of the oils produced at pilot scale were tested by analysing a representative sample of oil from all 4 condensers. As with the oil produced at bench scale, the results at pilot scale demonstrated no significant effect of temperature on the HHV of the oil (Figure 5.38). The energy content of the oils produced at 450, 500, and 550 °C were all within the average range of 41.9-42.5 MJ/kg, which is similar to the HHV of the oils obtained at bench scale of 42.5-43.4 MJ/kg. Therefore, scaling up to pilot scale did not affect the HHV of the oil. The HHV of the oil was comparable to that of diesel (42.8-45.8 MJ/kg), and only slightly lower than that of gasoline (43.4-46.5 MJ/kg) (Sharuddin *et al*., 2016).

Similar to the bench scale results, the oil obtained at pilot scale had HHVs higher than the average of the raw feedstocks of 37.2-39.8 MJ/kg in Table 5.14. The gross energy recovered from the feedstock at the temperature of 550 °C was 88±3%. This recovery is about 7 to 12% lower than what was achieved at bench scale at 450 °C of greater than 95%, due mainly to the lower oil yield at pilot scale because of the product losses as explained in the previous section.
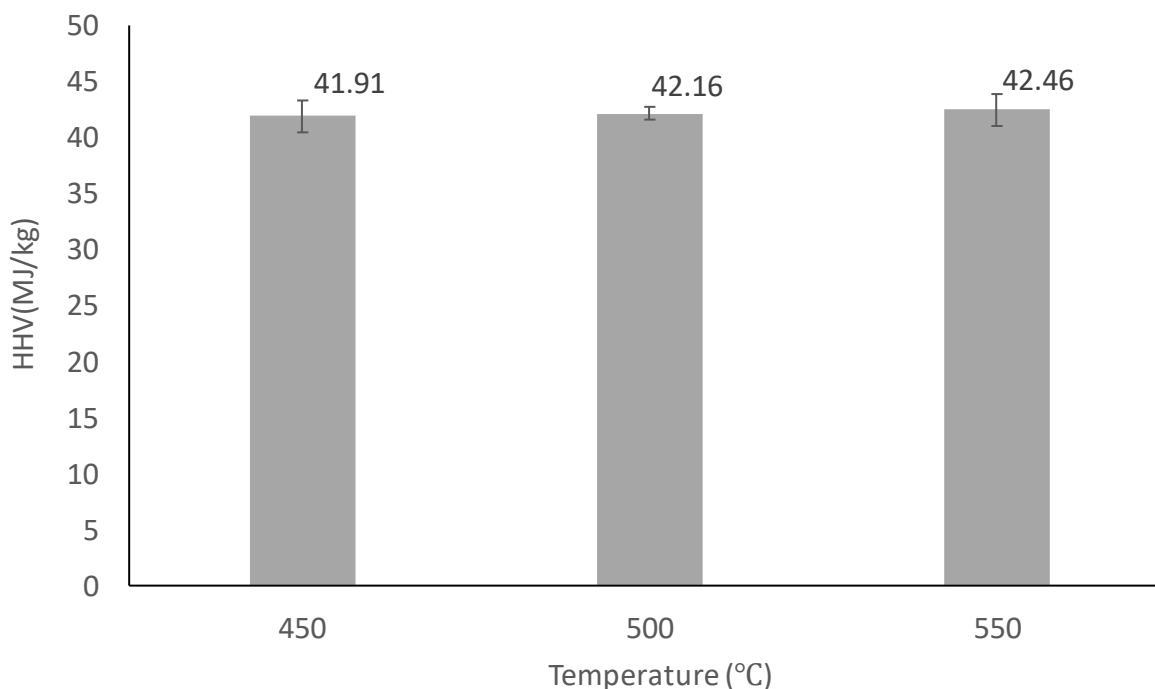
Figure 5.38: HHV analysis of contaminated high-density PS pyrolysis oil at pilot scale

The composition of the oils produced at pilot scale were determined in terms of the styrene, ethylbenzene, toluene, α-methylstyrene, and styrene dimer content. The oil product collected from the pyrolysis of the contaminated high-density PS at pilot scale was composed of an average of 68±2 wt.% of these compounds at all tested temperature conditions (450 °C, 500 °C, 550 °C). This proves that the oil was composed of at least 68 wt.% aromatic compounds. Aromatic content in fuel causes soot formation on combustion, which is detrimental to the engine (Zetterdahl *et al.*, 2017). This is why commercial gasoline and diesel typically have a low aromatic content of less than 35 vol% (SANS 1598, 2006) and about 5 vol% (Zetterdahl *et al.*, 2017) respectively. Therefore, blending of this oil with commercial fuel could be done to make it viable at a commercial level.

As stated in the bench scale section, the styrene yield is an additional point of interest aside from the use of the oil for fuel applications. The effect of temperature on the yields of styrene and the other 4 compounds is illustrated in Figure 5.39. A temperature increase from 450 to 550 °C resulted in an increase in the styrene yield from 31.1±0.9 to 39.4±3.5 wt.%. However, from 500 to 550 °C there was no significant difference in styrene yield. This would make sense if the styrene yield was to start to

reach the optimum in this temperature range. Indeed, other researchers determined that a styrene yield optimum was reached around 500 °C (Mo *et al*., 2014; Artexte *et al*., 2015). The optimum point in literature arose due to an increase in ethylbenzene, toluene and α-methylstyrene, accompanied by a decrease in styrene oligomers (such as dimer and trimer) yield as temperature increased (Mo *et al*., 2014; Artexte *et al*., 2015). Consistent with literature, Figure 5.39 illustrates similar trends with regards to the ethylbenzene, toluene and styrene dimer yields, indicating that at 550 °C greater depolymerisation occurred than at 450 °C. At bench scale it was found that temperature did not have a significant effect on the styrene, ethylbenzene, toluene, and styrene dimer yields (Section 5.2.4). It is possible that the temperature effect on the compound yields was significant at pilot scale but not at bench scale due to the difference in reactor configurations, specifically longer expected volatile residence times at pilot scale. Mo *et al*. (2014) and Artexte *et al*. (2015) found that the volatile residence effected the compound yields due to increased cracking at longer volatile residence times. Therefore, it is possible that the volatile residence time had an interacting effect on the temperature effect.

The maximum achieved styrene yield at pilot scale of 39.4±3.5 wt.% (Figure 5.39) was lower than the average yield achieved at bench scale of 48.3±6.1 wt.% (Table 5.18). This could be due to the longer expected volatile residence time (resulting in more cracking) at pilot scale compared to bench scale as discussed in the previous paragraph. This assumption is comforted by the fact that the maximum achieved pilot scale yields of ethylbenzene, toluene and α-methylstyrene of 4.9±0.8, 4.00±0.3 and 4.1±0.1 wt.% respectively (Figure 5.39) were higher than the average yields at bench scale of 1.4±0.9, 2.2±1.1 and 2.3±1.1 wt.% respectively (Table 5.18). Additionally, the maximum styrene dimer yield at pilot scale of 6.46±0.11 wt.% (Figure 5.39) was lower than the average yield at bench scale of 12.4±1.8 wt.% (Table 5.18). This is in accordance with findings by Artexte *et al*. (2015), who determined that as volatile residence time increased, the yields of ethylbenzene, toluene and α-methylstyrene increased and the yield of styrene dimer decreased, due to more cracking.
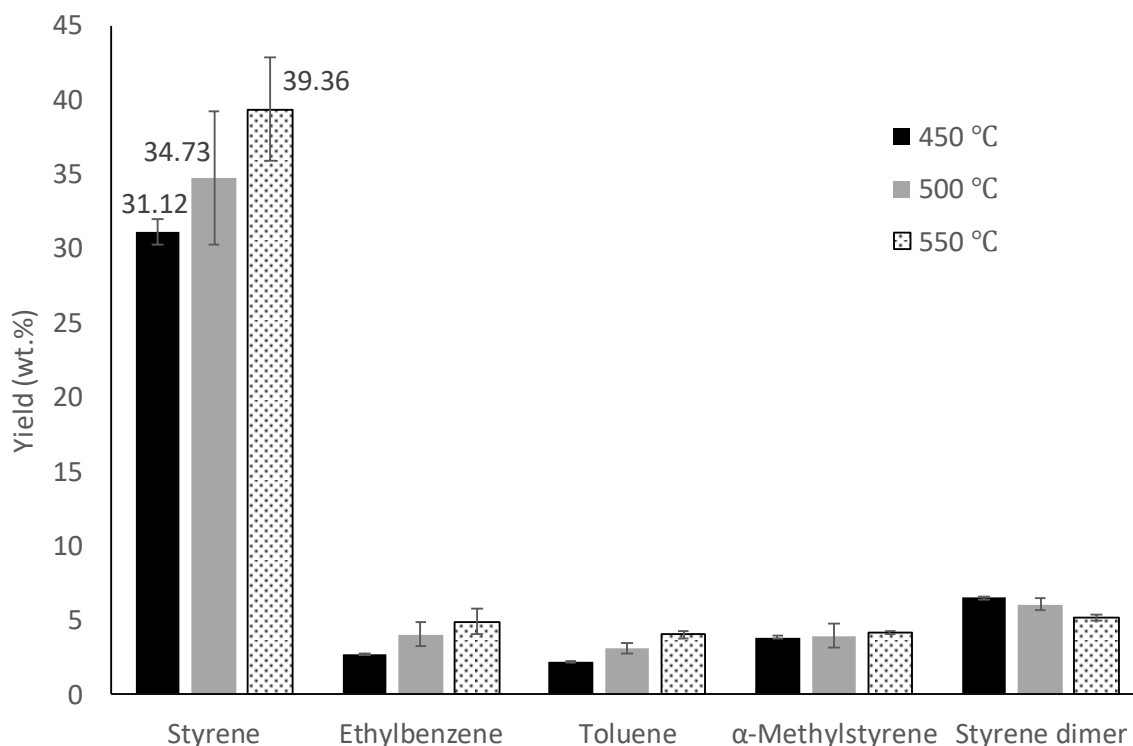
Figure 5.39: Yield of compounds in oil product from pilot scale pyrolysis of PS

5.5.1.3 Fuel properties of the oil product

Table 5.25 outlines the quality of the oil produced from the contaminated high-density PS at pilot scale in terms of some of the fuel properties that are considered important in standardisation of fuel for commercial use including ash content, pour point, flash point, sulphur content, viscosity, and distillation range (all tests were performed in duplicate). The properties are compared to SABS standards, SANS 342 for diesel and SANS 1598 for gasoline. Where the SABS standards do not specify the properties of interests, other sources were consulted to provide an indication of the relevant property value as outlined in Table 5.25.

Table 5.25 summarises the distillation behaviour of the PS derived oil and shows that the initial boiling point was at 137.0±1.4 °C, while the final boiling point was at 264.0±1.4 °C. The final boiling point was between what is specified by the SABS standards for gasoline and diesel of 210 and 360 °C. Additionally, Table 5.25 shows that at a distillation temperature of 154.0 °C, 80 vol% of the PS derived oil was recovered. As 154.0 °C is below the maximum boiling point for gasoline (210 °C), it proves that at least 80 vol% of the PS derived oil was in the gasoline range. The low boiling point of the PS derived oil makes sense as it was found that the majority of the oil (at least 68 wt.%) was composed of the single ring aromatics, styrene, ethylbenzene, toluene and α-methylstyrene. As these compounds have boiling points less than 165 °C (Daintith, 2008), the oil would be expected to have a corresponding low boiling point as evidenced by the distillation characterisation in Table 5.25. Therefore, the PS derived oil can be classified as predominantly gasoline and fractional distillation can be useful to remove the heavier

compounds (< 20 wt.%), which may be more suitable in diesel applications.

The ash content of the PS derived oil in Table 5.25 was 0.001 wt.% which is below the maximum content specified for commercial grade diesel of 0.01 wt.%. Gasoline standards do not specify a maximum ash content. However, SANS 1598 does specify the maximum content of lead, magnesium and potassium in metal-containing gasoline as a total of 59 mg/L. Using the average density of gasoline, this can be translated to a maximum weight percentage for these metals as 0.008 wt.%. This means that the maximum ash content of commercial grade gasoline would be at least 0.008 wt.%. Therefore, the PS derived oil would be suitable for gasoline as well as diesel applications in terms of ash content. The ash content of the PS derived oil was also substantially less than the ash content determined for the contaminated high-density feedstock of 3.27±1.38 wt.% (Table 5.14). This makes sense as it is expected that the inorganic fraction of the feedstock would partition to the char product, which is one of the ways that pyrolysis produces a value-added fuel (compared to the raw feedstock as fuel). The evidence of a more valuable fuel product (due to the reduced ash content) is reflected in the HHV of the oils, which were found to be higher than for the raw feedstocks (by about 4 MJ/kg) as discussed in Sections 5.2.4 and 5.5.1.2.

The density of the PS derived oil was 0.9232 kg/L (Table 5.26), which is about 9% higher than the commercial grade diesel range at 0.805-0.850 kg/L and 19% higher than the commercial grade gasoline range at 0.720-0.775 kg/L. The flash point of the PS derived oil of 30.5±0.7 °C was significantly greater than what is typically measured for commercial grade gasoline of -43 °C, but below the minimum specified for commercial grade diesel of 55 °C as outlined in Table 5.25. Therefore, in terms of the flash point, the suitability of the PS derived oil was not indicated for gasoline or diesel. Miandad *et al.* (2016b) achieved a similar flash point for PS derived oil of 30.2 °C.

As for the sulphur content, it was found to be 0.03 wt.% (Table 5.25) which is higher than the maximum amount specified for commercial grade gasoline and diesel of 0.001 wt.% according to SANS 342 and SANS 1598. However, it is below what is suitable for a 500 ppm (0.05 wt.%) grade fuel. The sulphur content was also significantly less than what was determined in the contaminated high-density PS feedstock of 0.52 wt.%, indicating a more valuable fuel for combustion compared to the raw feedstock with less SO_x emissions expected. Table 5.25 shows that the PS derived oil kinematic viscosity of 0.88±0.01 cSt was significantly lower than the range specified for commercial diesel of 2.0-4.5 cSt. However, the kinematic viscosity was only slightly higher than what is typically measured for commercial gasoline (0.6 cSt).

In summary, the distillation characterisation proves that the oil had boiling point predominantly in the gasoline range. Additionally, the oil was similar to commercial grade gasoline in terms of the ash

content, density, sulphur content and viscosity. However, as stated previously, the aromatic content in the oil was at least 68 wt.%. This means that the oil would not be suitable for use as gasoline as SANS 1598 specifies a maximum aromatic content in gasoline of 35 vol%. Therefore, blending of the oil will be essential to reduce the aromatic content.

Table 5.25: Fuel properties of PS derived oil at 550 °C

	PS derived oil	Diesel	Gasoline	References
Ash content, wt.%	<0.002	0.01 (max)	ns	(SANS 342, 2006)
Density at 15 °C, kg/L	0.9232±0.0001	0.805 (min) 0.850 (max)	0.720 (min) 0.775 (max)	(SANS 342, 2006; SANS 1598, 2006)
Flash point, °C	30.5±0.7	55 (min)	-43 ns	(SANS 342, 2006; Flash point – Liquids, n.d.)
Sulphur content, wt.%	0.03±0.01	0.001 (max)	0.001 (max)	(SANS 342, 2006; SANS 1598, 2006)
Kinematic viscosity at 40 °C, cSt	0.88±0.01	2.0 (min) 4.5 (max)	0.6	(SANS 342, 2006; Viscosity of liquids and gases, n.d.)
Distillation				
Initial boiling point, °C	137.0±1.4	ns	ns	-
10% Recovery, °C	142.0±0.1	ns	ns	-
20% Recovery, °C	142.5±0.7	ns	ns	-
30% Recovery, °C	145.0±1.4	ns	ns	-
40% Recovery, °C	145.5±0.7	ns	ns	-
50% Recovery, °C	146.0±0.1	ns	ns	-
60% Recovery, °C	147.5±0.7	ns	ns	-
70% Recovery, °C	149.0±0.1	ns	ns	-
80% Recovery, °C	154.0±0.1	ns	ns	-
Final boiling point, °C	264.0±1.4	360 (max), 95 vol% recovered	210 (max)	(SANS 342, 2006; SANS 1598, 2006)

ns = not specified by standards

5.5.1.4 Gas composition and energy value

The gas product obtained from the pyrolysis of PS at pilot scale, was composed of C_1-C_5 hydrocarbons, as well as H_2, CO and CO_2 as summarised in Table 5.26. The values reported in Table 5.26 specify the concentration of the compounds in the gas fraction, meaning that the actual yield of gas compounds were very little as the gas yield was less than 0.5 wt.% (Figure 5.37). It can be seen that CH_4 and the C_2 to C_4 hydrocarbons increased (by a combined average of about 36 wt.%) as temperature increased from 450 to 550 °C as increased cracking occurred at higher temperatures to form smaller compounds. This was accompanied by a decrease in CO_2 concentration of approximately 35 wt.%. This means that the gas produced at higher temperatures (550 vs 450 °C), consisted of more hydrocarbons, and explains the increase in the energy value of the gas from 7±5 to 22±1 MJ/kg as temperature increased from 450 to 550 °C. Comparison with literature reveals that from 450 to 550 °C more CH_4

106

was obtained in this study at pilot scale (0.96-9.50 wt.%) than in the fluidised bed reactor study by Williams and Williams (1999b) (< 0.1 wt.%). The higher CH_4 is possibly due to the longer expected volatile residence time in this study. This assumption can be supported by the fact that the CH_4 produced at bench scale (which had a shorter expected volatile residence time than pilot scale processing) was below the detection limit (Table 5.19).

At 550 °C, with the HHV of the gas being 22±1 MJ/kg, the energy produced from the gas per mass of feedstock processed was 0.08 MJ/kg. The estimated energy required for pyrolysis of PS has been estimated and reported to be 0.68 MJ/kg feedstock by Brems *et al.* (2011). Therefore, the gas fraction can potentially supply about 12% of the heat required for the pyrolysis process via combustion.

Table 5.26: Composition (concentration) and energy value of gas produced from pilot scale pyrolysis of PS

	450 °C	500 °C	550 °C
H_2 (wt.%)	0.96±0.56	1.54±0.83	1.56±0.17
CO (wt.%)	9.42±5.22	5.92±5.53	8.13±0.62
CH_4 (wt.%)	0.96±1.36	4.45±0.16	9.50±0.58
CO_2 (wt.%)	76.58±4.45	56.91±1.52	41.64±1.48
C_2 (wt.%)	3.20±2.26	10.70±1.81	16.06±0.50
C_3 (wt.%)	3.93±2.66	11.28±1.75	15.06±0.53
C_4 (wt.%)	4.82±3.75	9.19±2.53	8.06±0.58
C_5 (wt.%)	0.14±0.20	0.02±0.02	nd
C_6 (wt.%)	nd	nd	nd
HHV (MJ/kg gas)	7.28±5.09	17.69±4.20	21.76±1.05
HHV (MJ/kg feedstock)	0.01±0.00	0.04±0.00	0.08±0.00

nd = not detected; C_i = hydrocarbons containing i atoms of carbon

5.5.1.5 Char use

The utilisation of the char from PS pyrolysis is not frequently discussed in literature, probably because the char yield is usually less than 5 wt.%. However, at an industrial scale, 5 wt.% can represent a significant amount that should ideally not be landfilled. Some plastic derived chars have been shown to be comparable to commercial activated carbon after steam activation (Brems *et al.* 2011). Exploring the utilisation of the PS derived char as activated carbon, it can be useful to estimate the ash content of the char. With typical char yields of less than 5 wt.% being obtained in this study at bench scale (Figure 5.21) and the ash content of the PS feedstock being 3.27±1.38 wt.% in Table 5.14, the char would have an ash content of greater than 50 wt.%. This is important as char with a high ash content reduces the adsorption capacity of the char (Menya *et al.*, 2019), and the greater than 50 wt.% ash content of the

char could hinder its application as activated carbon.

Frequently, the energy value of pyrolysis char is also of interest. If a rough estimation is made that the organic fraction of the char has an HHV of 40 MJ/kg (similar to the PS feedstock in Table 5.14) and the inorganic fraction (ash) has an HHV of 0 MJ/kg, then the char would have an HHV of about 16 MJ/kg. This makes it similar to lignite coal A, which has an HHV of 14.7-19.3 (Green & Perry, 2008).

If the char has to be sent to landfill, then it will be very important to determine the composition of the inorganic fraction to assess the environmental impact.

5.5.2 LDPE/PET multi-layer

The conversion of the multi-layer at pilot scale was performed using the contaminated multi-layer, where 0.16 wt.% dry dog food contamination was added to the already cut clean multi-layer samples before processing. The processing rate of the contaminated multi-layer at pilot scale was 1 kg/h.

5.5.2.1 Product yields

At bench scale the optimum oil/wax yield from the pyrolysis of the LPDE/PET multi-layer was achieved at 500 ℃. Therefore, the pilot scale testing was centred around this temperature. The final temperature points investigated were 475, 500, 550 and 600 ℃. Following are the important observations made during the pilot scale testing with the LDPE/PET multi-layer:

- Similar to the pilot scale testing with PS, the product collected in the char pot consisted of undegraded plastic and some wax. Char was also clearly visible in the char pot. The undegraded plastic and char typically formed as one chunk, with the wax surrounding it. The surrounding wax was separated by hand from the plastic/char chunk and included in the yield of oil/wax. The melted plastic/char chunk is referred to as the residue in the following discussion.

- Typically, most of the oil/wax was collected in the first and second condensers (depicted in the schematic of the reactor in Figure 4.14) as shown in Figure 5.40. The oil/wax collected in all the condensers were observed to be flowable at ambient temperature.

- As with the pilot scale testing with PS, some volatiles were observed to escape at the feeding point. Additionally, it was observed that as the feeding cylinder moved forward to push the plastic into the reactor, small wisps of volatiles escaped at the cylinder and rotary seals (depicted in the set-up schematic in Figure 4.14).

Figure 5.40: Typical distribution of LDPE/PET multi-layer derived oi/wax in pilot scale condensers 1 to 4 (as shown from left to right)

The average mass balance closure for all the experiments was 70±13 wt.% (data not shown). The variability was much higher than what was observed when PS was tested at pilot scale with a mass balance closure of 85.3±0.9 wt.%. This large variability was interpreted as a consequence of the high viscosity of the melted LDPE, which made mixing and forward flow of the melt in the reactor unpredictable and could have also caused unpredictable trends in the mass transfer of volatiles out of the molten plastic. The mass balance closures at pilot scale were about 20-30 wt.% lower than what was obtained at bench scale (> 89 wt.%) when pyrolyzing the multi-layer. This was likely due to the volatile losses observed at the feeding point and seals and also due to condensation of oil/wax in parts of the pilot set-up that could not be weighed to be included in the mass balance. Predominantly, the lost oil/wax condensed in the exit pipe from the reactor. A similar observation was made at bench scale, where condensable fraction was observed at the outlet of the reactor. This condensable fraction had a yellow colour consistent with PET condensable product (Chomba, 2018) and its early condensation was due to its high boiling point that has been reported at about 400 °C (Brems *et al.*, 2011). Other researchers have also observed this phenomenon and have reported that PET condensable product caused blockages in pipes, especially at larger scale (Sharuddin *et al.*, 2016). This is the reason that there are so few articles describing PET pyrolysis, even though PET is a common plastic. During pilot scale experimentation in this study, this problem was overcome by operating at a low feed rate and nitrogen flowrate (1 kg/h and 1 L/min respectively). Further discussion on this operational problem can be found later in Section 5.6.

The ANOVA for the experimental range of 475-600°C and dependent variable of oil/wax yield is presented in Table 5.27. With a p-value of 0.02, the temperature effect was found to be significant.

Table 5.27: ANOVA for single factor (temperature) statistical design for pilot scale pyrolysis of contaminated LDPE/PET multi-layer

	SS	df	MS	F	p
Temperature (°C)	1844.92	3	614.97	13.19	0.02
Error	186.51	4	46.63		
Total	2031.44	7			

The ANOVA model was tested for its adequacy with residual visualisation in Figure 5.41. Figure 5.41a shows that the residuals were normally distributed and Figure 5.41b indicates independence of the residuals on time. Figure 5.41c indicates the residuals had constant variance and therefore the data were homoscedastistic.
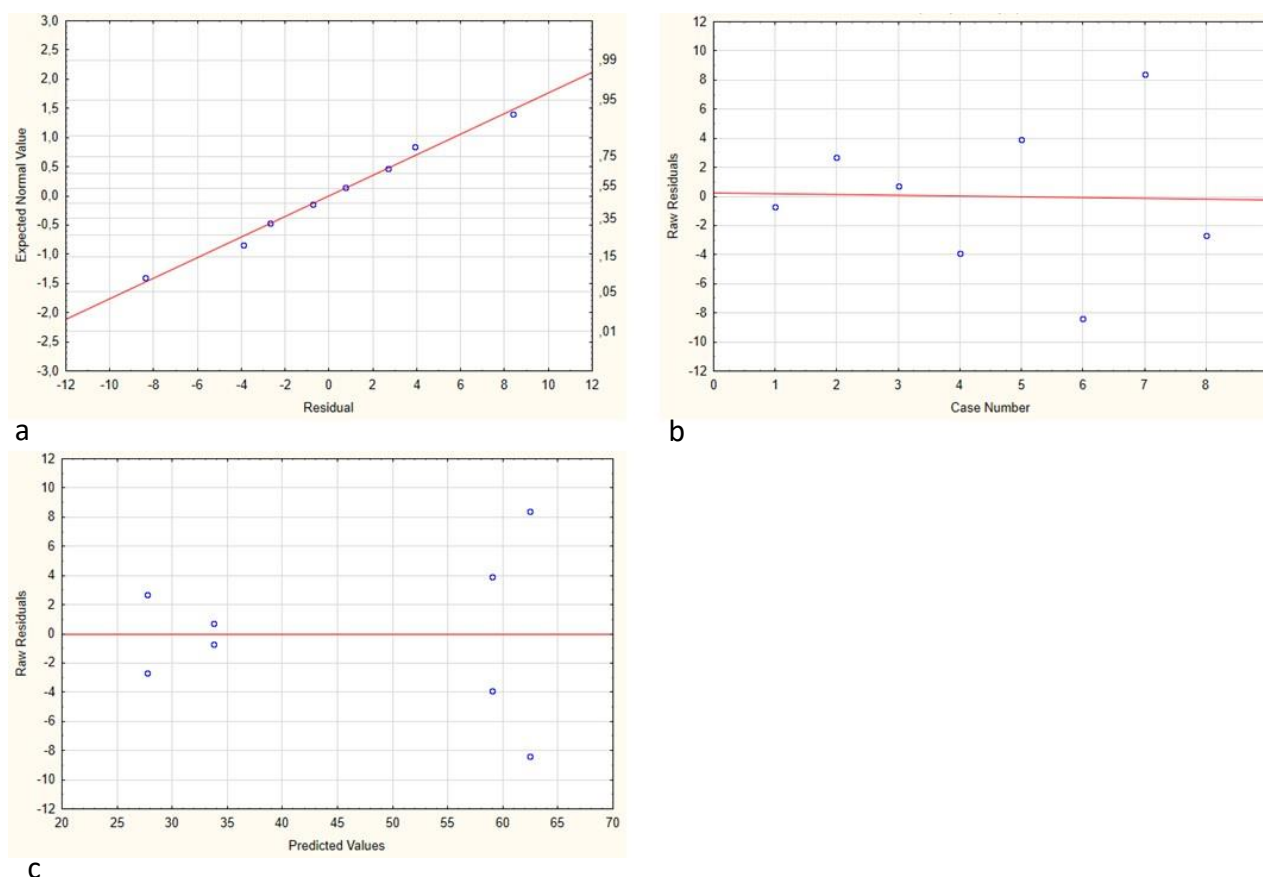
Figure 5.41: ANOVA model (contaminated LDPE/PET multi-layer oil/wax yield at pilot scale) adequacy check with residuals. a) normal probability of residuals; b) residuals vs run order/time (case number); c) residuals vs model predicted (oil/wax yield) values

The effect of temperature on the oil/wax yield is illustrated in Figure 5.42. It can be seen that the highest oil/wax yield of 62±12 wt.% was obtained at 475 °C. At 500 °C, the oil/wax yield of 59±6 wt.% was not significantly different to that achieved at 475 °C, whereas at bench scale there was a significant

increase in oil/wax yield (71.55±1.94 to 75.37±0.04 wt.% in Figure 5.29) when the temperature was increased from 475 to 500 °C. The fact that there was no significant difference in the oil/wax yield at these two temperatures at pilot scale is due to the large variability observed in the data. This large variability was due to the variability observed in the mass balances, as explained previously. Though it is not certain that the optimum temperature at pilot scale was 475 °C, instead of 500 °C (as was the case at bench scale), such difference (between bench and pilot scale) could be explained by the fact that clean multi-layer was considered for optimisation at bench scale (illustrated in Figure 5.29) while at pilot scale the contaminated multi-layer was used. This means that the optimum oil/wax yield could have shifted slightly to a lower temperature during pilot scale testing due to the catalytic effect from the inorganic fraction of the dog food contamination (this catalytic effect was proposed in Figure 5.31 during bench scale comparison of the clean and contaminated multi-layer). Furthermore, the catalytic effect could have been more pronounced at pilot scale than at bench scale, as was also proposed by Chireshe (2019) who made a similar observation while pyrolyzing biomass in a semi-continuous pilot scale rotary kiln reactor. As found by Chireshe (2019), the catalytic effect was more pronounced at pilot scale than at bench scale as the feedstock, volatiles and char mixed while moving through the rotary kiln reactor (whereas at bench scale with the batch reactor, the inorganic fraction remained in the sample boat and once the volatiles were swept away from the sample boat by the nitrogen flow, there was no more contact between the inorganic catalyst and the volatiles). This phenomenon resulted in more contact between the volatiles and the inorganic fraction of the contamination. Therefore, there could have been increased cracking of the volatiles at pilot scale, which caused the optimum oil/wax yield to shift to a lower temperature. When analysing differences in optimum temperature, differences in reactor configuration should also be considered and tests with the clean multi-layer at pilot scale could help with the interpretation of the results.

To test whether a greater oil/wax yield could be achieved at temperatures lower than 475 °C, an additional experiment was performed at 450 °C. This experiment resulted in 33 wt.% oil/wax yield (data not shown), due to limited feedstock conversion, which is significantly lower than the yield of 62±12 wt.% at 475 °C. Additionally, Figure 5.42 shows that further increase in temperature beyond 500 °C to 550 and 600 °C resulted in significant oil/wax yield decreases to 34±1 and 28±4 wt.% respectively. Therefore, the maximum oil/wax yield from the pyrolysis of contaminated LDPE/PET multi-layer at pilot scale was achieved at 475 to 500°C with 62±12 wt.% and 59±6 wt.% respectively, as shown in Figure 5.42. The maximum oil/wax yield achieved at pilot scale was about 9-13 wt.% lower than the yield at bench scale of 71.45±0.03 wt.% (Figure 5.31). This was due to the lower mass balance closures observed as explained previously.
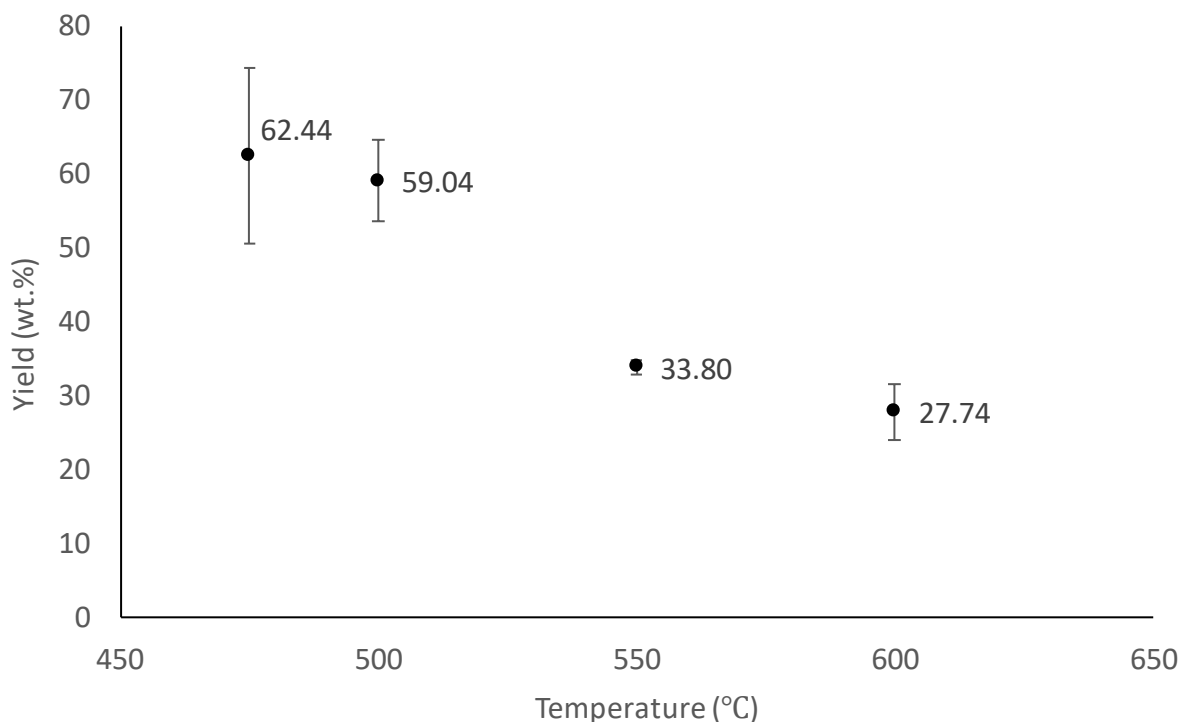
Figure 5.42: Effect of temperature on oil/wax yield from pilot scale pyrolysis of contaminated LDPE/PET multi-layer

Further insight into the process can be gained from Figure 5.43, which illustrates the yields of the flowable oil, wax, residue and gas. A very important feature in Figure 5.43 is the high flowable oil yields obtained at pilot scale, compared to what was achieved at bench scale (for example at a temperature of 500 °C, a flowable oil yield of 38±4 wt.% was achieved at pilot scale, compared to 12.56±1.61 wt.% at bench scale as seen in Figure 5.31). An explanation for this is that at bench scale the wax and oil were separated by the condensation of the heavier wax fraction in the first condenser at atmospheric temperature and the condensation of the oil fraction in the 4 condensers cooled with dry ice, as illustrated by the bench scale set-up in Figure 4.13. However, it was observed that the condensable fraction in the atmospheric condenser termed as "wax" was a mixture of wax and oil. At pilot scale the heavier wax fraction condensed in the char pot which was heated to 270 °C, while the oil condensed in the 4 downstream condensers, which facilitated better separation of the wax and the oil compared to bench scale. The more pronounced cracking of the wax fraction to smaller MW compounds at pilot scale, due to the proposed catalytic effect from the contamination, could also have contributed to the greater flowable oil yields. Figure 5.43 shows that the flowable oil yield was highest at 475 and 500°C (the same as with the oil/wax yield) with 39±10 wt.% and 38±4 wt.% yields respectively, which was about 26 wt.% more than the oil yield achieved at bench scale of 12.56±1.61 wt.% at a temperature of 500 °C (Figure 5.31). This was important as the flowable oil was found to be much easier to handle than the wax.

The wax yield illustrated in Figure 5.43, represents the wax collected in the char pot. At 475 and 500

°C, it constituted 24±2 and 21±2 wt.% respectively. As stated previously, the char pot had been heated to 270 °C to limit condensation of heavy compounds. Therefore, increased heating of the char pot would be necessary to further reduce the significant observed wax formation in the char pot.

In summary, from Figure 5.42, the maximum oil/wax yield at pilot scale was achieved at 475-500 °C (similar to bench scale) with 62±12 wt.% and 59±6 wt.% respectively (9-13 wt.% lower than at bench scale). The flowable oil yield at 475-500°C was 39±10 wt.% and 38±4 wt.% (Figure 5.43) which was about 26 wt.% more than what was achieved at bench scale. The wax fraction collected in the char pot was significant (> 20 wt.%) proving that heating of the char pot beyond 270 °C would be necessary to reduce its condensation here.
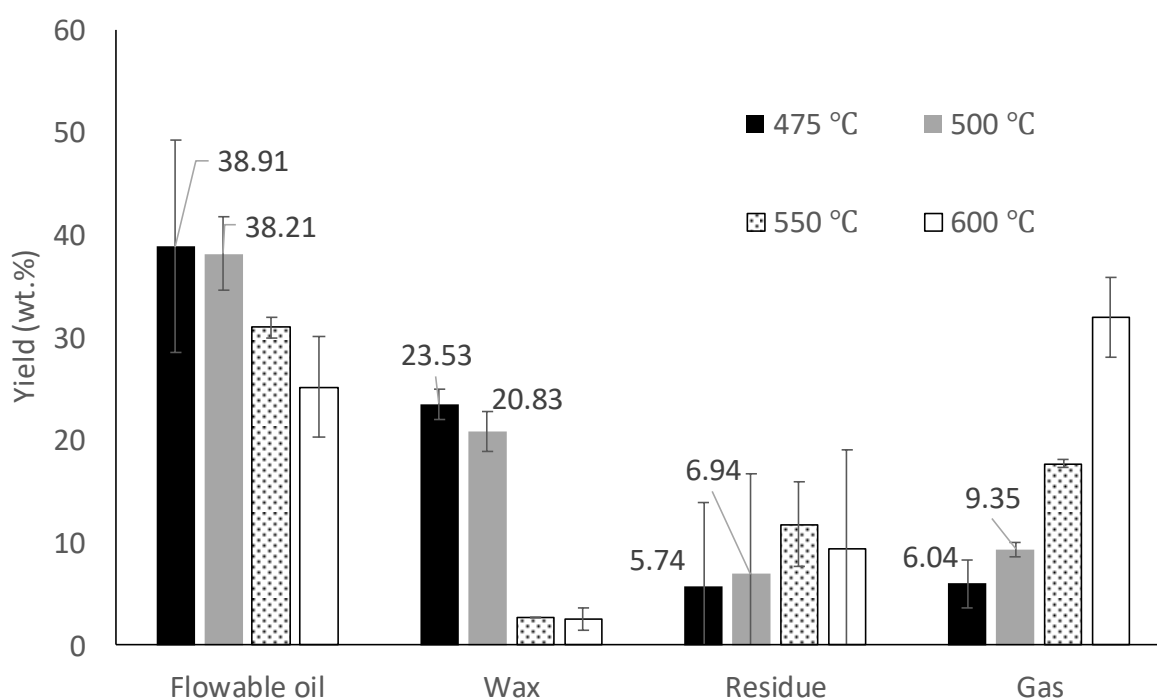
Figure 5.43: Effect of temperature on product yields from the pyrolysis of contaminated LDPE/PET multi-layer at pilot scale

5.5.2.2 Energy analysis of the oil/wax

The HHV analysis of the oil/wax was performed with a representative sample from all four condensers. Figure 5.44 illustrates the HHV of the oil/wax produced in the pilot reactor at the different temperatures tested. With a p-value of 0.58, it was determined that the temperature of the reactor had a non-significant effect on the HHV of the oil/wax. Figure 5.44 shows that the HHV of the oil/wax was in the range of 43.55-44.13 MJ/kg (comparable to commercial gasoline and diesel). This is similar to what was achieved at bench scale of 45.2±0.13 MJ/kg (Figure 5.32). The gross energy recovered in the oil/wax per mass of feedstock processed at 475 and 500 °C were 66±12 and 63±6% respectively.
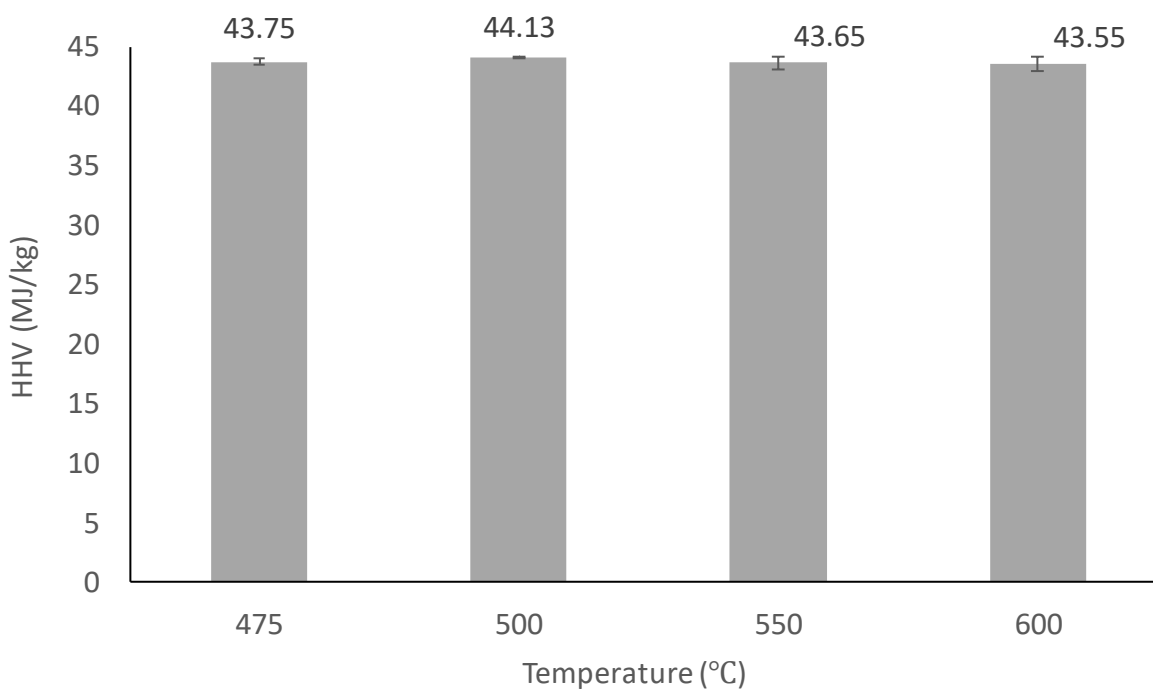
Figure 5.44: Effect of temperature on HHV of oil/wax from the pyrolysis of contaminated LDPE/PET multi-layer at pilot scale

5.5.2.3 Fuel properties of the oil/wax product

Table 5.28 summarises some of the fuel properties of the flowable oil produced from the LDPE/PET multi-layer at pilot scale at the temperatures of 475 and 500 °C. The properties determined were ash content, pour point, density, flash point, sulphur content and viscosity.

The ash content of the flowable oil (0.005 and 0.004 wt.%) was lower than what is specified as the maximum content for commercial diesel by SANS 342, making it suitable for use as diesel in terms of the ash content. Furthermore, the ash content was significantly less than what was determined for the raw feedstock of 4.83±0.11 wt.% in Table 5.20. This indicates that the majority of the inorganic contamination in the multi-layer formed part of the char product, as was also seen to be the case with the PS (Section 5.5.1.3). The suitability of the flowable oil for commercial diesel applications were also indicated by the density and the kinematic viscosity, both of which were within the commercial diesel range as shown in Table 5.28.

Table 5.28 indicates that the sulphur content of the flowable oil was 0.03 wt.%. This was more than what is specified as the maximum amount for ultra-low sulphur grade diesel at 0.001 wt.%. However, it meets the specification for a 500 ppm (0.05 wt.% max) sulphur grade diesel. The pour points of the flowable oils derived from pyrolysis at 475 and 500 °C were 16.0 and 15.0 °C respectively. This is significantly greater than the pour point of commercial diesel of (-18) – (-12) °C as reported by Güngör *et al*. (2015) and Dehaghani and Rahimi (2018). The pour point is the minimum temperature at which

114

the fuel flows (Miandad *et al.*, 2016b), and therefore the flowable oil would be more suitable in hot environments. The flash points of 18.0 and 20.0 °C indicated that the flowable oil would already ignite at ambient temperature when exposed to an ignition source. The flash points were significantly lower than the minimum flash point specified for diesel of 55 °C. The low flash point indicates the presence of very light, volatile compounds.

The distillation of the oil/wax could not be performed as it contained appreciable amounts of residual matter (heavy compounds) and therefore the distillation test method (ASTM D86) was not applicable. Overall, the properties of the flowable oil indicate that several properties were similar to commercial diesel. However, further upgrading would be necessary due to the presence of very light flammable compounds and very heavy compounds. Fractional distillation could be done to separate the heavier fraction from the light fraction that was indicated by the low flash point. After which the heavier fraction could be processed via fluid catalytic cracking (as suggested by Wong *et al.* (2015)) to produce lighter compounds in the diesel range.

Table 5.28: Fuel properties of LDPE/PET multi-layer derived flowable oil at 475 and 500 °C

	Flowable oil at 475 °C	Flowable oil at 500 °C	Diesel	Gasoline	References
Ash content, wt.%	0.005	0.004	0.01 (max)	ns	(SANS 342, 2006)
Density at 15 °C, kg/L	0.8355	0.8347	0.805 (min) 0.850 (max)	0.720 (min) 0.775 (max)	(SANS 342, 2006; SANS 1598, 2006)
Pour point, °C	16.0	15.0	(-18) – (-12)	ns	(Güngör *et al.*, 2015; Dehaghani & Rahimi, 2018)
Flash point, °C	Ambient at 18.0	Ambient at 20.0	55 (min)	-43 ns	(SANS 342, 2006; Flash point – Liquids, n.d.)
Sulphur content, wt.%	0.03	0.03	0.001 (max)	0.001 (max)	(SANS 342, 2006; SANS 1598, 2006)
Kinematic viscosity at 40 °C, cSt	3.79	4.1	2.0 (min) 4.5 (max)	0.6	(SANS 342, 2006; Viscosity of liquids and gases, n.d.)

ns = not specified by standards

5.5.2.4 Gas composition and energy value

As detailed in Table 5.29, the gas fraction produced from the pyrolysis of the contaminated multi-layer at pilot scale was composed of C_1-C_4 hydrocarbons as well as H_2, CO and CO_2. A difference from the bench scale pyrolysis at the optimum temperature of 500 °C (Table 5.23) is that C_5 hydrocarbons were not detected at pilot scale (Table 5.29), which could be due to the increased influence of the catalytic activity from the dry food contamination at pilot scale, which resulted in more intense cracking of C_5 hydrocarbons into lighter hydrocarbons as was explained in Section 5.5.2.1. It could also be due

to the change in reactor configuration from bench scale to pilot scale, with increased volatile residence time (and therefore increased secondary cracking) being expected at pilot scale.

Table 5.29 shows that, in terms of the energy content of the gasses, a gas fraction with a greater HHV (36.7±0.5 MJ/kg) was produced at 500 °C (compared to 30.3±0.7 MJ/kg at 475 °C), due to the decreased production of CO_2 and corresponding increase of the other high energy compounds at 500 °C. The HHV of the gas per kg of feedstock processed was 1.83±0.00 and 3.43±0.01 MJ/kg at 475 and 500 °C respectively. This resulted in gross energy recoveries of 4.5±0.1% at 475 °C and 8.3±0.1% at 500 °C. Brems *et al.* (2011) estimated in their study that the heat required for pyrolysis of polyethylene was 0.26 MJ/kg feedstock. Therefore, the gas fractions produced from the pyrolysis of the multi-layer at 475 and 500 °C could provide 7 and 13 times respectively the heat required. A similar result was found by Ghodrat *et al.* (2019) who pyrolysed a plastic mixture composed predominantly of polyethylene. This study found that the gas fraction could produce about 20 times the heat required for pyrolysis at 600 °C. It means that combustion of the gas product would make the pyrolysis process energy self-sufficient and some additional energy could be used for other activities.

Table 5.29: Gas composition and energy value at 475 and a pyrolysis temperature of 500 ℃

	475 °C	**500 °C**
H_2 (wt.%)	0.21±0.01	0.26±0.00
CO (wt.%)	9.07±0.22	7.97±0.11
CH_4 (wt.%)	5.52±0.15	7.77±0.12
CO_2 (wt.%)	32.66±0.97	21.15±1.11
C_2 (wt.%)	10.99±0.09	15.40±0.31
C_3 (wt.%)	25.97±0.82	30.99±0.53
C_4 (wt.%)	15.58±0.31	16.48±0.03
C_5 (wt.%)	nd	nd
C_6 (wt.%)	nd	nd
HHV (MJ/kg gas)	30.34±0.72	36.71±0.52
HHV (MJ/kg feedstock)	1.83±0.00	3.43±0.01

nd = not detected; C_i = hydrocarbons containing i atoms of carbon

5.5.2.5 Char use

As LDPE derived char has been reported to be less than 1 wt.% after complete degradation (Williams & Williams, 1999; Marcilla *et al.*, 2009; Gunasee *et al.*, 2017), its use is not often explored. However, PET derived char has been studied for its use as activated carbon by Brems et al. (2011) as studies have

obtained high char yields of 15-25 wt.%. These authors found that after steam activation, the char from PET pyrolysis was comparable to commercial activated carbon in terms of specific area and pore volume. However, the char from the conversion of the multi-layer sample considered in this study would have an ash content greater than 50 wt.%; this is based on a char yield of about 8 wt.% (Figure 5.30) and an ash content in the feedstock of 4.83±0.11 wt.% (Table 5.20). Therefore, its value as activated carbon would be diminished as a high ash content reduces the adsorption capacity of the char (Menya *et al.*, 2019). If the char were to be landfilled, it would be important to determine the composition of the inorganic fraction to assess the environmental impact.

5.6 Major difficulties and solutions

A major part of this study was to identify and resolve operational difficulties presented by the different natures of the investigated plastic feedstocks, in order to evaluate the viability of the pyrolysis process at a larger scale. These processing difficulties and solutions are presented here.

The major processing difficulty associated with the PS was the very low bulk density of the PS punnets investigated. This created two main problems: firstly the rate of processing at pilot scale would have been very low due to volumetric restrictions, which would affect the favourability of an economic analysis; and secondly, the lightness and bulkiness of the PS meant that it caused blockages in the feeding system of the pilot reactor, which made it physically impossible to process at pilot scale. The blockages occurred because the light and bulky PS would partially melt in the pipe underneath the feed hopper (Figure 4.14), which was hot due to its proximity to the reactor. This caused the PS to stick to the inside of the pipe, which eventually resulted in it getting blocked. The solution employed was to use densified PS at pilot scale, which resolved the major issue of blockage and allowed for a greater average feed rate of 2.3±0.6 kg/h. Therefore, the viability of the process was improved by densifying the PS. However, even the densified PS sometimes caused some blockages in the feeding system but to a much lesser degree than the high-absorbent PS. Therefore, it is further suggested that the feeding hopper drop-pipe be cooled with a cooling jacket to limit this effect.

As for the multi-layer, it presented several challenges. The major anticipated challenge was the presence of PET in the multi-layer, which has been known to produce condensables which de-sublimate at a very high temperature and cause blockages in the piping of a pyrolysis system (Sharuddin *et al.,* 2016). These blockages were observed during earlier testing with the multi-layer at pilot scale as shown in Figure 5.45. Two possible solutions were considered: firstly to set the second heating zone of the reactor to 400 °C to force the PET condensable to de-sublimate in this zone and fall in the char pot with the char fraction; and secondly reduce the feeding rate of the multi-layer feedstock and operate at a very low nitrogen flowrate to prevent high degrees of blockages during testing.

For the first solution, an insulation between the heating zones had to be installed in order to be able to set the first zone to temperatures above 475 ℃, while maintaining the second zone at 400 ℃. After installation of the insulation, the maximum difference in temperature between the two heating zones that could be achieved was 60 ℃. To test the viability of this solution, one test was performed, whereby the first heating zone was set to 475 ℃ which resulted in a temperature of 415 ℃ in the second zone (from conduction and convection from the first zone). The test proved that this would not be a viable solution with this reactor set-up as the temperature was not high enough to ensure adequate degradation of the plastic feedstock and resulted in a large amount of undegraded plastic in the reactor exit pipe (Figure 5.46) and char pot.

The second solution to decrease the feeding rate of the multi-layer feedstock and operate at a low nitrogen flowrate proved adequate to limit the blockage of the pipes so that the experimental runs could be completed. However, for this process to be viable at a larger scale, a solution, that can deal with continuous processing of the multi-layer as opposed to simply just testing, will need to be implemented. To this end, it is suggested that a filtration system be considered in future. During pilot testing when blockages did occur, it was noticed that the blockages were mainly at positions where there was either a narrowing of the pipes or a mesh (as at the gas exit). This suggests that a filtration system will be adequate to remove the PET condensables from the gas stream. Furthermore, through experience with the pilot scale reactor, it can be suggested that a mesh filtration system be used at the end of the heated exit pipe (Figure 4.14) in such a way that it can periodically be removed and exchanged for a new mesh (for example two mesh filters with a valve system that can divert the gas flow from one to the other).

The other difficulty experienced with the processing of the multi-layer was the size reduction of the feedstock. The plastic film was difficult to cut and mill. Eventually it was determined that by first shredding the plastic in an industrial paper shredder and then processing in a rotating blade mill, the size of the plastic particles could be adequately reduced to be able to feed samples to the pilot scale rotary kiln reactor.

Figure 5.45: PET condensables blockages in pipes at pilot scale

Figure 5.46: Melted plastic in exit pipe

6 Summary of results

To answer the key questions and objectives as outlined in Section 3, a summary of the important results is provided in this section.

6.1 Polystyrene single-layer

1. **Feedstock characterisation**

    Characterisation of the contamination present in PS waste could scarcely be found in literature, and therefore it was considered as an important first step in the approach to this study. The contamination in the contaminated high-absorbent PS was predominantly water (about 46.5 wt.%), proving that it would need to undergo drying before pyrolysis. The dry contamination in the dried contaminated high-absorbent PS was 15.9±1.3 wt.% and had the effect on feedstock characterisation of increasing the N, O and fixed carbon content consistent with what is expected from protein contamination. The contaminated high-density PS had less nitrogen than the contaminated high-absorbent PS, and higher sulphur and ash content than both high-absorbent batches. Overall, the three PS batches were found to be suitable for a pyrolysis process targeting the hydrocarbon oil product and had similar HHVs in the range of 37.2-39.8 MJ/kg, which is slightly lower than the HHV of conventional diesel.

    The clean and contaminated high-absorbent PS had similar thermal degradation behaviour, except for an earlier initial degradation temperature observed for the contaminated high-absorbent PS, which was attributed to the protein contamination degrading at a lower temperature. The contaminated high-density PS degraded earlier and had a lower peak degradation temperature than the clean high-absorbent PS, which was possibly due to a catalytic effect from the higher inorganic fraction (as supported by the higher ash content) or due to the densification process degrading the structure of this PS batch.

2. **Bench scale pyrolysis**

    The PS feedstocks produced only oil in the condensable fraction, with no wax being produced. The heating rate (tested range of 25-200 °C/min) had a non-significant effect on the oil yield, while temperature in the range of 450-550 °C had a significant effect. The maximum oil yield from the pyrolysis of clean PS of 93.2±1.4 wt.% was achieved at 600 °C. As the oil yield at 450 °C (89.8±0.4 wt.%) was only 3.4 wt.% lower than the maximum, this condition was not excluded as it saves on the energy requirement with only a small decrease in oil yield from the maximum. The HHV of the oil was not significantly affected by temperature or heating rate in the studied ranges. Furthermore, the oil had a greater HHV than the raw feedstocks, resulting in gross energy

recoveries of greater than 95%. The oil was found to be predominantly composed of aromatic compounds (> 72 wt.%) with a styrene yield of 48.3±6.1 wt.%.

The effect of contamination on bench scale pyrolysis of PS was an important consideration in this study that does not seem to be frequently discussed in literature. Heavy contamination of the PS with meat juice (about 16 wt.% dry contamination) reduced the oil yield by 7.3 wt.% at a pyrolysis temperature of 450 ℃, due to increased char and gas yields brought about by the protein contamination (after drying). The contaminated densified PS batch, which was a more representative sample of what would be collected in industry with lower degree of contamination, had a similar oil yield to the clean PS. The HHV of PS pyrolysis oil was not significantly affected by contamination and was in the range of 42.5-43.4 MJ/kg for the clean and contaminated PS batches. The composition of the oils derived from the contaminated PS batches were also predominantly aromatic.

3. Pilot scale pyrolysis

To our knowledge, studies investigating the scale-up of pyrolysis bench scale results to pilot scale are limited, making the results obtained in this study valuable to further our understanding of this aspect. Pilot scale testing resulted in lower mass balance closures due to increased losses of volatiles from equipment seals and losses of oil product in the equipment parts other than the condensers. It seemed that the feedstock residence time at pilot scale was less than at bench scale (30 min) due to fast forward flow of the melted PS in the rotary kiln pilot reactor which caused more significant residue yields at lower temperatures (450 ℃). The highest oil yield of 82.5±1.4 wt.% was reached at 550 ℃ during pilot scale testing, which was about 10 wt.% less than at bench scale due to more significant losses at pilot scale.

The HHV of the oil product from pilot scale testing (41.9-42.5 MJ/kg) was similar to what was achieved at bench scale, making the oil comparable in terms of energy content to conventional gasoline and diesel. However, due to the lower oil yield at pilot scale, the gross energy recovered in the oil (88±3%) was lower at pilot scale than at bench scale by about 7-12%. It was determined that the gas product from pilot scale pyrolysis of PS could potentially supply about 12% of the heat required for the pyrolysis process via combustion.

4. Oil use as fuel

The distillation characterisation of the PS derived oil proved that at least 80 vol% of the oil fell within the gasoline range specification. The ash content, density, sulphur content and viscosity

of the oil also compared well with commercial gasoline. The HHV of the oil was only slightly lower than that of commercial gasoline. The major quality concern then seemed to be the high aromatic content (> 68 wt.% at pilot scale), as commercial gasoline is limited to 35 vol% (SANS 1598, 2006). Therefore, upgrading of the oil by blending with conventional fuel could be considered.

5. **Major operational difficulties**

The major operational difficulty associated with the scale up of the PS pyrolysis process to pilot scale was the low bulk density of the feedstock, which made it practically impossible to feed it to the specific pilot reactor. It was determined that it was essential to densify the PS feedstock before pilot scale pyrolysis. This had the additional very important benefit of increasing the processing rate of the PS and therefore improving the viability of the process. To our knowledge, work pertaining to the pyrolysis of densified PS has not been considered in literature. Therefore, the study of the densified PS in terms of its characterisation, bench and pilot scale pyrolysis were a key element in this study. The universal benefit of densifying the PS (aside from being more practical in this particular study) is that it increased the processing rate of the PS. Whether the extra energy requirements necessary for densification can be justified would need to be assessed via a techno-economic analysis in future work.

6.2 LDPE/PET multi-layer

1. **Feedstock characterisation**

Characterisation of the LDPE/PET multi-layer was considered an important first step in this study as literature pertaining to the pyrolysis of LDPE/PET mixtures (both clean and contaminated) were found to be very limited, especially in the form of a multi-layer plastic.

To our knowledge, the method of deconvolution of peaks has not been applied to TGA data from an LDPE/PET multilayer, and in this study it was used to determine the amounts of LDPE and PET in present in the multi-layer. From this it was determined that pure LDPE and PET constituted about 76.6 and 18.6 wt.% respectively with the balance being inorganic (determined from ash quantification). However, the PET quantification seemed to be an overestimation, as it predicted a higher oxygen content in the multi-layer than what was determined via the ultimate analysis. This meant that the PET peak observed in the TGA data was not pure PET.

In terms of the proximate, ultimate and energy content analysis, it was determined that contamination did not have a significant effect (due to the low determined amount of

contamination of 0.16 wt.%). Both the clean and contaminated multi-layers were found to be suitable for a pyrolysis process where the hydrocarbon oil/wax yield is targeted, in terms of the proximate and ultimate analysis, and with HHVs (40.7-41.2 MJ/kg) similar to commercial diesel.

Contamination did not have an effect on the thermal degradation behaviour as determined with TGA. Finally, from the TGA results, possible interaction between LDPE and PET seemed to be limited.

2. Bench scale pyrolysis

Bench scale experiments were performed with the clean and the contaminated multi-layer to optimise the yield and quality of the oil/wax. Many bench scale pyrolysis studies have been done with LDPE and a few with PET. Only some studies have investigated LDPE and PET mixtures (with proportions pre-determined by the researchers) However, nothing (according to our knowledge) was available concerning the bench scale pyrolysis with an LDPE/PET multi-layer or the effect of contamination.

It was found that the condensable fraction was composed of oil and wax. Temperature had a significant effect (in the range of 475 to 700 °C) on the oil/wax yield with the optimum (when pyrolyzing the clean multi-layer) of 75.37±0.04 wt.% being achieved at 500 °C. The results from the pyrolysis of the contaminated multi-layer at 500 °C showed that the oil/wax yield decreased to 71.45±0.03 wt.%, with a corresponding increase in gas yield. This pointed toward a possible catalytic effect from the inorganic fraction of the dog food contamination. The effect of temperature (in the range of 475 to 650 °C) and contamination on the HHV of the oil/wax was non-significant with values in the range of 43.72-45.15 MJ/kg. Only at 700 °C did the HHV decrease to 40.65±2.03 MJ/kg which was likely due to the increased production of PAHs at this high temperature.

Finally, the gas composition was determined, which showed that more lighter hydrocarbons such as CH_4, C_2 to C_4 were produced when pyrolyzing the contaminated multi-layer as compared to the clean. This again pointed toward a possible catalytic effect from the inorganic fraction of the dog food contamination and resulted in a gas fraction with a higher energy value of 38.7±0.8 MJ/kg.

3. **Pilot scale pyrolysis**

The scale-up of the bench scale results to pilot scale were important as studies investigating this aspect are scarcely found. Scaling up resulted in a 20-30 wt.% reduction in mass balance closure due to more significant losses at pilot scale. Additionally, large variability was observed which was attributed to unpredictable mixing and forward flow of the high viscosity plastic melt in the reactor. The highest oil/wax yield of 62±12 wt.% was obtained at 475 °C during pilot scale testing. This was about 9 wt.% lower than at bench scale due to more condensable losses at pilot scale. The temperature at which the highest oil/wax yield was achieved (475-500 °C) was also slightly lower than the optimum temperature at bench scale (500 °C). This was attributed to the catalytic effect from the dry dog food contamination, which could have been more pronounced at pilot scale than at bench scale. It could also have been due to the different pilot reactor configuration compared to the bench reactor, where volatile residence times were expected to be longer at pilot scale resulting in increased secondary cracking. Furthermore, pilot scale pyrolysis of the multi-layer resulted in flowable oil of 39±10 and 38±4 wt.% at 475 and 500 °C respectively, which was about 26 wt.% more than was obtained at bench scale. This was a positive outcome as it was found that the flowable oil was easier to handle than the wax.

The HHV of oil/wax was not significantly affected by scaling up to pilot scale, with values in the range of 43.5-44.13 MJ/kg. The gross energy recovered from the oil/wax (obtained during pyrolysis at 475 °C) was determined as 66±12%. Finally, it was determined that combustion of the gas fraction could potentially supply about 7 to 13 times the heat required for pyrolysis.

4. **Oil/wax use as fuel**

The HHV of the oil/wax (43.5 to 44.13 MJ/kg) was found to be similar to that of commercial gasoline and diesel. The fuel characteristics of the flowable oil from pilot scale pyrolysis were comparable to the standard properties of commercial diesel (in terms of the density, viscosity, and the ash and sulphur content), but with a lower flash point and a higher pour point. It was also determined that the flowable oil contained appreciable amounts of heavy compounds. Further upgrading of the flowable oil would be necessary (possibly fractional distillation followed by fluid catalytic cracking) to make the flowable oil suitable for combustion in a diesel engine.

5. **Major operational difficulties**

The description of the difficulties associated with pilot scale pyrolysis of plastics in general can hardly be found in literature. The major operational difficulties associated with the scale-up of

the multi-layer pyrolysis to pilot scale were the blocking of the pipes from the condensables produced from the PET fraction and the size reduction of the multi-layer to be suitable at pilot scale in terms of feeding. The blockage problem during testing was overcome by reducing the feed rate of the feedstock and the flowrate of nitrogen. However, a solution that is able to cope with larger feed rates and prolonged continuous processing will be necessary and it is suggested that a mesh filtration system could be a viable solution. The size reduction of the multi-layer was accomplished by first shredding the multi-layer bags in an industrial paper shredder and then processing in a rotating blade mill, which was able to reduce the particle size to an adequate size for easier feeding to the pilot reactor.

7 Conclusions and recommendations

This study focussed on the pyrolysis of two plastic waste fractions that have been identified as problematic in South Africa's waste streams, due to their mixed and/or contaminated nature which excludes them from recycling via established secondary means. The two plastic wastes were a polystyrene single-layer used to package raw meat and an LDPE/PET multi-layer used to package dry dog food. The main aim of the study was to optimise the oil/wax product yield and to determine its quality as a fuel, with specific focus on the effect of contamination and the scale-up of the process to pilot scale.

7.1 Polystyrene single-layer

This study showed at bench scale that "worst-case" contaminated PS with about 16 wt.% contamination (after drying) can be processed via pyrolysis to produce an oil yield of 83.4±1.2 wt.%, which was about 7.3 wt.% less than the oil yield obtained with clean PS. Additionally, contamination was found to not affect the HHV of the oil. This proves that a high oil yield can be obtained despite contamination with gross energy recoveries of greater than 95% having been achieved.

To process the PS at pilot scale, it was found to be beneficial to use densified PS as it resulted in more effective feeding and would mean that the feedstock could be processed at a faster rate. To achieve the maximum oil yield at pilot scale, the temperature had to be increased from 500 °C (the maximum point at bench scale) to 550 °C, probably due to a shorter feedstock residence time at pilot scale (from the flow of the melted PS) compared to bench scale. Additionally, the product losses at pilot scale caused about a 10 wt.% decrease in the maximum oil yield compared to bench scale. The gross energy recovered at pilot scale at the maximum point was 88±3%.

The oil showed similarity to conventional gasoline in terms of HHV, boiling point range, ash content and sulphur content. The HHV of the oil was higher than that of the feedstock while the ash and sulphur

contents were lower than that of the feedstock, which is as a result of the inorganic fraction portioning to the char product, leading to an upgraded fuel product. The viscosity, density and flash point of the oil did not meet specification for gasoline. The composition of the oil was determined to be at least 68 wt.% aromatic. Some commercial transportation fuel must comply to a limited aromatic content (for example gasoline is limited to 35 vol%), therefore blending of the oil with commercial grade fuel is suggested. As aromatic compounds cause toxic emissions (Zetterdahl *et al*., 2017), it is important to consider a life cycle assessment (LCA) which compares the utilisation options of the oil. In this study it would be important to consider not just the harmful aromatic emissions from combustion but also the contribution this would make to CO_2 emissions and climate change. Another option for the utilisation of the fuel is to recover valuable chemicals, particularly styrene.

The following recommendations for further work with the PS can be made:

- A techno-economic analysis will be useful to determine whether increases in temperature can justify the small increases in oil yield in the temperature range of 500-550 °C at pilot scale. The techno-economic analysis will also be essential to determine if the energy required for densification of the PS can be justified by the increased processing feed rate.

- The feeding hopper drop-pipe can be fitted with a cooling jacket to reduce its temperature and to further limit melting of PS and blockage formation in the feeding section. However, densification of the PS would still be necessary even if the cooling jacket is installed to enable a greater feeding rate.

- The blending ratio of the PS derived oil with conventional gasoline must be investigated with a focus on required blending ratios and its effect on oil composition and fuel properties.

- An LCA analysis regarding the utilisation of the oil will be useful, especially as the high aromatic content of the oil can cause harmful emissions when combusted.

7.2 LDPE/PET multi-layer

The multi-layer was determined to be composed of 76.6±2.6 wt.% LDPE and less than 18.6±2.5 wt.% PET. The optimum oil/wax yield of 75.37±0.04 wt.% at 500 °C was achieved from the bench scale pyrolysis of the clean multi-layer. The dry dog food contamination was determined to have a potential catalytic effect with 0.16 wt.% contamination causing a 3.92±0.07 wt.% decrease in oil/wax yield, but had no significant effect on the HHV.

Pilot scale pyrolysis of the contaminated multi-layer proved that the multi-layer can successfully be processed at pilot scale even with the presence of the PET, which has been known to cause blockages

in a continuous process system. The formation of blockages was mitigated by decreasing the feedstock feeding rate and utilising a low nitrogen flowrate. The installation of a filtration system is proposed to mitigate this problem further. The flow of the melted polymer through the reactor behaved unpredictably causing large variation around the maximum oil/wax yield point. However, the data suggested that the maximum point may have shifted to the lower temperature of 475 °C, compared to 500 °C at bench scale. This could be due to longer expected volatile residence times at pilot scale or it could be due to a more pronounced catalytic effect at pilot scale. Processing with clean multi-layer would be useful to gain further insight. Losses at pilot scale caused about a 9 wt.% reduction in the maximum oil/wax yield compared to bench scale. The gross energy recovered from the multi-layer at pilot scale was 66±12%.

In terms of the quality of the oil/wax, it showed similarity to diesel in terms of HHV, ash content, sulphur content, density and viscosity. Distillation characterisation could not be performed because of the presence of heavy wax compounds, and the pour point was higher than diesel for the same reason. The flash point was lower than diesel due to the presence of very light compounds. Therefore, to upgrade the oil/wax for fuel application, it is suggested to separate the light and heavy fractions via fractional distillation and to further crack the heavy fraction via fluid catalytic cracking.

For further work with the multi-layer, the following recommendations are made:

- Pilot scale tests with clean multilayer could help in understanding the influence of different reactor configurations when scaling-up and confirm potential catalytic effect of the contamination component.
- The heating on the char pot and reactor outlet line must be improved to prevent the condensation of significant wax fraction (> 20 wt.%) in the char pot.
- A mesh filtration system must be designed and installed on the pilot reactor to facilitate the removal of the condensables (from the PET fraction) from the gas stream and so overcome the problem of blockages of the pipes at higher feedstock feeding rates.
- Lastly, the upgrading of the flowable oil product via fractional distillation and fluid catalytic cracking and the effect on the fuel properties should be tested.

8 References

Aboulkas, A., El harfi, K., Nadifiyine, M. & Benchanaa, M. 2011. Pyrolysis Behaviour and Kinetics of Moroccan Oil Shale with Polystyrene. *Journal of Petroleum and Gas Engineering*, 2(6):108–117.

Aboulkas, A., El harfi, K. & El bouadili, A. 2008. Pyrolysis of olive residue/low density polyethylene mixture: part I thermogravimetric kinetics. *Journal of Fuel Chemistry and Technology*, 36(6):672–678.

Adhesive resins and tie layers: Polymer Properties Database. 2019. [Online]. Available: http://polymerdatabase.com/Films/Tie%20Layers.html [2019, September 11].

Aguado, R. 2003. Kinetics of polystyrene pyrolysis in a conical spouted bed reactor. *Chemical Engineering Journal*, 92(1–3):91-99.

Aguado, J. & Serrano, D.P. 1999 *Feedstock recycling of plastic wastes*. Cambridge: The Royal Society of Chemistry.

Ahmad, I., Khan, M.I., Khan, H., Ishaq, M., Tariq, R., Gul, K. & Ahmad, W. 2015. Pyrolysis Study of Polypropylene and Polyethylene Into Premium Oil Products. *International Journal of Green Energy*, 12(7):663-671.

Al-Salem, S.M., Lettieri, P. & Baeyens, J. 2009. Recycling and recovery routes of plastic solid waste (PSW): A review. *Waste Management*, 9(10):2625–2643.

Angyal, A., Miskolczi, N. & Bartha, L. 2007. Petrochemical feedstock by thermal cracking of plastic waste. *Journal of Analytical and Applied Pyrolysis*, 79:409-414.

Artexte, M., Lopez, G., Amutio, M., Elordi, G., Olazar, M. & Bilbao, J. 2010. Operating Conditions for the Pyrolysis of Poly-(ethylene terephthalate) in a Conical Spouted-Bed Reactor. *Industrial & Engineering Chemistry Research*, 49:2064-2069.

Artexte, M., Lopez, G., Amutio, M., Barbarias, I., Arregi, A., Aguado, R., Bilbao, J. & Olazar, M. 2015. Styrene recovery from polystyrene by flash pyrolysis in a conical spouted bed reactor. *Waste Management*, 45:126-133.

Bagri, R. and Williams, P.T. 2002. Catalytic pyrolysis of polyethylene. *Journal of Analytical and Applied Pyrolysis*, 63:29–41.

Bockhorn, H., Hornung, A. & Hornung, U. 1998. Stepwise pyrolysis for raw material recovery from plastic waste. *Journal of Analytical and Applied Pyrolysis*, 46(1):1-13.

Bockhorn, H., Hornung, A. & Hornung, U. 1999. Mechanisms and kinetics of thermal decomposition of plastics from isothermal and dynamic measurements. *Journal of Analytical and Applied Pyrolysis,* 50:77-101.

Brems, A., Baeyens, J., Vandecasteele, C. & Dewil, R. 2011. Polymeric Cracking of Waste Polyethylene Terephthalate to Chemicals and Energy. *Journal of the Air & Waste Management Association*, 61(7):721-731.

Bridgwater, A.V. 2012. Review of fast pyrolysis of biomass and product upgrading. *Biomass and Bioenergy*, 38:68–94.

Caillat, S. & Vakkilainen, E. 2013. Large-scale biomass combustion plants: an overview, in L. Rosendahl (ed). *Biomass Combustion Science, Technology and Engineering.* Cambridge: Woodhead Publishing Limited. 189-224.

Callister, W.D. & Rethwisch, D.G. 2011. *Materials Science and Engineering, SI Version.* 8th edition. John Wiley and Sons, Inc.

Çengel, Y.A. & Boles, M.A. 2008. *Thermodynamics: an Engineering Approach.* 7th edition. Boston: McGraw-Hill Higher Education.

Chen, D., Yin, L., Wang, H. & He, P. 2014. Pyrolysis technologies for municipal solid waste: A review. *Waste Management*, 34:2466-2486.

Chen, L., Wang, S., Meng, H., Wu, Z. & Zhao, J. 2017. Synergistic effect on thermal behavior and char morphology analysis during co-pyrolysis of paulownia wood blended with different plastics waste. *Applied Thermal Engineering,* 111:834-846.

Chireshe, F. 2019. Production of an upgraded bio-oil by catalytic pyrolysis of forest residues. Unpublished master's thesis. Stellenbosch: Stellenbosch University.

Chomba, E.M. 2018. Pyrolysis of waste plastics into chemicals as an alternative to landfilling or incineration. Unpublished master's thesis. Stellenbosch: Stellenbosch University.

Cit, I., Smag, A., Yumak, T., Ucar, S., Misirhoglu, Z. & Canel, M. 2010. Comparative pyrolysis of polyolefins (PP and LDPE) and PET. *Polymer Bulletin*, 64:817-834.

Collard, F-X. & Blin, J. 2014. A review on pyrolysis of biomass constituents: Mechanisms and composition of the products obtained from the conversion of cellulose, hemicelluloses and lignin. *Renewable and Sustainable Energy Reviews*, 38:594–608.

Curve fitting to get overlapping peak areas [Online]. 2012. Available: http://matlab.cheme.cmu.edu/2012/06/22/curve-fitting-to-get-overlapping-peak-areas/. [2019, August 19].

Daintith, J. 2008. *Dictionary of Chemistry*. Oxford: Oxford University Press.

Demirbas, A. 2004. Pyrolysis of municipal plastic wastes for recovery of gasoline-range hydrocarbons. *Journal of Analytical and Applied Pyrolysis*, 72:97–102.

Dehaghani, A.H.S. & Rahimi, R. An experimental study of diesel fuel cloud and pour point reduction using different additives. *Petroleum,* 4-7.

Diaz-Silvarrey, L.S. & Phan, A.N. 2016. Kinetic study of municipal plastic waste. *International Journal of Hydrogen Energy*, 41(37):16352–16364.

Diaz-Silvarrey, L.S., Mcmahon, A. & Phan, A.N. 2018. Benzoic acid recovery via waste poly (ethylene terephthalate) (PET) catalytic pyrolysis using sulphated zirconia catalyst. *Journal of Analytical and Applied Pyrolysis*, 134:621-631.

Engel, T. & Reid, P. 2013. *Thermodynamics, Statistical Thermodynamics, & Kinetics*. 3rd edition. Pearson Education, Inc.

Fahim, M.A., Alsahhaf, T.A. & Elkinlani, A. 2010. *Fundamentals of petroleum refining*. Oxford: Elsevier.

Faravelli, T., Bozzano, G., Scassa, C., Perego, M., Fabini, S., Ranzi, E. & Dente, M. 1999. Gas product distribution from polyethylene pyrolysis. *Journal of Analytical and Applied Pyrolysis,* 52(1):87-103.

Faravelli, T., Pinciroli, M., Pisano, F., Bozzano, G., Dente, M. & Ranzi, E. 2001. Thermal degradation of polystyrene. *Journal of Analytical and Applied Pyrolysis,* 60(1):103-121.

Figueiredo, F. & Gomes, M.I. 2013. The Skew-Normal Distribution in SPC. *REVSTAT-Statistical Journal*, 11(1):83-104.

Flashpoints – Liquids [Online]. [n.d.]. Available: https://www.engineeringtoolbox.com/flash-point-

fuels-d_937.html [2019, November 9].

Fogler, H.F. 2014. *Elements of chemical reaction engineering*. Harlow: Pearson Education Limited.

Ganeshan, G., Shadangi, K.P. & Mohanty, K. 2018. Degradation kinetic study of pyrolysis and co-pyrolysis of biomass with polyethylene terephthalate (PET) using Coats – Redfern method. *Journal of Thermal Analysis and Calorimetry*, 131(2):1803-1816.

Gao, F. 2010. Pyrolysis of Waste Plastics into Fuels. Unpublished doctoral dissertation. Christchurch: University of Canterbury.

Ghodrat, M., Alonso, J.A., Hagare, D., Yang, R. & Samali, B. 2019. Economic feasibility of energy recovery from waste plastic using pyrolysis technology: an Australian perspective. *International Journal of Environmental Science and Technology,* 16(7):3721–3734.

Green, D.W. & Perry, R.H. 2008. *Perry's Chemical Engineers' Handbook*. 8th edition. New York: McGraw-Hill.

Gunasee, S.D., Danon, B., Görgens, J.F. & Mohee, R. 2017. Co-pyrolysis of LDPE and cellulose: Synergies during devolatilization and condensation. *Journal of Analytical and Applied Pyrolysis*, 126:306-314.

Güngör, C., Serin, H., Özcanli, M., Serin, S. & Aydin, K. 2015. Engine Performance and Emission Characteristics of Plastic Oil Produced from Waste Polyethylene and Its Blends with Diesel Fuel. *International Journal of Green Energy,* 12(1):98-105.

Havelcova, M., Bicakova, O., Sykorova, I., Weishauptova, Z. & Melegy, A. 2016. Characterization of products from pyrolysis of coal with the addition of polyethylene terephthalate. *Fuel Processing Technology*, 154:123–131.

Hemighaus, G., Boval, T., Bosley, C., Organ, R., Lind, J., Brouette, R., Thompson, T., Lynch, J. & Jones, J. 2006. *Alternative Jet Fuels*. Chevron Corporation.

Hujuri, U., Ghoshal, A.K. & Gumma, S. 2008. Modeling pyrolysis kinetics of plastic mixtures. *Polymer Degradation and Stability*, 93(10):1832–1837.

Hujuri, U., Ghoshal, A. K. & Gumma, S. 2010. Temperature-dependent pyrolytic product evolution profile for low-density polyethylene from gas chromatographic study. *Waste Management*, 30(5):814–820.

Izzatie, N., Basha, M.H., Uemura, Y., Hashim, M.., Amin, N.A.M. & Hamid, M.F.B. 2017. Co-pyrolysis of rice straw and Polyethylene Terephthalate (PET) using a fixed bed drop type pyrolyzer. *Journal of Physics: Conference Series,* 908(1).

Jayanarayanan, K., Thomas, S. & Joseph, K. 2016. Effect of blend ratio on the dynamic mechanical and thermal degradation behaviour of polymer-polymer composites from low density polyethylene and polyethylene terphphalate. *Iranian Polymer Journal*, 25(4):373-384.

Kalargaris, I., Tian, G. & Gu, S. 2017. Combustion, performance and emission analysis of a DI diesel engine using plastic pyrolysis oil. *Fuel Processing Technology*, 157:108–115.

Kaminsky, W., Predel, M. & Sadiki, A. 2004. Feedstock recycling of polymers by pyrolysis in a fluidised bed. *Polymer Degradation and Stability*, 85:1045–1050.

Kebelmann, K., Hornung, A., Karsten, U. & Griffiths, G. 2013. Intermediate pyrolysis and product identification by TGA and Py-GC/MS of green microalgae and their extracted protein and lipid components. *Biomass and Bioenergy*, 49(0):38-48.

Kim, S.S. & Kim, S. 2004. Pyrolysis characteristics of polystyrene and polypropylene in a stirred batch reactor. *Chemical Engineering Journal*, 98(1–2):53–60.

Kotz, J.C., Treichel, P.M. & Townsend, J.R. 2009. *Chemistry and chemical reactivity*. Belmont: Thompson Higher Education.

Kunwar, B., Cheng, H.N., Chandrashekaran, S.R. & Sharma, B.K. 2016. Plastics to fuel: a review. *Renewable and Sustainable Energy Reviews*, 54:421–428.

Letcher, T.M. & Vallero, D.A. 2011. *Waste: A handbook for management*. Burlington: Elsevier.

Levchik, S.V. & Weil, E.D. 2004. A review on thermal decomposition and combustion of thermoplastic polyesters. *Polymers for Advanced Technologies*, 15(12):691–700.

Li, A.M., Li, X.D., Ren, Y., Chi, Y., Yan, J.H. & Cen, K.F. 1999. Pyrolysis of solid waste in a rotary kiln: influence of final pyrolysis temperature on the pyrolysis products. *Journal of Analytical and Applied Pyrolysis,* 50:149-162.

Liu, J. & Zhang, Y. 2011. Effect of ethylene-acrylic acid copolymer on flame retardancy and properties of LLDPE/EAA/MH composites. *Polymer Degradation and Stability,* 96(12):2215-2220.

Liu, Y., Qian, J. & Wang, J. 2000. Pyrolysis of polystyrene waste in a fluidized-bed reactor to obtain styrene monomer and gasoline fraction. *Fuel Processing Technology*, 63(1):45–55.

López, A., de Marco, I., Caballero, B.M., Laresgoiti, M.F. & Adrados, A. 2010. Pyrolysis of municipal plastic wastes: Influence of raw material composition. *Waste Management*, 30(4):620-627.

López, A., de Marco, I., Caballero, B.M., Laresgoiti, M.F. & Adrados, A. 2011. Influence of time and temperature on pyrolysis of plastic wastes in a semi-batch reactor. *Chemical Engineering Journal*, 173:62–71.

Marcilla, A., Beltrán, M.I. & Navarro, R. 2009. Evolution of products during the degradation of polyethylene in a batch reactor. *Journal of Analytical and Applied Pyrolysis.* 86(1):14–21.

Martín-Gullón, I., Esperanza, M. & Font, R. 2001. Kinetic model for the pyrolysis and combustion of poly-(ethylene terephthalate) (PET). *Journal of Analytical and Applied Pyrolysis*, 58–59:635–650.

Masri, S., Li, L., Dang, A., Chung, J.H., Chen, J-C., Fan, Z-H. & Wu, J. 2018. Source characterization and exposure modeling of gas-phase polycyclic aromatic hydrocarbon (PAH) concentrations in Southern California. *Atmospheric Environment*, 177:175–186.

McKeen, L.W. 2014. Plastics Used in Medical Devices, in K. Modjarrad (ed.) *Handbook of Polymer Applications in Medicine and Medical Devices*. William Andrew Publishing. 21-53.

Menya, E., Olupot, P.W., Storz, H., Lubwama, M., Kiros, Y. & John, M.J. 2018. Optimization of pyrolysis conditions for char production from rice husks and its characterisation as a precursor for production of activated carbon. *Biomass Conversion and Biorefinery*.

Miandad, R., Barakat, M.A., Aburiazaiza, A.S., Rehan, M., Ismail, I.M.I. & Nizami, A.S. 2016a. Effect of plastic waste types on pyrolysis liquid oil. *International Biodeterioration and Biodegradation*, 119:239–252.

Miandad, R., Nizami, A.S., Rehan, M., Barakat, M.A., Khan, M.I., Mustafa, A., Ismail, I.M.I. & Murphy, J.D. 2016b. Influence of temperature and reaction time on the conversion of polystyrene waste to pyrolysis liquid oil. *Waste Management*, 58:250–259.

Mo, Y., Zhao, L., Wang, Z., Chen, C.L., Tan, G.Y.A. & Wang, J.Y. 2014. Enhanced styrene recovery from waste polystyrene pyrolysis using response surface methodology coupled with Box-Behnken design. *Waste Management*, 34(4):763–769.

Montgomery, D.C. 2013. *Design and analysis of experiments*. 8th edition. John Wiley & Sons, Inc.

National Plastics Recycling Survey-2016. 2017. PlasticsSA.

National Waste Information Baseline Report. 2012. RSA: Department: Environmental Affairs.

Nunes, L.J.R., de Oliveira Matias, J.C. & da Silva Catalao. 2018. *Torrefaction of Biomass for Energy Applications*. Academic Press.

Ojha, D.K. & Vinu, R. 2015. Resource recovery via catalytic fast pyrolysis of polystyrene using zeolites. *Journal of Analytical and Applied Pyrolysis*, 113:349–359.

Park, B.I., Bozzelli, J.W., Booty, M.R., Bernhard, M.J., Mesuere, K., Pettigrew, C.A., Shi, J.C. & Simonich, S. L. 1999. Polymer pyrolysis and oxidation studies in a continuous feed and flow reactor: Cellulose and polystyrene. *Environmental Science and Technology*, 33(15):2584–2592.

Park, J.J., Park, K., Park, J-W. & Kim, D.C. 2002. Characteristics of LDPE pyrolysis. *Korean Journal of Chemical Engineering*, 19(4):658–662.

Park, J.J., Park, K., Park, J-W. & Kim, D.C. 2003. Characterization of Styrene Recovery from the Pyrolysis of Waste Expandable Polystyrene. *Korean Journal of Chemical Engineering*, 19(4):658-662.

Park, S.S., Seo, D.K., Lee, S.H., Yu, T.U. & Hwang, J. 2012. Study on pyrolysis characteristics of refuse plastic fuel using lab-scale tube furnace and thermogravimetric analysis reactor. *Journal of Analytical and Applied Pyrolysis*, 97:29–38.

Parku, G.K. 2019. Pyrolysis of waste polypropylene plastics for energy recovery: Investigation of operating parameters and process development at pilot scale. Unpublished master's thesis. Stellenbosch: Stellenbosch University.

Pek, W.K. & Ghosh, U.K. 2015. Effect of binary mixture of waste plastics on the thermal behavior of pyrolysis process. *Environmental Progress & Sustainable Energy*, 34(4): 1113–1119.

SANS 1598: Unleaded Petrol. 2006. Pretoria: South African Bureau of Standards.

SANS 342: Automative Diesel Fuel. 2006 Pretoria: South African Bureau of Standards.

Shah, J. & Jan, M.R. 2014. Thermo-catalytic pyrolysis of polystyrene in the presence of zinc bulk catalysts. *Journal of the Taiwan Institute of Chemical Engineers*, 45(5):2494–2500.

Shah, S.H., Khan, Z.M., Raja, I.A., Mahmood, Q., Bhatti, Z.A., Khan, J., Farooq, A., Rashid, N. & Wu, D. 201. Low temperature conversion of plastic waste into light hydrocarbons. *Journal of Hazardous Materials,* 179(1-3):15-20.

Sharuddin, S.D.A., Abnisa, F., Daud, W.M.A.W. & Aroua, M.K. 2016. A review on pyrolysis of plastic wastes. *Energy Conversion and Management*, 115:308–326.

Silderber, M.S. 2009. *Chemistry: The molecular nature of matter and change.* 5th edition. New York: McGraw-Hill.

Singh, R.K., Ruj, B., Sadhukhan, A.K. & Gupta, P. 2019. Thermal degradation of waste plastics under non-sweeping atmosphere: Part 1: Effect of temperature, product optimization, and degradation mechanism. *Journal of Environmental Management*, 239:395–406.

Sogancioglu, M., Ahmetli, G. & Yel, E. 2017. A Comparative Study on Waste Plastics Pyrolysis Liquid Products Quantity and Energy Recovery Potential. *Energy Procedia*, 118:221–226.

Sogancioglu, M., Yel, E. & Ahmetli, G. 2017. Investigation of the Effect of Polystyrene (PS) Waste Washing Process and Pyrolysis Temperature on (PS) Pyrolysis Product Quality. *Energy Procedia*, 118:189–194.

Speight, J.G. 2015. *Handbook of petroleum product analysis*. New Jersey: John Wiley & Sons.

The New Plastics Economy: Catalysing Action. 2016. Ellen MacArthur Foundation.

Viscosity of liquids and gases [Online]. [n.d.]. Available: http://hyperphysics.phy-astr.gsu.edu/hbase/Tables/viscosity.html [2019, November 9].

Wei, X., Ma, X., Peng, X., Yao, Z., Yang, F. & Dai, M. 2018. Comparative investigation between co-pyrolysis characteristics of protein and carbohydrate by TG-FTIR and Py-GC/MS. *Journal of Analytical and Applied Pyrolysis*, 135(381):209–218.

Williams, E.A. & Williams, P.T. 1997. The Pyrolysis of Individual Plastics and a Plastic Mixture in a Fixed Bed Reactor. *Journal of Chemical Technology and Biotechnology.* 70:9-20.

Williams, P.T., Horne, P.A. & Taylor, D.T. 1993. Polycyclic aromatic hydrocarbons in polystyrene derived pyrolysis oil. *Journal of Analytical and Applied Pyrolysis*, 25:325–334.

Williams, P.T. & Williams, E.A. 1999a. Fluidised bed pyrolysis of low density polyethylene to produce petrochemical feedstock. *Journal of Analytical and Applied Pyrolysis*, 51(1):107–126.

Williams, P.T. & Williams, E.A. 1999b. Product Composition from the Fast Pyrolysis of Polystyrene. *Environmental Technology*, 20:1109–1118.

Wiriyaumpaiwong, S. & Jamradloedluk, J. 2017. Distillation of Pyrolytic Oil Obtained from Fast Pyrolysis of Plastic Wastes. *Energy Procedia*, 138:111–115.

Wong, S.L., Ngadi, N., Abdullah, T.A.T. & Inuwa, I.M. 2015. Current state and future prospects of plastic waste as source of fuel : A review. *Renewable and Sustainable Energy Reviews*, 50:1167–1180.

Yi, L., Liu, H., Lu, G., Zhang, Q., Wang, J., Hu, H. & Yao, H. 2017. Effect of Mixed Fe/Ca Additives on Nitrogen Transformation during Protein and Amino Acid Pyrolysis. *Energy and Fuels*, 31(9):9484–9490.

Yue, L., Li, G., He, G., Guo, Y., Xu, L. & Fang, W. 2016. Impacts of hydrogen to carbon ratio (H/C) on fundamental properties and supercritical cracking performance of hydrocarbon fuels. *Chemical Engineering Journal*, 283:1216–1223.

Zetterdahl, M., Salo, K., Fridell, E. & Sjöblom, J. 2017. Impact of Aromatic Concentration in Marine Fuels on Particle Emissions. *Journal of Marine Science and Application*, 16:352–361.

Zhang, Z., Hirose, T., Nishio, S., Morioka, Y., Azuma, N., Ueno, A., Ohkita, H. & Okada, M. 1995. Chemical Recycling of Waste Polystyrene into Styrene over Solid Acids and Bases. *Industrial & Engineering Chemistry Research*, 34(12):4514–4519.

Zhao, D., Jin, Y. & Wang, M. 2012. Study on viscosity of polymer melt flowing through microchannels considering the wall-slip effect. *Polymer Engineering & Science*, 52(8), pp. 1806–1814.

Zhou, J., Qiao, Y., Wang, W., Leng, E., Huang, J., Yu, Y. & Xu, M. 2016. Formation of styrene monomer, dimer and trimer in the primary volatiles produced from polystyrene pyrolysis in a wire-mesh reactor. *Fuel*, 182:333–339.

Appendices

Appendix A: Data

A.1 Polystyrene single-layer

Table A.30: Bench scale data with clean high-absorbent PS testing effect of nitrogen flow rate

Nitrogen flow rate (L/min)	Char (wt.%)	Oil (wt.%)	Gas (wt.%)
0.5	2.50	91.50	5.95
2	2.30	64.02	33.68

Table A.31: Bench scale data with clean high-absorbent PS

	Temperature (°C)	Heating rate (°C/min)	Char (wt.%)	Oil (wt.%)	Gas (wt.%)	HHV (MJ/kg)
2-Factor factorial design	550	200	4.40	92.41	0.65	41.61
	550	25	4.60	93.39	0.84	41.62
	450	200	4.81	89.48	0.28	42.81
	450	25	4.60	90.10	0.36	41.92
	500	112.5	4.50	90.40	0.64	41.64
	500	112.5	4.70	93.09	0.44	42.06
	500	112.5	4.70	92.00	0.54	42.72
Data at 600 °C	600	200	3.49	96.34	0.17	-
	600	200	4.60	91.90	3.50	-

Table A.32: Bench scale data with contaminated high-absorbent PS

Temperature (°C)	Heating rate (°C/min)	Char (wt.%)	Oil (wt.%)	Gas (wt.%)	HHV (MJ/kg)
450	200	8.90	83.20	1.73	45.39
450	200	9.20	82.40	1.67	43.04
450	200	8.40	84.70	3.98	41.85

Table A.33: Bench scale data with contaminated high-density PS

Temperature (°C)	Heating rate (°C/min)	Char (wt.%)	Oil (wt.%)	Gas (wt.%)	HHV (MJ/kg)
450	200	4.43	88.52	0.18	42.77
450	200	4.83	92.91	0.16	42.25

Table A.34: Pilot scale data with contaminated high-density PS

Temperature (°C)	Residue (wt.%)	Oil (wt.%)	Gas (wt.%)	HHV (MJ/kg)
450	19.57	66.35	0.109	42.83
450	15.63	68.31	0.210	40.99
500	6.30	79.35	0.223	42.21
500	5.35	78.54	0.189	42.12
550	2.20	83.51	0.289	43.06
550	3.90	81.48	0.415	41.86

A.2 LDPE/PET multi-layer

Table A.35: Bench scale data with LDPE/PET multi-layer

	Temperature (°C)	Char (wt.%)	Oil/wax (wt.%)	Oil (wt.%)	Wax (wt.%)	Gas (wt.%)	HHV (MJ/kg)
Clean	475	11.30	70.18	8.93	61.25	7.11	44.66
	475	9.87	72.92	10.90	62.02	7.33	44.89
	500	8.16	75.34	9.16	66.18	7.36	43.36
	500	8.27	75.40	8.30	67.10	8.50	45.11
	550	7.67	61.09	12.07	48.92	25.10	43.68
	550	7.67	64.40	10.83	53.40	19.89	43.77
	600	7.50	56.52	12.47	43.85	35.15	46.47
	600	7.56	56.68	13.83	42.85	40.10	42.78
	650	7.50	44.12	14.00	29.56	69.19	43.15
	650	7.47	49.25	14.96	34.16	57.73	45.49
	700	7.33	31.62	17.39	12.80	81.36	39.22
	700	7.34	30.42	15.49	13.90	72.29	42.08
Contaminated	500	8.03	71.48	11.43	60.05	9.50	45.06
	500	7.93	71.43	13.70	57.73	11.11	45.24

Table A.36: Pilot scale data with LDPE/PET multi-layer

Temperature (°C)	Residue (wt.%)	Oil/wax (wt.%)	Flowable Oil (wt.%)	Wax (wt.%)	Gas (wt.%)	HHV (MJ/kg)
475	0.00	54.05	31.57	22.48	6.00	43.59
475	11.49	70.83	46.25	24.58	6.07	43.9
500	13.89	55.14	35.66	19.48	8.61	44.1
500	0.00	62.94	40.76	22.18	10.10	44.15
550	8.88	33.07	30.30	2.77	17.73	43.26
550	14.76	34.52	31.74	2.77	17.74	44.03
600	16.20	30.41	28.63	1.78	37.96	43.96
600	2.70	25.07	21.78	3.30	26.04	43.14

Appendix B: LDPE and PET quantification Matlab code

B.1 Deconvolution of two signals with skew gauss shape

```
Data_table=readtable('Sample_1 Run_1.xls'); %import data from excel
Data_array=table2array(Data_table); %convert imported table data to
an array
dW=-Data_array(:,5); %assign weight loss data, in mg, to "dW"
T=Data_array(:,2); %assign temperature data, in ℃, to "T"

coeff_guess=[450,40,-5,10,500,30,-4,60]; %estimate the coefficients
of the mathematical model
signals_guess=twosignal_skewgauss(coeff_guess,T); %create estimated
two signal curve using function twosignal_skewgauss
coeff_real = nlinfit(T,dW,@twosignal_skewgauss,coeff_guess);
%determine real coefficients through non-linear fit of estimated
curve
signals_real = twosignal_skewgauss(coeff_real,T); %create real two
signal curve using function twosignal_skewgauss (Appendix B.2)
PET_coeff = coeff_real(1:4); %extract PET coefficients
LDPE_coeff = coeff_real(5:8); %extract LDPE coefficients
PET_signal = skewgauss(PET_coeff,T); %create individual PET curve
using function skewguass (Appendix B.3)
LDPE_signal = skewgauss(LDPE_coeff,T); %create individual LDPE curve
using function skewguass (Appendix B.3)

%plot signals
hold on
plot(T,dW,'c-');
plot(T,signals_guess,'r--');
plot(T,signals_real,'b--');
plot(T,PET_signal,'g-');
plot(T,LDPE_signal,'k-');
title('Deconvolution of PET/LDPE TGA data (S1.1)')
xlabel('Temperature (℃)')
ylabel('dWeight/dTemperature (mg/℃)')

%numerical integration under deconvoluted curves using function
trapz
PET_area = trapz(T,PET_signal); %area = PET wt.%
LDPE_area = trapz(T,LDPE_signal); %area = LDPE wt.%
```

B.2 Function twosignal_skewgauss

```
function f = twosignal_skewgauss(coeff,x)
c1=coeff(1); %location coefficient of PET signal
c2=coeff(2); %scale coefficient of PET signal
c3=coeff(3); %shape coefficient of PET signal
c4=coeff(4); %height coefficient of PET signal
c5=coeff(5); %location coefficient of LDPE signal
c6=coeff(6); %scale coefficient of LDPE signal
c7=coeff(7); %shape coefficient of LDPE signal
```

```
c8=coeff(8); %height coefficient of LDPE signal
PET_coeff = [c1,c2,c3,c4];
LDPE_coeff = [c5,c6,c7,c8];
PETsignal=skewgauss(PET_coeff,x); %create PET curve using function
skewgauss (Appendix B.3)
LDPEsignal=skewgauss(LDPE_coeff,x); %create LDPE curve using
function skewgauss (Appendix B.3)
f=PETsignal+LDPEsignal; %create convoluted curve by summing PET and
LDPE curves
```

B.3 Function skewgauss

```
function f = skewgauss(coeff,x)
c1 = coeff(1); %location coefficient
c2 = coeff(2); %scale coefficient
c3 = coeff(3); %shape coefficient
c4 = coeff(4); %signal height
f = 2/c2*(1/sqrt(2*pi()))*exp(-1/2*((x-
c1)/c2).^2)).*(1/2*(1+erf(c3*(x-c1)/c2/sqrt(2))))*c4; %mathematical
model (equation 4, Section 4.2.6)
```

Appendix C: Sample calculations

C.1 Gas yield

This section illustrates the calculation of the gas yield based on the GC results and equations 8 to 12 in Section 4.5.1. The raw data (grey shaded) and calculated data are given in Table C.37 from bench scale pyrolysis of the clean LDPE/PET multi-layer at 500 °C.

Equation 8 was used to calculate the volume of compound i in the sample Tedlar bag, for example at the first time-interval and H_2 as compound i:

$$V_{H_2,bag} = \frac{V\%_{H_2}}{V\%_{N_2}} \times \dot{V}_{N_2} \times t_{sampling} \qquad [8]$$

$$V_{H_2,bag} = \frac{0.144}{80.473} \times 0.5 \times 2 = 1.790 \times 10^{-3} \, L$$

The moles of H_2 in the bag can then be calculated using equation 9:

$$n_{H_2,bag} = \frac{V_{H_2,bag}}{22.4} \qquad [9]$$

$$n_{H_2,bag} = \frac{1.790 \times 10^{-3}}{22.4} = 7.989 \times 10^{-5} \, mol$$

The mass of H_2 in the bag is calculated with equation 10:

$$m_{H_2,bag} = n_{H_2,bag} M_{H_2}$$ [10]

$$m_{H_2,bag} = (7.989 \times 10^{-5})(2.016) = 1.610 \times 10^{-4} \, g$$

The total mass of H_2 evolved during the experiment can then be calculated as the sum of H_2 in all the bags as in equation 11:

$$m_{H_2,experiment} = \sum m_{H_2,bags}$$ [11]

$$m_{H_2,experiment} = [1.610 + 2.847 + 1.979 + 1.040 + 1.488 + 3.087 + 7.404 + 6.755 + 8.862 \\ + 9.208 + 7.324 + 5.585 + 4.969 + 3.887 + 5.270 + 6.836] \times 10^{-4} = 0.008 \, g$$

The total mass of gas evolved during the experiment is then the sum of all compounds evolved during the experiment as follows:

$$m_{gas} = 0.008 + 0.182 + 0.182 + 0.589 + 0.479 + 0.633 + 0.132 + 0.005 = 2.210 \, g$$

The yield of gas is then calculated using equation 12:

$$Gas \; yield \; (wt.\%) = \frac{m_{gas}}{m_{sample}} \times 100$$ [12]

$$Gas \; yield \; (wt.\%) = \frac{2.210}{30.01} \times 100 = 7.363 \; wt.\%$$

Table C.37: GC data and sample calculation

Time interval (min)	N_2 (vol%)	H_2				CO				CH_4				CO_2			
		H_2 (vol%)	Volume (L)	Moles (mol)	Mass (g)	CO (vol%)	Volume (L)	Moles (mol)	Mass (g)	CH_4 (vol%)	Volume (L)	Moles (mol)	Mass (g)	CO_2 (vol%)	Volume (L)	Moles (mol)	Mass (g)
2.0	80.473	0.144	1.790E-03	7.989E-05	1.610E-04	0.000	0.000E+00	0.000E+00	0.000E+00	0.000	0.000E+00	0.000E+00	0.000E+00	0.155	1.922E-03	8.580E-05	3.776E-03
3.0	90.621	0.191	3.163E-03	1.412E-04	2.847E-04	0.000	0.000E+00	0.000E+00	0.000E+00	0.000	0.000E+00	0.000E+00	0.000E+00	0.062	1.031E-03	4.602E-05	2.025E-03
2.0	94.442	0.208	2.199E-03	9.816E-05	1.979E-04	0.000	0.000E+00	0.000E+00	0.000E+00	0.000	0.000E+00	0.000E+00	0.000E+00	0.048	5.117E-04	2.284E-05	1.005E-03
2.0	94.680	0.109	1.156E-03	5.160E-05	1.040E-04	0.000	0.000E+00	0.000E+00	0.000E+00	0.000	0.000E+00	0.000E+00	0.000E+00	0.327	3.454E-03	1.542E-04	6.785E-03
2.0	91.699	0.152	1.654E-03	7.383E-05	1.488E-04	0.406	4.423E-03	1.974E-04	5.530E-03	0.000	0.000E+00	0.000E+00	0.000E+00	0.940	1.025E-02	4.576E-04	2.014E-02
2.0	87.492	0.300	3.430E-03	1.531E-04	3.087E-04	0.953	1.090E-02	4.865E-04	1.363E-02	0.263	3.001E-03	1.340E-04	2.149E-03	1.839	2.102E-02	9.383E-04	4.130E-02
3.0	84.170	0.462	8.227E-03	3.673E-04	7.404E-04	2.000	3.565E-02	1.591E-03	4.458E-02	0.691	1.232E-02	5.500E-04	8.821E-03	3.236	5.767E-02	2.575E-03	1.133E-01
3.0	81.872	0.410	7.506E-03	3.351E-04	6.755E-04	2.380	4.361E-02	1.947E-03	5.453E-02	1.315	2.409E-02	1.075E-03	1.725E-02	3.770	6.907E-02	3.084E-03	1.357E-01
3.0	81.150	0.533	9.847E-03	4.396E-04	8.862E-04	1.680	3.105E-02	1.386E-03	3.883E-02	2.096	3.875E-02	1.730E-03	2.775E-02	2.951	5.454E-02	2.435E-03	1.072E-01
3.0	82.455	0.562	1.023E-02	4.568E-04	9.208E-04	0.737	1.340E-02	5.983E-04	1.676E-02	2.518	4.580E-02	2.045E-03	3.280E-02	1.550	2.820E-02	1.259E-03	5.540E-02
3.0	84.650	0.459	8.138E-03	3.633E-04	7.324E-04	0.352	6.243E-03	2.787E-04	7.807E-03	2.271	4.025E-02	1.797E-03	2.882E-02	0.881	1.560E-02	6.966E-04	3.066E-02
3.0	86.726	0.359	6.206E-03	2.771E-04	5.585E-04	0.000	0.000E+00	0.000E+00	0.000E+00	1.859	3.215E-02	1.435E-03	2.302E-02	0.641	1.108E-02	4.947E-04	2.177E-02
3.0	87.299	0.321	5.522E-03	2.465E-04	4.969E-04	0.000	0.000E+00	0.000E+00	0.000E+00	1.648	2.831E-02	1.264E-03	2.027E-02	0.564	9.693E-03	4.327E-04	1.905E-02
3.0	82.086	0.236	4.319E-03	1.928E-04	3.887E-04	0.000	0.000E+00	0.000E+00	0.000E+00	0.564	1.031E-02	4.602E-04	7.382E-03	0.313	5.724E-03	2.555E-04	1.125E-02
3.0	87.677	0.342	5.856E-03	2.614E-04	5.270E-04	0.000	0.000E+00	0.000E+00	0.000E+00	0.654	1.119E-02	4.997E-04	8.014E-03	0.313	5.350E-03	2.388E-04	1.051E-02
3.0	90.876	0.460	7.596E-03	3.391E-04	6.836E-04	0.000	0.000E+00	0.000E+00	0.000E+00	0.522	8.615E-03	3.846E-04	6.169E-03	0.276	4.561E-03	2.036E-04	8.961E-03
Total					0.008				0.182				0.182				0.589

Table C.37 ctd.

	C₂				C₃				C₄				C₅		
C₂ (vol%)	Volume (L)	Moles (mol)	Mass (g)	C₃ (vol%)	Volume (L)	Moles (mol)	Mass (g)	C₄ (vol%)	Volume (L)	Moles (mol)	Mass (g)	C₅ (vol%)	Volume (L)	Moles (mol)	Mass (g)
0.045	5.649E-04	2.522E-05	7.329E-04	0.000	1.850E-06	8.260E-08	3.643E-06	0.000	0.000E+00	0.000E+00	0.000E+00	0.000	0.000E+00	0.000E+00	0.000E+00
0.027	4.438E-04	1.981E-05	5.757E-04	0.001	1.293E-05	5.774E-07	2.546E-05	0.001	1.501E-05	6.702E-07	3.895E-05	0.000	0.000E+00	0.000E+00	0.000E+00
0.035	3.680E-04	1.643E-05	4.774E-04	0.001	1.343E-05	5.996E-07	2.644E-05	0.002	1.628E-05	7.269E-07	4.225E-05	0.000	0.000E+00	0.000E+00	0.000E+00
0.048	5.075E-04	2.265E-05	6.583E-04	0.026	2.707E-04	1.208E-05	5.329E-04	0.002	1.767E-05	7.890E-07	4.586E-05	0.000	0.000E+00	0.000E+00	0.000E+00
0.176	1.916E-03	8.553E-05	2.485E-03	0.124	1.352E-03	6.037E-05	2.662E-03	0.007	7.191E-05	3.210E-06	1.866E-04	0.000	0.000E+00	0.000E+00	0.000E+00
0.416	4.755E-03	2.123E-04	6.169E-03	0.342	3.905E-03	1.743E-04	7.688E-03	0.057	6.476E-04	2.891E-05	1.680E-03	0.002	1.926E-05	8.598E-07	6.204E-05
0.998	1.779E-02	7.942E-04	2.308E-02	0.756	1.348E-02	6.017E-04	2.653E-02	0.109	1.949E-03	8.701E-05	5.057E-03	0.003	4.880E-05	2.179E-06	1.572E-04
1.774	3.251E-02	1.451E-03	4.218E-02	1.388	2.543E-02	1.135E-03	5.006E-02	0.067	1.229E-03	5.485E-05	3.188E-03	0.004	7.894E-05	3.524E-06	2.543E-04
2.747	5.077E-02	2.267E-03	6.587E-02	2.124	3.925E-02	1.752E-03	7.728E-02	0.085	1.574E-03	7.028E-05	4.085E-03	0.006	1.143E-04	5.102E-06	3.681E-04
3.444	6.265E-02	2.797E-03	8.128E-02	2.769	5.038E-02	2.249E-03	9.919E-02	0.384	6.978E-03	3.115E-04	1.811E-02	0.008	1.502E-04	6.707E-06	4.839E-04
3.246	5.752E-02	2.568E-03	7.463E-02	2.831	5.017E-02	2.240E-03	9.877E-02	0.473	8.378E-03	3.740E-04	2.174E-02	0.011	1.882E-04	8.404E-06	6.063E-04
2.716	4.697E-02	2.097E-03	6.093E-02	2.531	4.377E-02	1.954E-03	8.618E-02	0.497	8.590E-03	3.835E-04	2.229E-02	0.012	2.124E-04	9.484E-06	6.842E-04
2.457	4.221E-02	1.885E-03	5.476E-02	2.330	4.004E-02	1.788E-03	7.883E-02	0.491	8.430E-03	3.763E-04	2.187E-02	0.013	2.174E-04	9.707E-06	7.003E-04
1.009	1.845E-02	8.235E-04	2.393E-02	1.100	2.010E-02	8.973E-04	3.957E-02	0.254	4.647E-03	2.075E-04	1.206E-02	0.008	1.467E-04	6.549E-06	4.725E-04
1.043	1.784E-02	7.964E-04	2.314E-02	1.048	1.792E-02	8.001E-04	3.529E-02	0.246	4.200E-03	1.875E-04	1.090E-02	0.007	1.237E-04	5.523E-06	3.985E-04
0.837	1.382E-02	6.168E-04	1.793E-02	0.941	1.554E-02	6.936E-04	3.059E-02	0.255	4.205E-03	1.877E-04	1.091E-02	0.008	1.242E-04	5.544E-06	4.000E-04
Total			0.479				0.633				0.132				0.005

C.2 Uncertainty calculations

The uncertainty represented by error bars in the graphs were calculated as the standard deviation of a sample as follows:

$$\sigma = \sqrt{\frac{\sum(x - \bar{x})^2}{n - 1}}$$

For example, taking the oil/wax yield data from bench scale pyrolysis of the clean LDPE/PET multi-layer at 500 °C as given in Table A.35. First the average oil/wax yield is calculated:

$$\bar{x} = \frac{75.34 + 75.40}{2} = 75.37 \, wt.\%$$

Then the uncertainty can be calculated as:

$$\sigma = \sqrt{\frac{(75.34 - 75.37)^2 + (75.40 - 75.37)^2}{2 - 1}} = 0.042 \, wt.\%$$